ULTIMATE STRENGTH IN DIAGONAL SPLITTING OF REINFORCED CONCRETE THIN WALL RIBBED PANELS

Alfred Abdulezer

A THESIS

in

The Department

of

Civil Engineering

Presented in Partial Fulfillment of the Requirements for the Degree of Master of Engineering at Sir George Williams University Montreal, Canada

April, 1974

In memory of my father

ABSTRACT

ULTIMATE STRENGTH IN DIAGONAL SPLITTING OF REINFORCED CONCRETE THIN WALL PANELS

Alfred Abdulezer

ABSTRACT

On the basis of previous research carried out on reinforced concrete beams and especially on deep beams [6,7], it appears that inclined cracking due to shear does not terminate the work of a beam if there is sufficient web reinforcement, and the main tensile reinforcement is well anchored beyond the support. Beams, even with inclined cracks will be able to withstand further loading, until they reach the diagonal splitting strength limit due to what can be called, arch behaviour.

We have attempted in this thesis to develop a formula which will allow the estimation of the strength after diagonal splitting has occurred, and provide the necessary web reinforcement. The amount of web reinforcement required for the above ultimate condition is, in most cases, less than that required, according to the traditional shear theory and present requirements for deep beams (ACI-318-71, Section 11.9). But, in the other cases, more web reinforcement is required than ACI Practice provides, which implies that ACI-318-71, Section 11.9, is dangerous to follow, a situation which must be corrected.

ACKNOWLEDGEMENTS

ACKNOWLEDGEMENTS

The investigation reported herein was supported by the National Research Council (NRC).

The author expresses his gratitude to Dr. Zenon A. Zielinski for his invaluable guidance and advice, during all the stages of the research program and the preparation of this thesis.

The author is indebted to Sir George Williams University for the use of its Structural Laboratory facilities, and also to the Laboratory technicians, Sonny Karnick, Steven Muenz, Louis Stankevicius, Milan Wichterle, and to all the others who assisted during the various testing stages.

A special word of thanks also goes to the students of the Civil Engineering Class of 1973, for their assistance, and to all those who contributed to the completion of this thesis.

TABLE OF CONTENTS

TABLE OF CONTENTS

LIST OF TABLES

LIST OF TABLES

LIST OF ILLUSTRATIONS

LIST OF ILLUSTRATIONS

NOTATIONS

NOTATIONS

a	=	Shear span, distance between concentrated load and concentrated reaction at support.
a_2	=	Shear span as defined in Fig. 2.4.
a_{eff}	=	Effective inclined splitting span, as defined in Fig. 2.4.
a_i	=	Shear span as defined in Fig. 2.4.
A_s	=	Area of tension reinforcement, sq. in.
A_{sh}	=	Area of shear reinforcement parallel to the main tension reinforcement.
A_{sv}	=	Area of shear reinforcement perpendicular to main reinforcement within a distance a_{eff} or a_i, sq. in.
A_v	=	Area of shear reinforcement perpendicular to main reinforcement within a distance s, sq. in.
A_{vh}	=	Area of shear reinforcement parallel to the main tension reinforcement within a distance s_2, sq. in.
b	=	Width of compression face of member.
b_w	=	Web width.
d	=	Distance from extreme compression fiber to centroid of tension reinforcement.
DSC	=	Diagonal splitting crack
f'_c	=	Ultimate compressive strength of concrete, psi.
$\sqrt{f'_c}$	=	Square root of ultimate compressive strength of concrete.
f_{ct}	=	Compressive strength of concrete under combined bi-directional compression and tension.
f_{tc}	=	Tensile strength of concrete under combined bi-directional tension and compression.
f_{tt}	=	Strength of concrete under combined bi-directional tension.

f_{cc} = Strength of concrete under combined bi-directional compression.

f_y = Yield strength of reinforcement.

h = Total depth of beam.

H = Force in tension reinforcement.

ℓ = Total span.

ℓ' = Span, measured center-to-center of supports.

ℓ_n = Clear span measured face-to-face of supports.

LHS = Left-hand side of the load.

M_u = Applied load moment at a section.

P_u = Concentrated loading force.

RHS = Right-hand side of the load.

s = Shear reinforcement spacing in a direction parallel to the longitudinal reinforcement.

s_2 = Shear reinforcement spacing in a direction perpendicular to the longitudinal reinforcement.

S = Diagonal splitting force.

u = Bond stress

v = Shear stress

v_c = Nominal permissible shear stress carried by concrete.

v_t = Principal tension stress in shear.

v_u = Nominal total design shear stress.

V = Shear force

V_a = Shear force at the moment of diagonal splitting.

V_h = Part of the shear force taken by the horizontal web reinforcement.

V_u = Total shear force at section.

V_v = Part of the shear force taken by the vertical web reinforcement.

α = Diagonal splitting angle as defined in Fig. 2.4.

Σ_o = Perimeter of reinforcing bars.

ρ_h = A_{sh}/bh, ratio of reinforcement in horizontal projection.

ρ_v = A_{sv}/ba_2, ratio of reinforcement in vertical projection.

ρ_w = $A_s/b_w d$

CHAPTER 1

INTRODUCTION

CHAPTER 1

INTRODUCTION

The problem of determining the shearing strength of reinforced concrete beams has received a great deal of attention in the technical literature. A large number of laboratory investigations have been reported both in the North American continent and overseas, and empirical methods have been proposed for predicting the shearing strength of beams with web reinforcement, as for example, the formulas proposed by ACI-318-71 (Section 11.9) for deep beams, which we found to be dangerous to follow in certain cases. However, the complexity of the problem is so great that as yet, no adequate analytical solution of the problem has been developed, comparable to the simplified flexural ultimate strength design method being now used by ACI-318-71.

1.1 STRENGTH LIMITS OF REINFORCED CONCRETE BEAMS

Strength limits of beams in general, can be defined by limit deformation or by material failure. Reinforced concrete beams are made of two materials - steel and concrete. Failure of the composing materials simultaneously or separately describes the strength of a beam. In the case of steel, the failure is defined by the yield. The failure of concrete is defined by cracking.

1.1.1 Main Modes of Cracking Failure of Concrete in Beams

Three main modes of cracking failure of concrete in beams can be identified as illustrated in Figure 1.1. They are defined as follows:

Mode 1 - Uni-axial tension stresses and cracking perpendicular to the stress.

Mode 2 - Uni-axial compression stresses and cracking parallel to the stress.

Mode 3 - Bi-directional tension and compression stresses leading to cracking, perpendicular to the tension stress, and valid for "shear" or "moment and shear" loaded zones of the beam.

The knowledge of combined bi-directional strength of concrete is essential for proper evaluation of the cracking strength limits of beams.

On the basis of previous research [6,7], it appears to be adequately accurate for practical design purposes to assume the combined strength of concrete in the bi-directional stress condition, as a linear function, as presented in Figure 1.2.

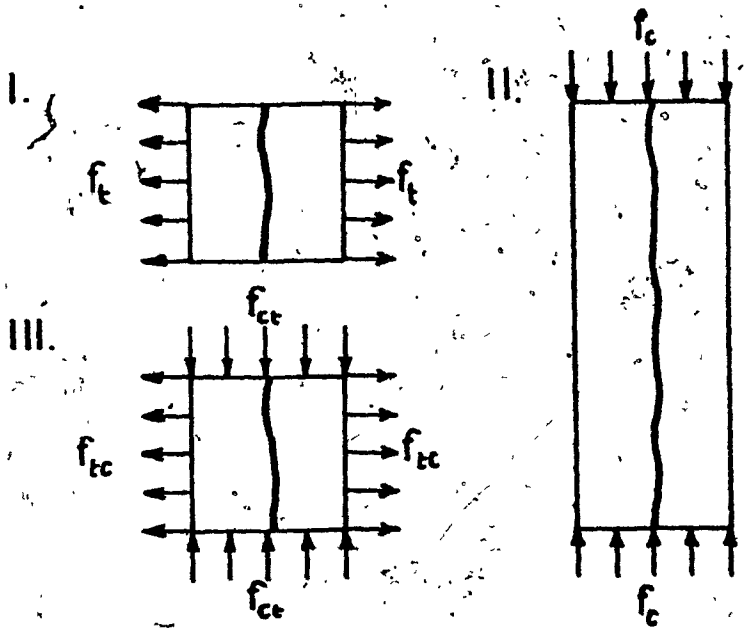

Fig. 1.1 - Basic causes of failure of concrete: (i) uni-axial tension stress, (ii) uni-axial compression stresses, (iii) bi-directional tension and compression stresses.

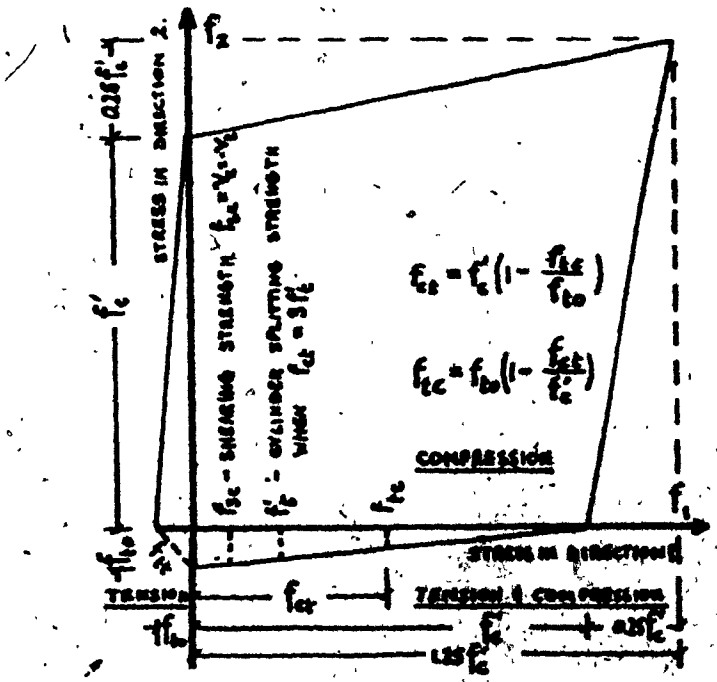

Fig. 1.2 - Combined bi-directional strength of concrete.

1.1.2 Strength Limits for Reinforced Concrete Beams

In general, we can now identify the following strength limits for reinforced concrete beams:

Strength Limit No. 1 - First flexural cracking (equal to ultimate failure as in the case of a concrete beam with no, or with very little tensile reinforcement.)

Strength Limit No. 2 - Inclined cracking under moment and shear due to beam work.

Strength Limit No. 3 - Diagonal splitting due to arch work.

Strength Limit No. 4 - Ultimate flexural failure due to yield (or rupture) of tensile reinforcement or crushing of concrete in compression.

For economical reasons, our aim should be to design a beam with the maximum possible load-carrying capacity defined by the ultimate flexural strength - Strength Limit No. 4, and to eliminate earlier failures which may be caused by any one of Strength Limits Nos. 1, 2 and 3. The ultimate flexural Strength Limit No. 4, is by now, quite well de-

fined and verified by tests.

1.2 SEQUENCE OF APPEARANCE OF CRACKS

The first cracks to appear are usually the flexural cracks (cracking Mode 1, and reaching the maximum tensile strength.) They tend to develop vertically. They define Strength Limit No. 1.

Next to appear will be cracks in shear-moment loaded zones of the beam. They originally begin as vertical (up to the main reinforcement level) but develop further at an angle (up to 45° in the middle portion of the beam). These cracks define Strength Limit No. 2.

These cracks have been conventionally called shear cracks, however, they are appearing due to the bi-axial compression and tension stress condition (cracking Mode 3) created in the beam by the bond between steel and concrete. There are no such cracks in beams with unbonded reinforcement.

The last cracks which may appear in beams, in areas of high shear, are the SPLITTING CRACKS, Strength Limit No. 3. These are diagonal cracks extending in the direction from the support to the load application point. They appear due to arch work and also due to reaching the ultimate combined strength of concrete under bi-directional

compression and tension (cracking Mode 3) or uni-axial compression strength (cracking Mode 2). These cracks may appear in beams with unbonded, as well as bonded reinforcement. The appearance of these SPLITTING CRACKS means the ultimate failure of beams which do not have sufficient web reinforcement. One of the aims of our test program was to develop a method of calculating the splitting strength and providing web reinforcement in such an amount that diagonal splitting will not cause the beam to fail before the maximum ultimate flexural strength is reached.

In the following Chapters, we are attempting to develop such formulas.

CHAPTER 2

INCLINED CRACKING STRENGTH LIMITS

CHAPTER 2

INCLINED CRACKING STRENGTH LIMITS

A definition of the strength limits for a reinforced concrete beam is presented hereunder; leading to the development of formulas allowing the calculation of the ultimate capacity of the beam at diagonal splitting, and the estimation of the total area of web reinforcement required.

We shall not discuss here Strength Limit No. 1, dealing with first flexural cracking, which is rather well-known, but limit ourselves to Strength Limit No. 2, describing 45^{o} inclined cracking, conventionally called shear cracks, and to Strength Limit No. 3, dealing with diagonal splitting at arch action.

2.1 STRENGTH LIMIT NO. 2 - INCLINED CRACKING

Inclined cracking described as Strength Limit No. 2, is illustrated by B4 and B5 cracks, in Figure 2.1. It takes place because of the so-called beam work, and the presence of bond between the flexural reinforcement and the surrounding concrete.

What we conventionally call shear stress:

$$v = \frac{V}{bjd} \qquad (2.1)$$

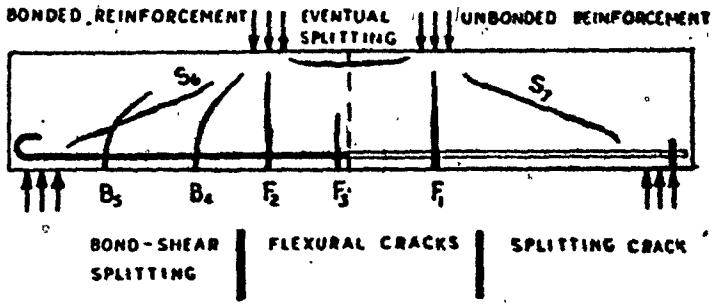

Fig. 2.1 - Generalized crack propagation in the beam with bonded or unbonded reinforcement. F_1-F_3 - flexural vertical cracks, B_4-B_5 - inclined cracks due to the bond and beam work, S_6-S_7 - diagonal splitting cracks due to arch work. Nos. 1,2,3,etc., show the order of crack appearance.

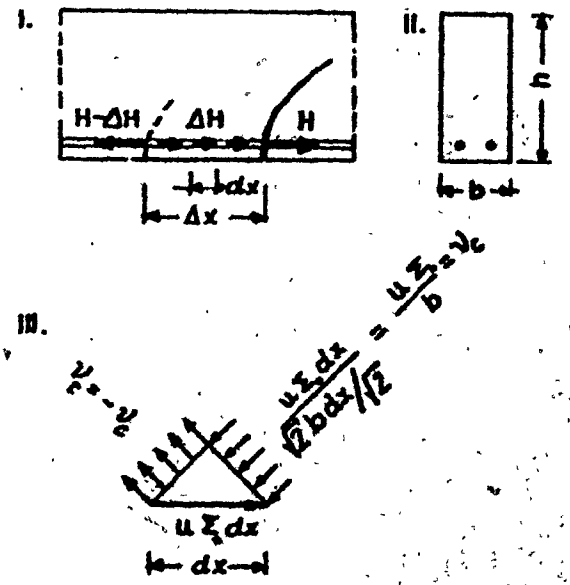

Fig. 2.2 - Definition of bi-directional stress condition at inclined cracking of the beam caused by bond: (i) segment of beam, (ii) cross-section, (iii) stress in concrete due to bond.

depends on the bond stress:

$$u = \frac{V}{\Sigma_o jd} \tag{2.2}$$

Mainly, the bond resistance $u\Sigma_o dx$ as described in Figure 2.2 evokes in the beam a bi-directional stress condition of

$$v_c = - v_t = \frac{u\Sigma_o}{b} \tag{2.3}$$

By substituting in formula (2.3) for u we can show that

$$v_c = - v_t = \frac{V\Sigma_o}{\Sigma_o jdb} = \frac{V}{bjd} = v \tag{2.4}$$

which is the conventionally called shear stress, that proves the dependence of the shear stress v on the bond stress u.

In the case of a beam with unbonded reinforcement, there is no bond resistance ($u = 0$) which means also that

$$v = v_c = -v_t = o$$

and inclined cracks cannot be expected at all. Thus, the presence of bond between reinforcement and concrete evokes bi-directional inclined stresses of $v_c = -v_t$ which are additive to the flexural normal stresses due to the moment. On the neutral axis where the flexural stresses are equal to zero, the strength of the beam is governed only by the bi-directional equal stresses of $v_c = -v_t$ inclined under 45^o.

When these stresses reach their strength limit, as defined earlier in Figure 1.2 as

$$f_{sc} \simeq .9 f_{to}$$

the beam will be subjected to 45° inclined cracking described as Strength Limit No. 2 (cracking Mode 3, Figure 1.1).

A beam with unbonded reinforcement, from the very beginning, works as a tied arch, provided that the main flexural reinforcement is well anchored beyond the support.

Tests [6,7] prove that a beam with bonded reinforcement well anchored beyond the support, works at the tied arch scheme, after the appearance of 45° inclined cracks, until they reach the diagonal splitting Strength Limit No. 3, as defined later.

Hence, it appears that 45° inclined cracking could be accepted in the design practice the same way as flexural cracking is. An additional argument in favor is the fact that inclined cracking usually occurs after flexural cracking.

As in the case of flexural cracking, also in the case of Inclined Cracking, it would be uneconomical to eliminate inclined cracks by means of additional reinforcement.

Tests show [6,7] that at the moment of cracking, the strain in concrete is in the order of:

$$\varepsilon = 0.0001 \text{ to } 0.00015 \text{ in/in}$$

which means that the accompanying stress in steel will be

$$f_s = \varepsilon E = (.0001 \text{ to } .00015)\ 30 \times 10^6 = 3000 \text{ psi} - 4000 \text{ psi}$$

which is not much at all (only 5-10% of f_y).

For example, 1% of web reinforcement stressed to $f_s = 3000$ psi, in the case of concrete with a bi-directional strength of $f_{sc} = 300$ psi, the increase in cracking resistance due to that web reinforcement would be only of the order of 10%, which may be negligible.

We should rather accept the existence of 45° inclined cracks, but ensure additional load-carrying capacity beyond the flexural and the 45° inclined cracking stages, and reach a higher strength limit at arch work - Strength Limit No. 3, being discussed next.

2.2 STRENGTH LIMIT NO. 3 - DIAGONAL SPLITTING DUE TO ARCH WORK

Diagonal splitting due to arch action could be best visualized in a beam loaded at one or two points. The working condition in such a beam is illustrated in Figure 2.3.

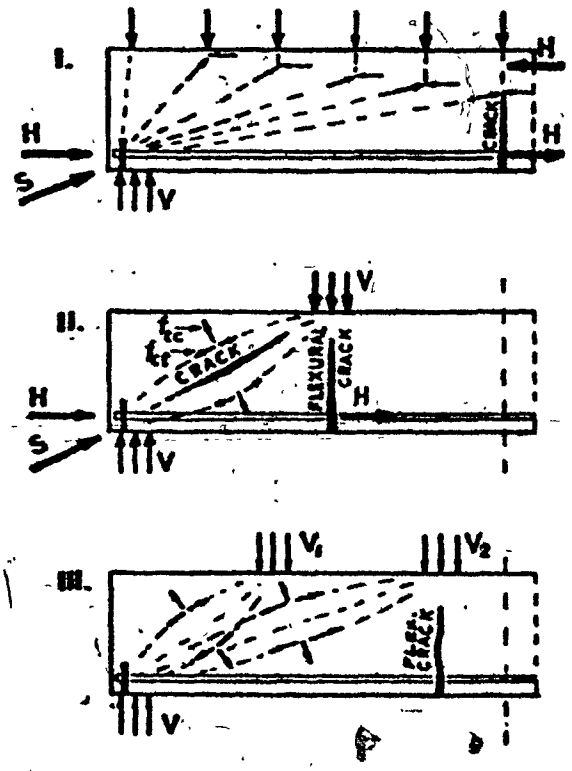

Fig. 2.3 - Basic loading schemes describing arch strength of reinforced concrete beam with unbonded reinforcement: (i) uniformly loaded beam, (ii) one or two-point loaded beams, (iii) three or more-point loaded beams.

Because of the geometry of the support-segment (between load and support) of the beam, streams of compression stresses f_{ct} will be curvilinear and will be accompanied by simultaneous tangential tensile stresses f_{tc}. In the limit state, this stress condition may lead to diagonal splitting.

It appears possible for practical design purposes, to assume a simplified rectangular stress block in the support-load segment of the beam, as shown in Figure 2.4. The above assumption is comparable to a similar design practice assuming a rectangular stress block for the flexural compression zone.

Referring to Figure 2.4, bi-directional stresses depend on the geometry of the support-segment and can be defined for a beam without web reinforcement as

$$f_{ct} = \frac{S}{bh} \cdot \cos\alpha = \frac{H}{bh} \qquad (2.5)$$

$$f_{tc} = \frac{S}{ba_2} \cdot \sin\alpha = \frac{V}{ba_2} \qquad (2.6)$$

$$\frac{f_{ct}}{f_{tc}} = \frac{Ha_2}{Vh} = \frac{a_2^2}{h^2} \qquad (2.7)$$

The diagonal splitting will occur when the concrete in the middle portion of the support-load segment reaches

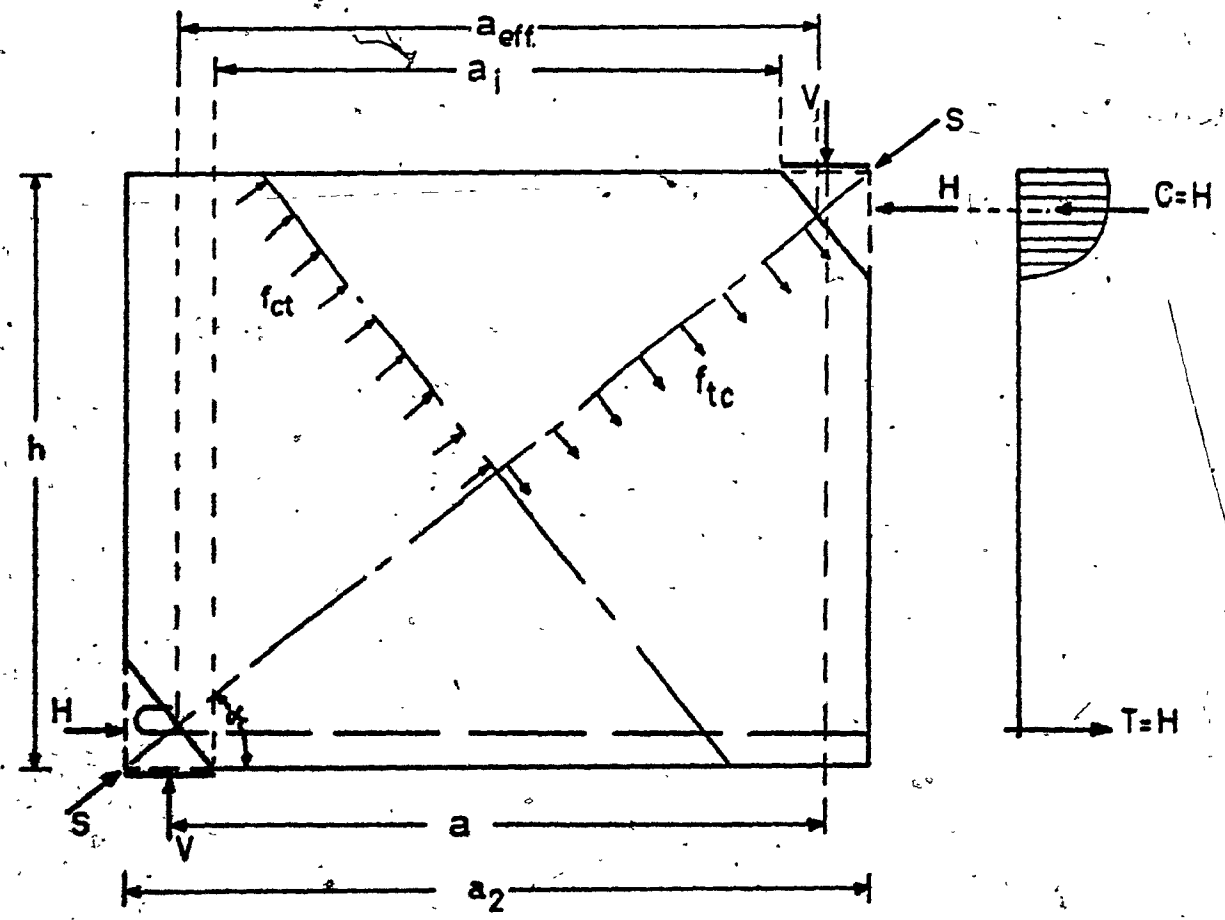

FIG. 2.4 - SIMPLIFIED STRESS DISTRIBUTION UNDER DIAGONAL COMPRESSION

f_{tc} - the limit strength for concrete in bi-directional tension and compression. Assuming a linear strength function describing biaxial strength of concrete, as presented in Figure 1.2, and applying formula (2.7)

$$f_{tc} = \frac{f'_c}{\frac{f'_c}{f_{to}} + \frac{a_2^2}{h^2}} \qquad (2.8)$$

The corresponding maximum load, in terms of a limit shear force V_a, will be:

$$V_a = f_{tc} a_2 b = \frac{f'_c a_2 b}{\frac{f'_c}{f_{to}} + \frac{a_2^2}{h^2}} \qquad (2.9)$$

Formulas (2.8) and (2.9) apply to beams with no web reinforcement.

In the case of a beam with web reinforcement, the corresponding formulas can be written as:

$$f_{ct} = \frac{H}{bh[1 + \frac{E_c}{E_s} \rho_h]} \qquad (2.10)$$

$$f_{tc} = \frac{V}{ba_2[1 + \frac{6000}{f_{tc}} \rho_v]} \qquad (2.11)$$

where $\rho_h = \frac{A_{sh}}{bh}$ and $\rho_v = \frac{A_{sv}}{ba_2}$.

The corresponding maximum load in terms of a limit shear force V_a is

$$V_a = f_{tc}\, ba_2[1 + \frac{6000}{f_{tc}} \rho_v] \qquad (2.12)$$

If the beam contains sufficient web reinforcement; reach of Strength Limit No. 3, as defined in formulas (2.5) to (2.12), does not mean the end of the working capability of the beam.

Having sufficient web reinforcement, able to take over the whole splitting force V_a, and to restrict the width of the splitting crack, the beam will be able to work further until it reaches V_u the ultimate shear force that will accompany the ultimate flexural failure. In which case, we will have a diagonally cracked support-load segment with the concrete working under diagonal uni-axial compression only, and with no resistance against the tangential tension and splitting action. The tangent splitting force will be carried totally by the web reinforcement.

The ultimate capacity, after diagonal splitting has occurred, can be computed from the following formulas:

1) Portion of the reaction force provided by the vertical web reinforcement (A_{sv})

$$V_v = \cos\alpha \sum_{i=1}^{n} A_{svi} f_{yi} \qquad (2.13)$$

2) Portion of the reaction force provided by the horizontal web reinforcement (A_{sh})

$$V_h = \sin\alpha \sum_{i=1}^{n} A_{shi} f_{yi} \qquad (2.14)$$

3) The summation of V_v and V_h gives the ultimate reaction force which could be carried at the support, refer to Figure 2.4

$$V_u = V_v + V_h = \cos\alpha \sum_{i=1}^{n} A_{svi} f_{yi} + \sin\alpha \sum_{i=1}^{n} A_{shi} f_{yi} \qquad (2.15)$$

In the following Chapter, we are discussing the strength tests carried out on panels designed in such a way that the reach of ultimate flexural strength would be simultaneous with diagonal splitting, as described above.

CHAPTER 3

RESEARCH PROGRAM

CHAPTER 3

RESEARCH PROGRAM

Precast modular thin-wall panels are being used in a variety of building projects to minimize construction time, labor and material consumption. Some of the possible ways as to their use are shown in Figures 3.1(a) to (f).

The same panel being used for floors and walls, has to be designed to be able to withstand the different loading situations including high shear, moment and torsion, depending upon its location in the structure.

The unique feature of these panels is the very thin - 1.5 inch concrete slab reinforced with a wire mesh. An 8 inch (or more) deep reinforced rib on the perimeter is provided for the rigidity of the whole element and the erected structure. Detailed drawings for the panels are shown in Appendix B. The shape of the rib on the long side, was chosen to provide a shear key for a side connection. The panels could be connected by welding, in which case, inserts are provided, or by having the main flexural reinforcement protruding to the outside and cast in situ concrete, thus creating a monolithic connection (Figure 3.1(g)).

The panels may work as bearing walls when placed in the long direction and support one or more concentrated

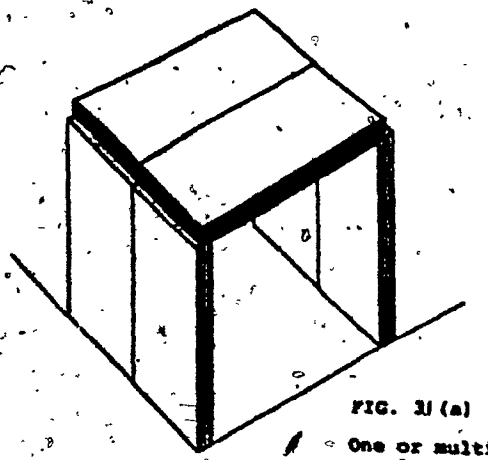

FIG. 3.1 (a)

One or multi-storey buildings having span equal to one panel using same panel for roof/floor and wall.

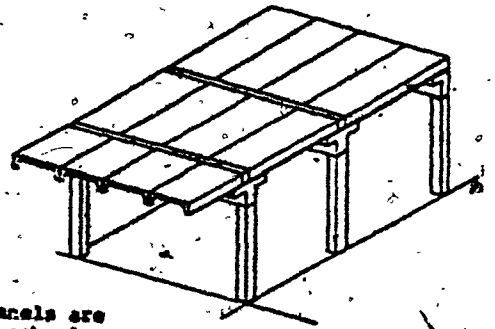

FIG. 3.1(b)

Large span buildings where panels are placed on precast beams (for schools, industrialized buildings).

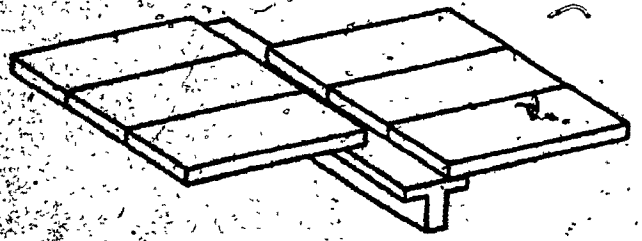

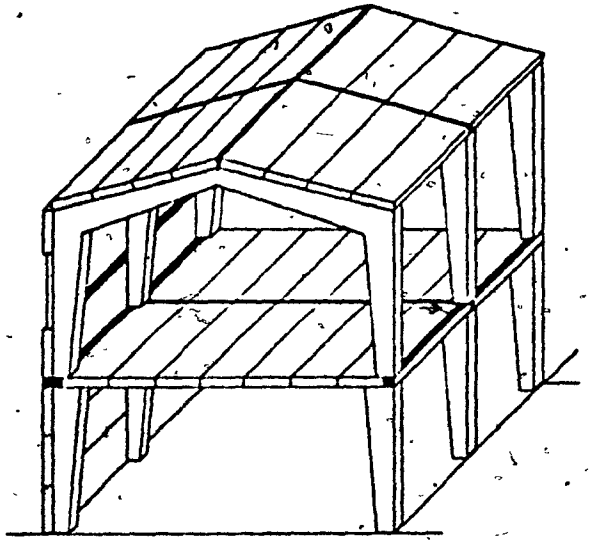

FIG. 3.1(c) Buildings with frame structures

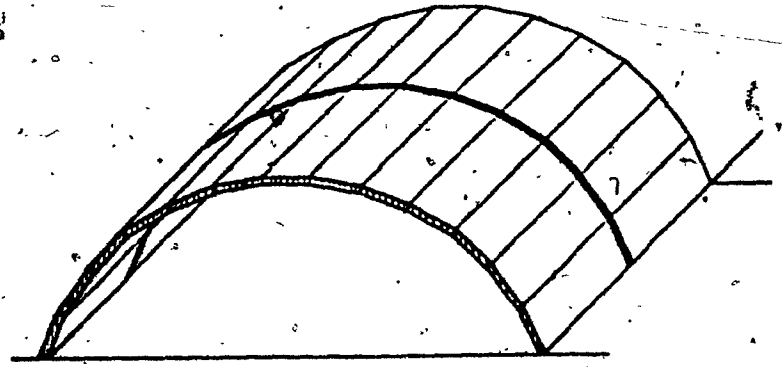

FIG. 3.1(d) Vault-like Building

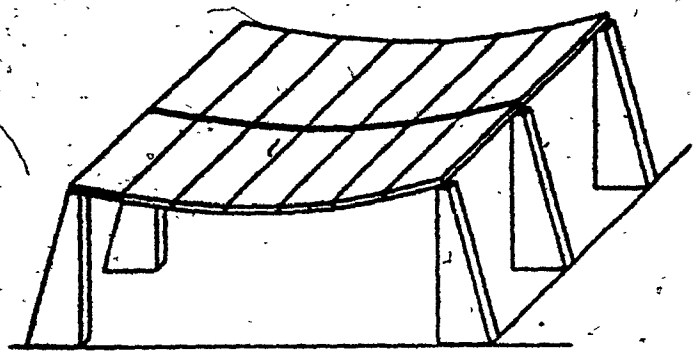

FIG. 3.1(e) Hanging roof

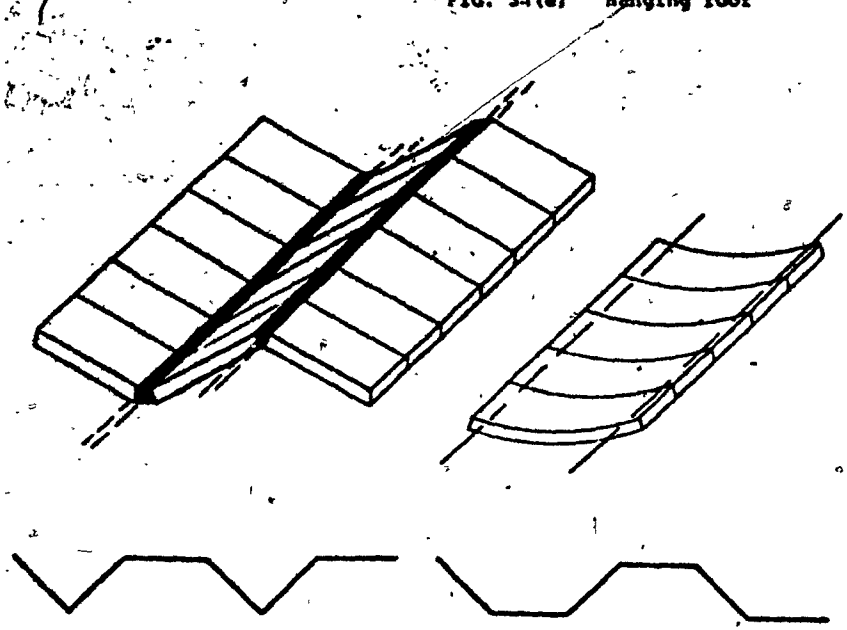

FIG. 3.1(f) Folded roofs with cast in situ edges with ordinary or post-tensioned reinforcement.

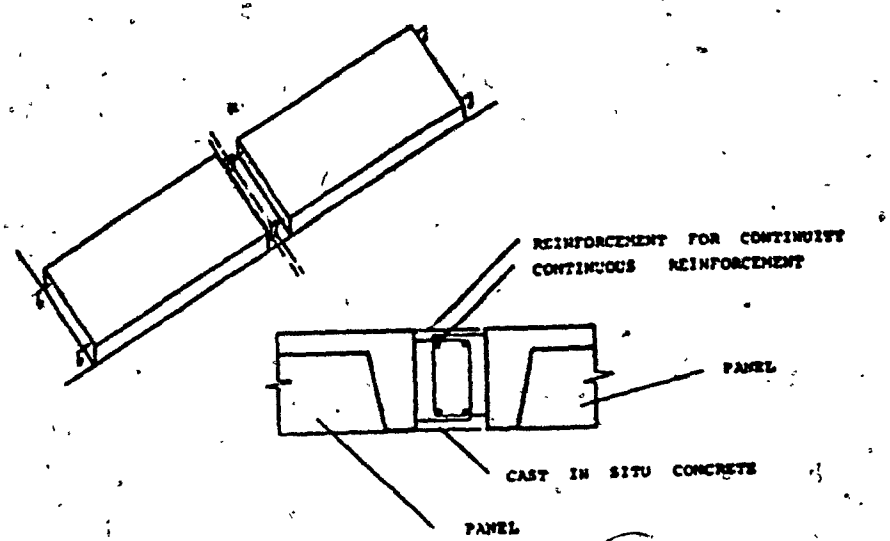

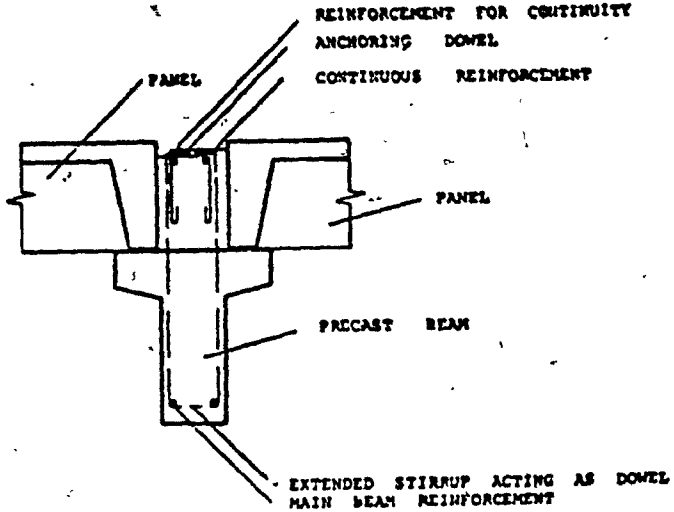

FIG. 3.1(g) Examples of connection between panels

loads from the walls above. The wall panel in such a case will be acting as a deep beam, and may be subjected to very high diagonal splitting stresses. The fact that the thin slab is the web of the beam, presents an excellent opportunity to study the propagation of cracks, and inclined splitting stresses. Both are highly apparent in such a thin web.

3.1 EXPERIMENTAL PROGRAM

An experimental program was initiated to test 4 ft. wide by 9 ft. long panels, having a slab 1.5 inch thick and an 8 inch deep rib all around (refer to any of the figures in Appendix B).

There were in total fourteen samples of seven different types. Details of the test programme are given in Table 3.1. The variables were, first the method of loading - some were loaded at mid-span and others at one third span, and second - the reinforcement. The basic features of the different panel types are described below.

Panel 168-5 (see Appendix B), contained a 66-1010 wire mesh (gage #10 wires spaced at 6 inches in both directions) as web reinforcement provided to withstand an ultimate diagonal splitting load in the range of 40 kips to 50 kips

TABLE 3.1- TEST SCHEDULE

LOADING CONDITION	TEST Nº	Nº OF SAMP.	P_u kips.	REINF. DETAIL
I 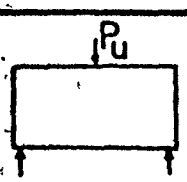	1	2	44	168-5
	2	2	58	168-6
	3	2	130	168-7
II 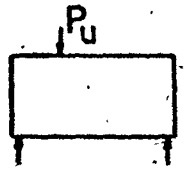	4	2	58	168-8
	5	2	80	168-9
III 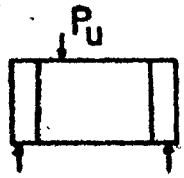	6	2	65	168-10
	7	2	90	168-11

Note -

P_u : Anticipated failure load.

applied at mid-span. The tensile reinforcement was provided in the bottom rib to provide flexural resistance. It consisted of 2-#5 reinforcing bars. Steel angles were welded to their ends to provide sufficient anchorage at the supports. The upper rib contained a nominal reinforcement of 1-#2 and 1-#3. A special stirrup reinforcement consisting of 2-#4 rebars was provided under the applied load to prevent local failure of the upper rib.

Panels 168-6 contained a 66-66 wire mesh as web reinforcement, which is slightly heavier than what was provided in panel 168-5. It was provided to resist an ultimate diagonal splitting load in the range of 50 kips to 60 kips applied at mid-span. The tensile reinforcement in the lower rib was 2-#6 rebars. The reinforcement in the upper rib was 1-#3 and 1-#4 rebars, and the stirrup reinforcement under the load was 2-#5.

Panels 168-7 were the most heavily reinforced of all; they contained <u>two</u> 66-66 wire meshes, as web reinforcement, the combination of which was to resist an ultimate diagonal splitting force of over 130 kips applied at mid-span. The lower rib tensile reinforcement was 2-#9. The nominal rebars in the upper rib were 1-#3 and 1-#4, the stirrups under the load were 4-#6.

Panels 168-8 were designed to be loaded at 1/3 of

their span to create two different support-segments of different height-to-width ratios. These panels contained one light wire mesh 146-1210 over the whole length of the web, plus an additional wire mesh 66-66 in the shorter support-segment. That segment is subject to a higher shear force in this case, being equal to 2/3 of the applied load, as compared to the longer segment taking the remaining 1/3 of that load. The wire mesh combination was provided to withstand an ultimate diagonal splitting force in the range of 50 kips to 60 kips. The tensile rebars in the lower rib were 2-#6, the rebars in the upper rib were 1-#2 and 1-#3 and the stirrups under the load were 2-#4.

Panels 168-9 were also to be loaded at 1/3 span. They contained one wire mesh 66-66 over the whole length of the web, plus an additional heavier wire mesh 66-11 in the shorter (1/3 span) support segment. The combination was provided to withstand an ultimate diagonal splitting load in the range of 70 kips to 80 kips. The lower rib tensile rebars were 1-#6 and 1-#8, the rebars in the upper rib were 1-#3 and 1-#4 and the stirrups under the load were 5-#4.

Panels 168-10 were similar to panels 168-8, as to the sizes of the wire meshes and reinforcing bars they contained. Except that, panel 168-10 had <u>two</u> internal ribs 6 inches deep, one at 1/6 of the span and the other at 5/6 of the span. The purpose of these ribs was to provide extra

rigidity to the web-slab, as well as to contain a fairly substantial additional web reinforcement (1-#2 in each rib). The panels were designed to be able to withstand a load in the range of 60 kips to 70 kips applied at 1/3 span.

Panels 168-11 were also to be loaded at 1/3 span. They contained one wire mesh 66-1010 over the whole length of the web, plus an additional heavier piece of wire mesh 66-11 in the shorter (1/3 span) support-segment. These panels had two 6 inches deep internal ribs at 1/6 and 5/6 of the span, the rebars inside them were 1-#3 and 1-#4, respectively. The wire meshes and rebars combination was provided to withstand a diagonal splitting load in the range of 80 kips to 90 kips. The lower rib tensile reinforcement was 1-#6 and 1-#8, the rebars in the upper rib were 1-#3 and 1-#4, and the stirrups under the load were 5-#4. The 168-11 series are comparable to the 168-9 series of panels.

3.2 FABRICATION

The production of panels was made by FRANCON(1966) LTEE, a local precasting firm.

The reinforcing cages were assembled prior to placement into the forms. The steel assembly was securely held in the proper location inside the form. Lifting inserts were provided for handling purposes (Fig. 3.2).

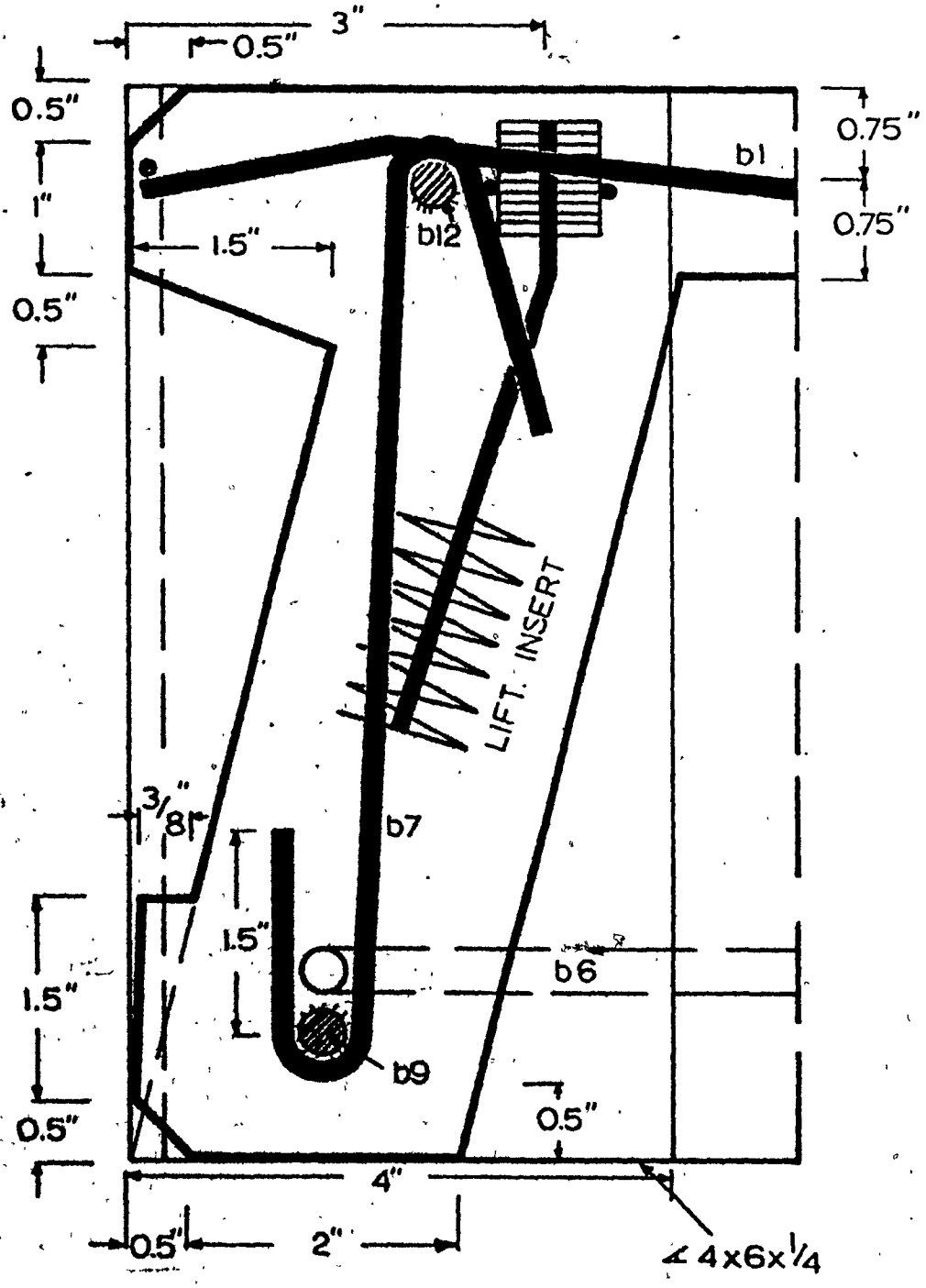

FIG. 3.2 - MAIN RIB DETAIL AND LIFTING INSERT.

The panels were cast in a form made of plywood with epoxy coating to give a smooth surface. The casting of all the panels was done in a single form, at the rate of one panel per day. All panels were air cured.

3.3 CONTROL SPECIMENS

3.3.1 Concrete

Three 6 in x 12 in. cylinder-specimens were taken for every panel type. They were cured under the same conditions as the panels. The cylinders were tested in compression. The recorded ultimate strengths of concrete f'_c were between 4050 psi and 5306 psi for the various panel types, as shown in Table 3.2. Also, stress-strain curves were drawn for some samples (see Figures in Appendix D).

3.3.2 Reinforcing Steel

Three 18 inches long samples from every kind of reinforcing bars and wire meshes used were tested. The stress-strain curves were automatically drawn by the testing apparatus, and the average yield stresses f_y are given in Table 3.3.

3.4 TEST PROCEDURE AND INSTRUMENTATION

The loading arrangement is shown in Figure 3.3 and photograph No. E.1 in Appendix E.

TABLE 3.2 - CONCRETE COMPRESSIVE STRESSES f'_c AS OBTAINED FROM TEST CYLINDERS.

CYLINDERS FOR PANEL TYPE	SAMPLE #1 f'_{c1} psi.	SAMPLE #2 f'_{c2} psi.	SAMPLE #3 f'_{c3} psi.	SAMPLES AVERAGE f'_c psi.	$f'_{c\ AVG.}$ psi.
168-5-2	6190	6084	5942	6072	5070
168-5-3	4244	3784	4174	4067	
168-6-2	4952	4244	3254	4150	4050
168-6-3	4244	3042	4563	3950	
168-7-1	5270	5553	3997	4940	5023
168-7-2	5553	5553	4209	5105	
168-8-1	4810	4952	5447	5070	5306
168-8-2	5518	5588	5518	5541	
168-9-1	4457	4952	5376	4928	5259
168-9-3	5518	5659		5589	
168-10-1	4563	4598	4633	4598	4698
168-10-2	4244	5022	5129	4798	
168-11-1	5235	5588	5659	5494	5073
168-11-2	4633	4669		4651	

TABLE 33- REINFORCING STEEL YIELD STRESSES f_y

REINFORCEMENT TYPE		NOMINAL AREA SQ. IN.	SAMPLE #1 f_{y1} psi.	SAMPLE #2 f_{y2} psi.	SAMPLE #3 f_{y3} psi.	AVERAGE f_y psi.
MESH 146 - 1210	GAGE # 10	0.0143	88811.2	81,818.2	83,916	85,314.7
	GAGE # 12	0.0087		86206.9	89,425.3	87,816.1
MESH 66-1010	GAGE # 10	0.0143	86,014	79,720.3	84,615.4	83,449.9
MESH 66-66	GAGE # 6	0.02895	71,157.2	70,811.7	76,683.9	72884.3
MESH 66-11	GAGE # 1	0.0629	86,009.5	56,438.8	86,645.5	76,364.6
REBAR	# 2	0.05	45,000	47,800	39,600	44,133.4
REBAR	# 3	0.11	54,500	55,454.5	55,700	55,218.2
REBAR	# 4	0.20	47,300	49,400	47,500	48,066.7
REBAR	# 5	0.31	50,000	49,193.6	50,000	49,731.2
REBAR	# 6	0.44	43,636.4	43,181.8	43,750	43,522.7
REBAR	# 6	0.44	~~50,568.2~~	51,136.4	51,590.9	51,098.8

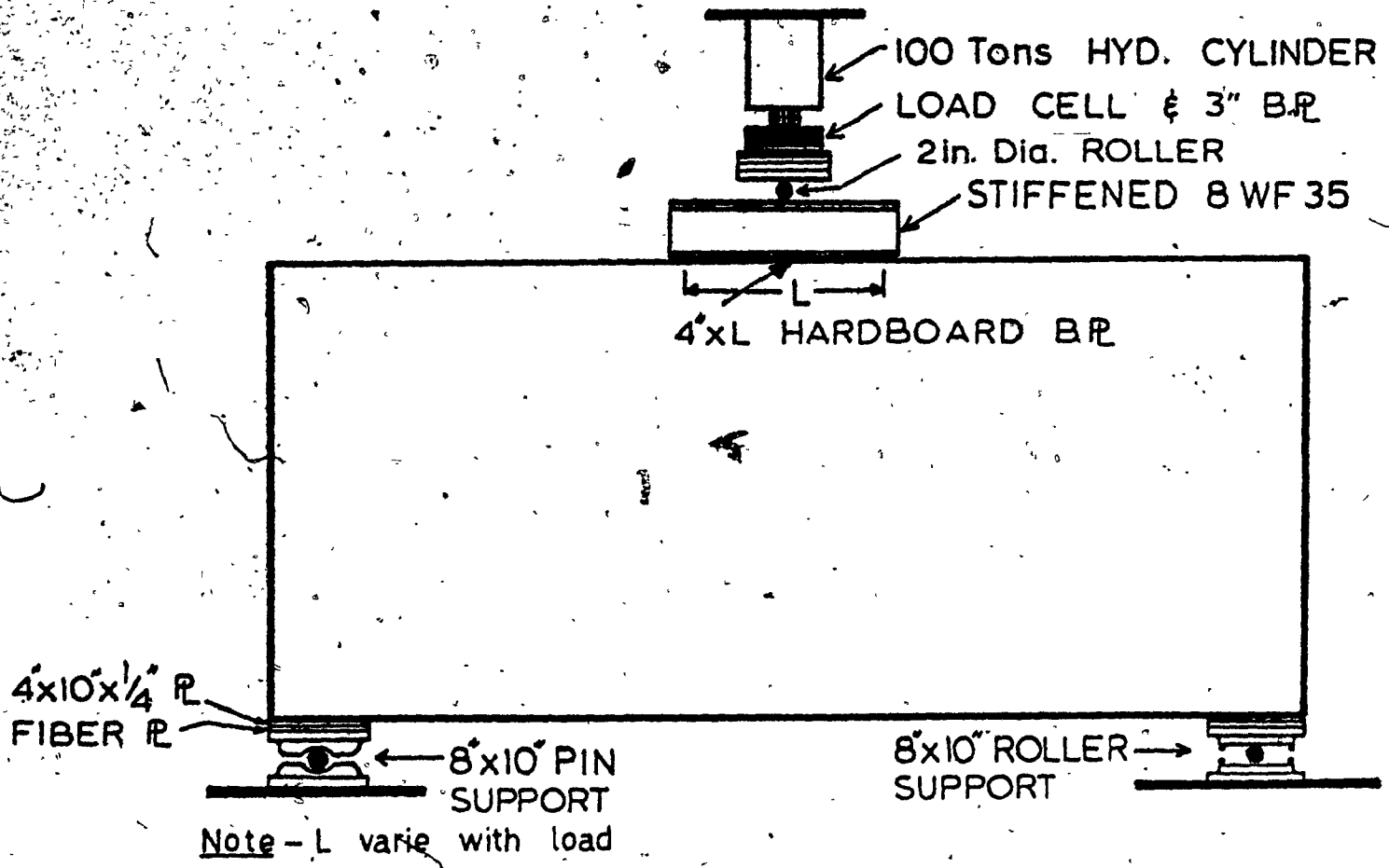

FIG. 33 - LOADING ARRANGEMENT, TYPICAL

The test panels were seated on 4 in x 10 in x 1/4 in. plates on top of the supports, so as to load at the centre of gravity of the section and thus avoid heavy torsion.

The load was applied by means of a hydraulic cylinder through a load cell, a roller, a stiffened loading beam, and a wooden fiber plate the length of which varied for different loads. The exact load was measured by means of a calibrated electronic load cell.

The compressive stresses in the web of the panels were recorded. Electric strain gages were used. They were fixed to the back of the panels by means of epoxy(Inter-technology Type GA 2). The strain gages were located on the line joining the point of load application with the point of support and the central line perpendicular to it, as shown in Figs. 3.4(a) and 3.4(b).

The tensile strains were also measured. They were read on 6 inch bases between the points shown on Figs. 3.5(a), 3.5(b) and 3.5(c). Small square metal bases were punched and glued with epoxy on each of those points to permit reading with a specially rigged dial gage of 0.0001 in accuracy.

Vertical (y-axis) and horizontal(z-axis) displacements were measured by specially developed precalibrated electric devices of 1" travel. They were preferred to dial gages because of their speed in reading the data. The measurements

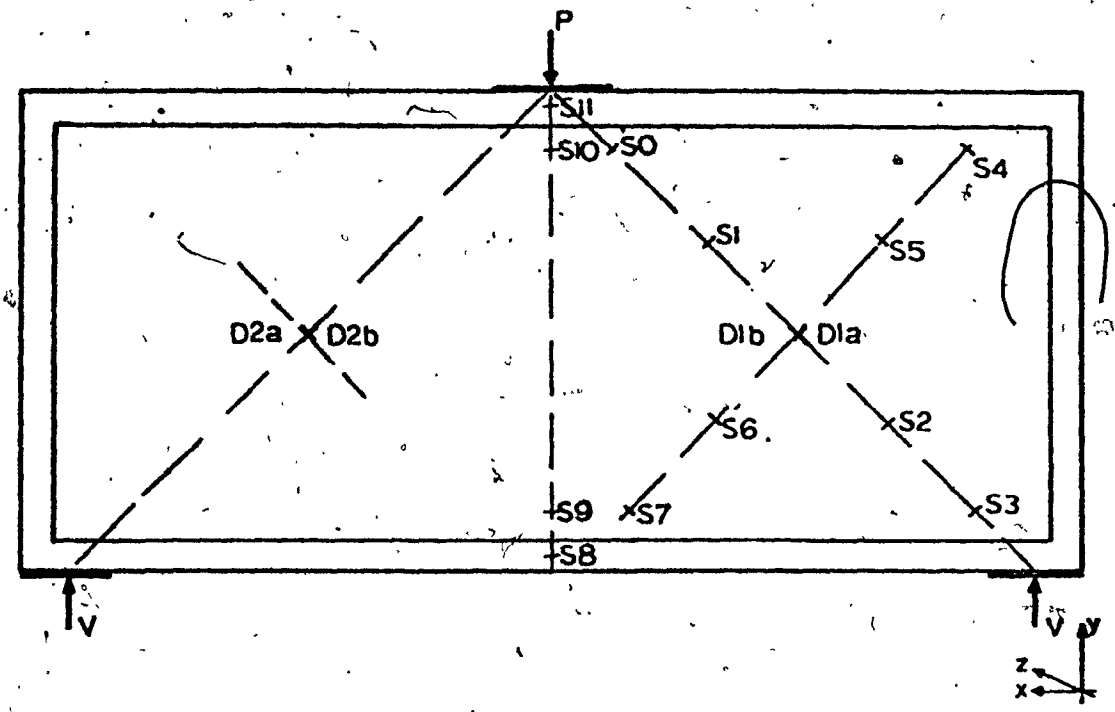

FIGURE 3.4(a) - STRAIN GAGE ARRANGEMENT FOR PANELS 168 - 5/6/7

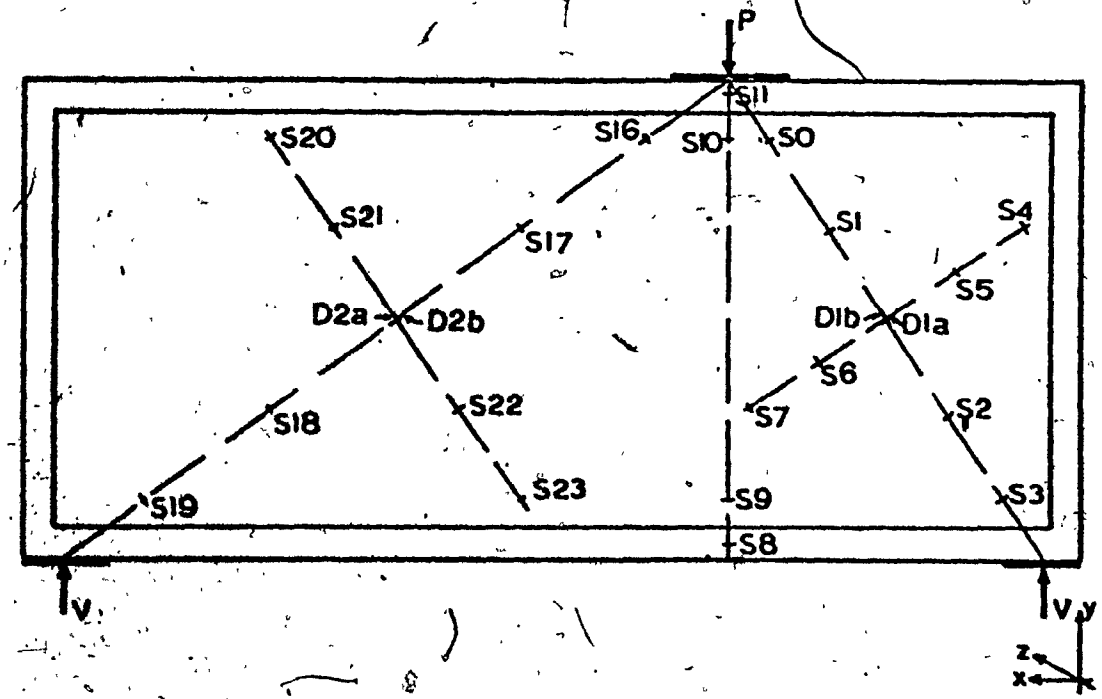

FIGURE 3.4(b) - STRAIN GAGE ARRANGEMENT FOR PANELS 168-8/9/10/11.

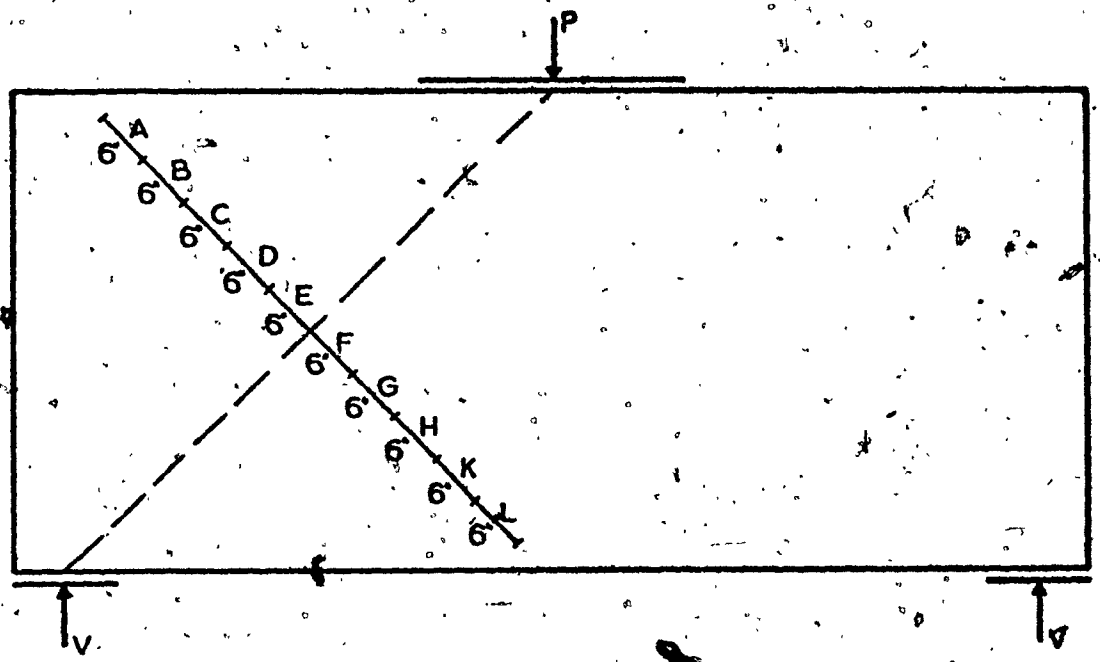

FIGURE 3.5(a) - TENSILE STRAINS MEAS. BASES, FOR PANELS 168-5-2, 168-6-2

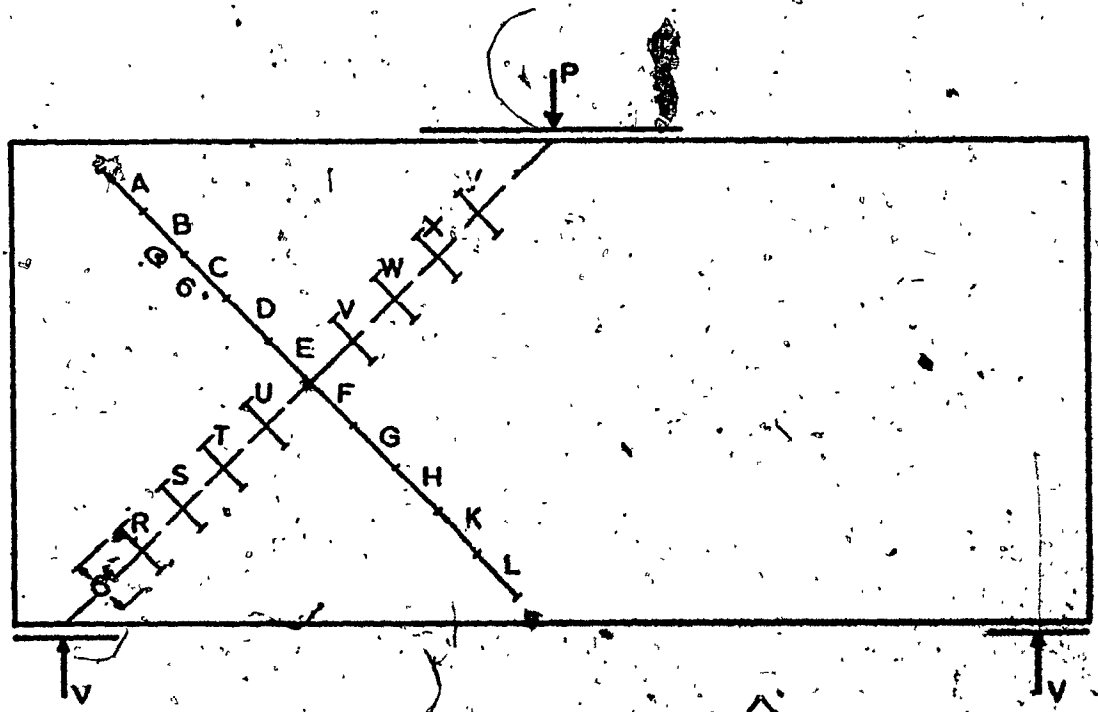

FIGURE 3.5(b) - TENSILE STRAINS MEASUREMENTS BASES FOR PANELS 168-6-3 & 168-7-1/2

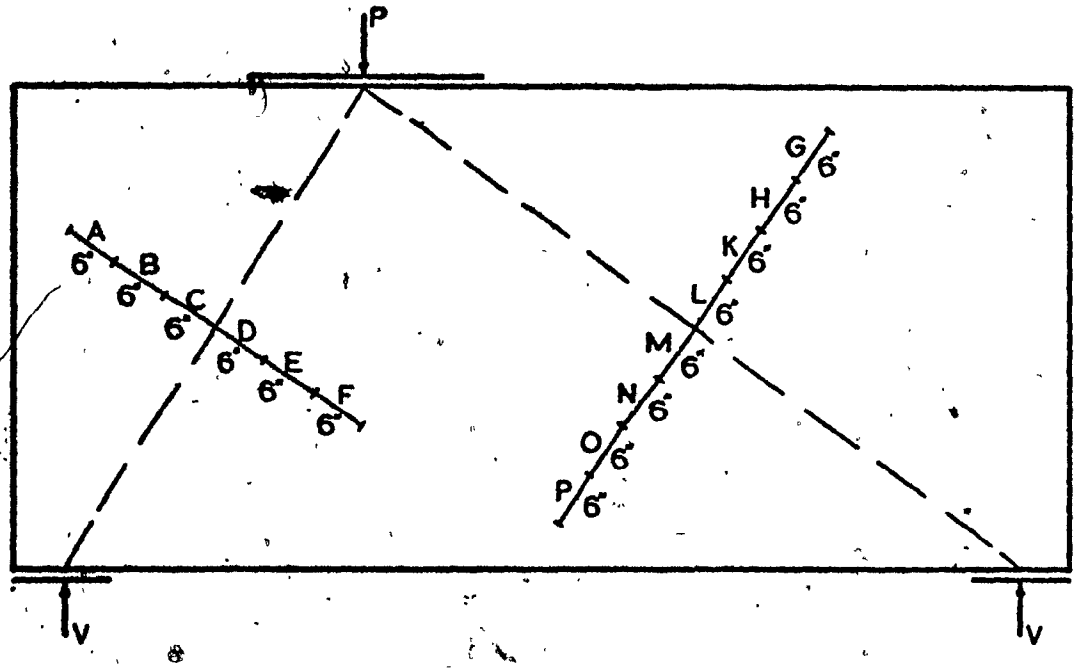

FIGURE 3.5(c) - TENSILE STRAINS MEAS. BASES, FOR PANELS 168-8 ; 168-9 , 168 - 10 & 168 - 11

were made on the points shown in Figs. 3.6(a) and 3.6(b).

To facilitate the recording of cracks and visual observation of the panel behavior during testing, the surfaces of the panel were brushed clean and a 1 ft square grid was drawn on the outside surface.

Each panel was very accurately positioned in the test frame. The allowable tolerances were ± 1/16 inch.

All the strain gages and the electric displacement reading devices were connected to a data acquisition system which would automatically take three readings and one calibration reading at each load increment and store them on a magnetic tape. The whole operation was performed within 10 seconds, thus nullifying the effect of any drop in the load.

A strain gage indicator was connected to the load cell, which was pre-calibrated. Calibration tables for load increments of 2 kips and 2.5 kips were used. The gage indicator would be set at its equivalent reading for every desired load increment and the load would then be applied to balance that reading.

At each load increment, readings for all electric devices and strain gages were taken, and the panel was checked for cracks which in the event of their occurrence were painted on the panel surface. At every second load increment,

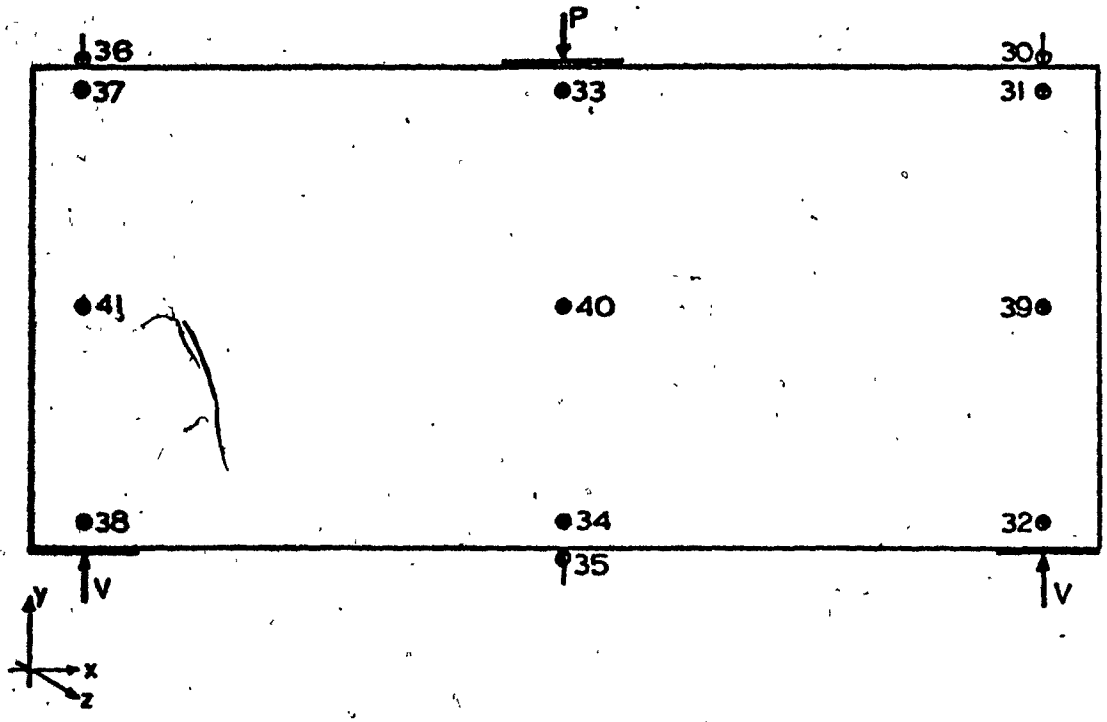

FIGURE 3.6 (a) - DISPLACEMENT READING POINTS FOR PANELS 168 - 5/6/7

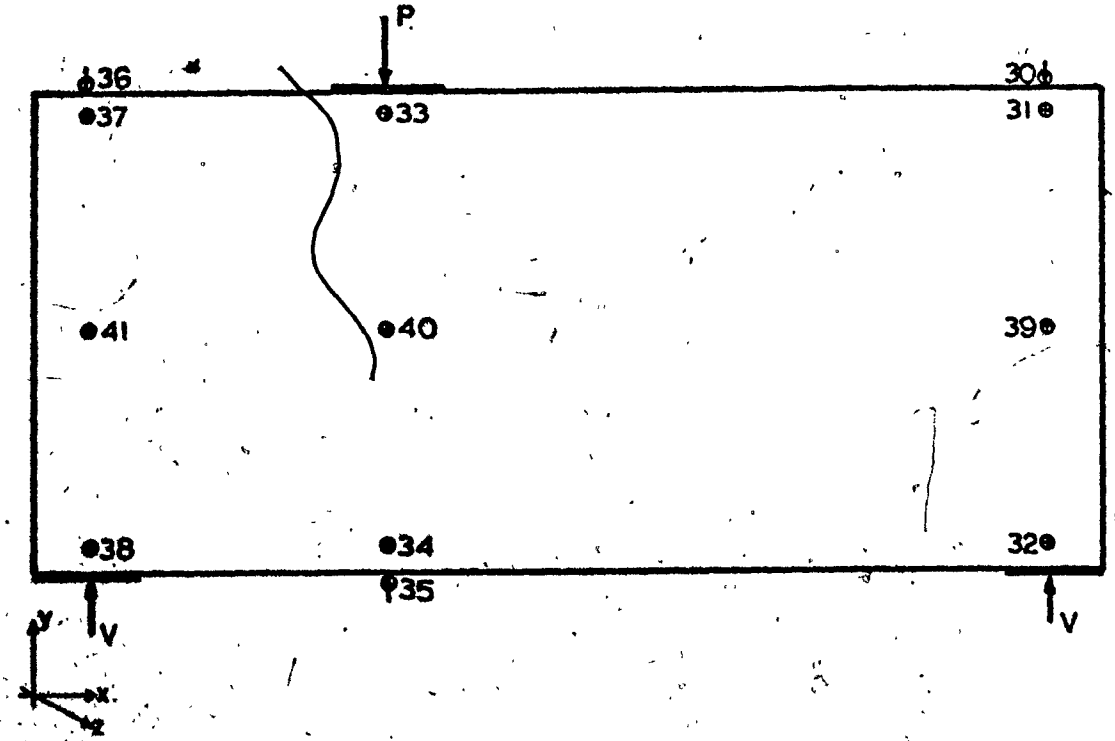

FIGURE 3.6 (b) - DISPLACEMENT READING POINTS FOR PANELS 168 - 8/9/10/11

tensile strain readings were taken.

The panels were loaded only once from zero and up to failure. After failure occurred, the load was relieved and the crack pattern sketched. Also, photograph documentation of the cracked panel was taken (see the photographs in Appendix E).

CHAPTER 4

TEST OBSERVATIONS AND RESULTS

CHAPTER 4

TEST OBSERVATIONS AND RESULTS

The following observations were made during tests:

1) Displacements in the vertical (y-axis) and horizontal (z-axis) directions (Figs. 3.6(a) and 3.6(b)).

2) Tensile strains, (Figs. 3.5(a), 3.5(b) and 3.5(c).

3) Cracks and their development pattern, (Figs. in Appendix C).

4) Mode and location of failure.

5) Failure loads (Table 5.1).

4.1 OBSERVATIONS COMMON TO ALL TEST PANELS

From Table 4.1, it is seen that the greatest deflections both horizontal and vertical occurred at the load points as had been expected. There were horizontal restraints on the panel at the region of application of the load, the top right corner and at the supports.

The maximum tensile strains were observed in the regions of diagonal splitting crack near the support and to the loading area. That implies that the web reinforcement was under maximum stress in those regions. This condition can be explained by superposition of the

TABLE 4.1 - MAXIMUM DISPLACEMENTS IN THE X & Y - Axes FOR THE POINTS DEFINED IN FIGS. 3.5(a) & 3.5(b).

TEST PANEL	HORIZONTAL (Z-Axis) DISPLACEMENT IN.									VERT. (Y-Axis) IN		
	37	41	38	33	40	34	31	39	32	36	35	30
168-5-2	0.77	0.44	0.08	0.26	0.50	0.38	0.0	0.40	-0.02	-0.20	-0.10	-0.26
168-5-3	0.65	0.32	0.0	0.08	0.04	0.03	0.06	0.0	-0.06	-0.12	-0.50	-0.25
168-6-2	0.39	0.20	0.0	0.14	0.47	0.51	0.08	0.06	-.015	0.09	-0.36	-0.06
168-6-3	1.20	0.53	0.05	0.34	0.56	0.11	0.13	0.07	-0.01	-0.21	-0.56	0.06
168-7-1	1.00	0.82	0.08	0.26	1.00	0.40	0.16	0.03	-0.06	-0.42	-0.35	-0.26
168-7-2	1.30	0.85	0.16	0.32	1.00	0.42	-0.15	-0.07	-0.07	-0.37	-0.62	-0.24
168-8-1	1.02	0.56	0.0	0.52	1.13	0.66	-0.18	-0.03	0.0	0.20	-0.01	-0.10
168-8-2	1.30	0.42	-0.04	0.30	0.82	0.47	-0.19	-0.12	-0.06	0.23	-.188	-0.04
168-9-1	0.78	0.41	0.07	0.42	0.50	0.29	-0.06	-0.03	0.0	—	-0.28	-0.06
168-9-3	1.33	0.60	0.0	0.43	0.79	0.49	0.0	-0.19	-0.08	-0.48	0.0	-0.38
168-10-1	0.83	0.37	0.0	0.33	0.78	0.45	-0.09	-0.02	-0.07	-0.05	0.0	-0.15
168-10-2	0.49	0.01	-0.02	0.04	0.18	0.21	-0.05	-0.03	0.96	-0.22	-0.06	-0.25
168-11-1	0.50	0.62	0.01	0.42	-1.35	0.45	-0.20	-0.36	-0.26	0.06	-0.09	-0.24
168-11-2	0.80	0.36	-0.01	0.10	0.30	0.27	-0.12	-0.17	-0.10	-0.23	0.0	-0.37

bond imposed stresses and the shear stresses.

4.2 OBSERVATIONS CONCERNING PANELS LOADED AT MIDSPAN

The flexural cracks appeared at the early stages of loading. They first appeared at the bottom tension zone at mid-span directly under the load, slightly above the lower rib, i.e., in the 1.5 inch web. Then, as the load was increased, the flexural cracks propagated vertically upwards towards the compression zone under the load. They stopped propagating any further at around 45% to 50% of the ultimate loads. If there was no flexural tensile reinforcement in the bottom rib, the panel would have failed under tension due to beam action.

The first inclined cracks started to appear later, after the appearance of the flexural cracks. The inclined cracks appeared adjacent to the flexural cracks, and they were running upwards at an angle.

As the load increased, the existing cracks developed further and new inclined cracks appeared adjacent to the older ones. The sequence of appearance of new inclined cracks was from mid-span, under the load; and towards the supports, on both sides.

At around 75% to 80% of the ultimate load, a sudden diagonal splitting crack showed up running from

the support to the load. Subsequently, another diagonal splitting crack appeared on the second half of the panel. The appearance of the diagonal splitting crack was simultaneously audible and visible.

At this stage, the panel would have been considered as having exhausted its capacity to carry any more load if there had been insufficient web reinforcement. The wire mesh web reinforcement takes over the splitting force and as the load was further increased, the diagonal splitting cracks were widening. It could be noted from the tensile strain readings at that stage and on, that the wire mesh across the diagonal splitting cracks was yielding until it snapped. This meant that the ultimate splitting strength had been reached. In fact, in most of the cases, the concrete around the failure zone was chipping off, and the snapped wire could be seen. Details of crack propagation are presented in the figures in Appendix C.

4.3 SPECIFIC OBSERVATIONS

4.3.1 Panel 168-5-2

The crack pattern conformed to the general trend, (compare the figure in Appendix C and the photograph in Appendix E). The first diagonal splitting crack (DSC) was observed at 24 kips on the right-hand side (RHS) support-

segment of the panel. Then it was followed by the second DSC on the left-hand side (LHS) support-segment at 30 kips. Failure occurred at 42 kips, along the second crack. Incidentally, the left side of the panel was supported on the pin support arrangement, i.e., with no freedom of horizontal movement.

4.3.2 Panel 168-5-3

The crack pattern conformed to the general trend, (compare the figure in Appendix C and the photograph in Appendix E). The first DSC appeared on the RHS support-segment of the panel between 25 kips and 30 kips. The second DSC followed at 30 kips and 40 kips on the LHS support segment and a third DSC occurred adjacent to the second at 45 kips. Failure ultimately occurred at the second DSC at 53 kips.

4.3.3 Panel 168-6-2

The crack pattern conformed to the general trend, (compare the figure in Appendix C and the photograph in Appendix E). The first DSC appeared at 30 kips on the RHS support-segment. The second DSC appeared at 35 kips, on the LHS support-segment and it ran between points E-F on the tension line. This crack widened suddenly at 50 kips and failure occurred at the second DSC at 60 kips.

4.3.4 Panel 168-6-3

The crack pattern conformed to the general trend, (compare the figure in Appendix C and the photograph in Appendix E). Two DSC appeared at 35 kips on the LHS and RHS support-segments. Then the RHS DSC kept on widening up to failure at 55 kips.

4.3.5 Panel 168-7-1

This panel contained exceptionally heavy web reinforcement. The crack pattern conformed to the general trend, (compare the figure in Appendix C and the photograph in Appendix E). A point to note was the absence of inclined cracks from a wide area at the middle of the panel. That could be explained by the use of a 32" long bearing plate covering all that area under the load, where only vertical flexural cracks appear. The first DSC appeared at 40 kips on the LHS support-segment, followed by the second DSC at 50 kips. Both DSC's kept on running towards the load, as the load was increased. They kept on widening until failure occurred at 95 kips at the right-hand side DSC.

4.3.6 Panel 168-7-2

The crack pattern conformed to the general trend, (compare the figure in Appendix C and the photograph in Appendix E). To note here also, was the absence of inclined cracks from a wide area at the middle of the panel.

The first DSC appeared at 60 kips on the LHS support-segment, followed by a loudly announced second DSC on the RHS at 65 kips. The DSC's were still propagating until failure occurred at the RHS support-segment DSC at 110 kips.

4.3.7 Panel 168-8-1

That panel was loaded at 1/3 span. The crack pattern conformed to the general trend, (compare the figure in Appendix C and the photograph in Appendix E). The first DSC appeared at 25 kips through point N on the RHS support-segment. The second DSC appeared at 45 kips on the LHS. Yielding was heard and observed at 43 kips. Failure occurred at 60 kips simultaneously in compression under the load due to beam action and yielding of the web reinforcement across the splitting crack at the LHS support-segment.

4.3.8 Panel 168-8-2

The crack pattern conformed to the general trend, (compare the figure in Appendix C and the photograph in Appendix E). The first DSC appeared at 27.5 kips on the RHS support-segment. The second DSC appeared at 32.5 kips on the LHS support-segment. Yielding was observed at the LHS diagonal splitting crack at 67.5 kips when compression flexural failure occurred.

4.3.9 Panel 168-9-1

The crack pattern conformed to the general trend, (compare the figure in Appendix C and the photograph in Appendix E). The first DSC appeared at 30 kips on the RHS support-segment followed by a second DSC at 40 kips on the LHS support-segment, which in turn, was followed by a third DSC on the LHS support-segment at 50 kips. At this point, excessive horizontal deflection (in the z-axis) was observed and extra bracing of the loading arrangement was required. Failure occurred at 63 kips at the third DSC on the RHS support-segment. It is suspected that the above displacement occurred due to improper alignment or insufficient horizontal bracing, which might have contributed to earlier failure.

4.3.10 Panel 168-9-3

The crack pattern conformed to the general trend, (compare the figure in Appendix C and the photograph in Appendix E). The first DSC occurred at 45 kips in the LHS support-segment, followed by the second DSC at 55 kips on the RHS support-segment. This second crack kept on propagating and widening until failure occurred at 87 kips.

4.3.11 Panel 168-10-1

The crack pattern conformed to the general trend, (compare the figure in Appendix C and the photograph in Appendix E). The first DSC occurred at 40 kips on the RHS support-segment. The second DSC appeared at 42.5 kips on the LHS support-segment. Yielding of the first crack was observed at 50 kips and it kept on widening until failure occurred at 60 kips.

4.3.12 Panel 168-10-2

The crack pattern conformed to the general trend, (compare the figure in Appendix C and the photograph in Appendix E). The first DSC appeared at 40 kips on the RHS support-segment. The second DSC appeared at 50 kips on the LHS support-segment. Yielding at the first DSC was from hereon observed, and until failure occurred at 57.5 kips.

4.3.13 Panel 168-11-1

The crack pattern conformed to the general trend, (compare the figure in Appendix C and the photograph in Appendix E). The first DSC appeared at 35 kips at the RHS support-segment. The second at 55 kips at the LHS support-segment, and the third at 70 kips at the RHS support-segment, which kept on widening and yielding until failure occurred at 90 kips.

4.3.14 Panel 168-11-2

The crack pattern conformed to the general trend, (compare the figure in Appendix C and the photograph in Appendix E). The first DSC occurred at 35 kips at the LHS support-segment. The second DSC occurred at 70 kips at the RHS support-segment. The first DSC kept on yielding, propagating and widening until failure at 85 kips.

CHAPTER 5

DISCUSSION OF TEST RESULTS AND CONCLUSIONS

CHAPTER 5

DISCUSSION OF TEST RESULTS AND CONCLUSIONS

Table 5.1 shows the values of the ultimate load-carrying capacities obtained from the tests.

A computational analysis was performed, to determine the ultimate load-carrying capacities of the support-load-segment-blocks for panels 168-5 to 168-11.

Formula (2.15) was applied considering, as effective only, the web reinforcement located within the distance a_{eff} or, within the distance a_i (compare Figure 2.4). The yield stresses f_{yi} of the reinforcing bars and wire meshes, as obtained from the tests, were used (Table 3.3).

Tables 5.2 and 5.3 show a summary of all the calculations.

These calculations were compared to the design practice for deep beams, recommended by the American Concrete Institute (ACI).

By applying the requirements of ACI-318-71, Section 11.9, we have to check the allowable concrete shear strength v_c using ACI Equation (11.22):

$$v_c = (3.5 - 2.5 \frac{M_u}{V_u d})(1.9\sqrt{f'_c} + 2500 \rho_w \frac{V_u d}{M_u})$$

CHAPTER 5

DISCUSSION OF TEST RESULTS AND CONCLUSIONS

CHAPTER 5

DISCUSSION OF TEST RESULTS AND CONCLUSIONS

Table 5.1 shows the values of the ultimate load-carrying capacities obtained from the tests.

A computational analysis was performed, to determine the ultimate load-carrying capacities of the support-load-segment-blocks for panels 168-5 to 168-11.

Formula (2.15) was applied considering, as effective only, the web reinforcement located within the distance a_{eff} or, within the distance a_i (compare Figure 2.4). The yield stresses f_{yi} of the reinforcing bars and wire meshes, as obtained from the tests, were used (Table 3.3).

Tables 5.2 and 5.3 show a summary of all the calculations.

These calculations were compared to the design practice for deep beams, recommended by the American Concrete Institute (ACI).

By applying the requirements of ACI-318-71, Section 11.9, we have to check the allowable concrete shear strength v_c using ACI Equation (11.22):

$$v_c = (3.5-2.5 \frac{M_u}{V_u d})(1.9\sqrt{f'_c} + 2500\ \rho_w \frac{V_u d}{M_u})$$

TABLE 5.1 - TEST RESULTS

LOADING CONDITION	TYPE	SAMP. Nº	FAIL. P_u k.	FAIL. SIDE	AVG. P_u k.
I 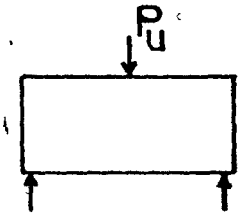	168-5	2	42	LHS	47.5
		3	53	LHS	
	168-6	2	60	LHS	57.5
		3	55	RHS	
	168-7	1	95	RHS	102.5
		2	110	LHS	
II 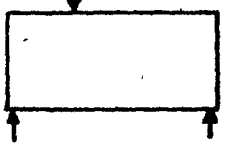	168-8	1	60	LHS	63.8
		2	67.5	LHS	
	168-9	1	63	RHS	75
		3	87	RHS	
III 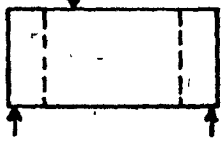	168-10	1	60	RHS	59
		2	58	RHS	
	168-11	1	90	RHS	87.5
		2	85	LHS	

Note –
P_u : ULTIMATE FAILURE LOAD

TABLE 5.2- CALCULATIONS ACCORDING TO DIAGONAL SPLITTING CONCEPT CONSIDERING WEB REINFORCEMENT WITHIN a_{eff}.

PANEL TYPE	PORTION	a_{eff} in	Cos α	Sin α	A_{sv1} sq.in	A_{sh1} sq.in	f_{y1} ksi	A_{sv2} sq.in	A_{sh2} sq.in	f_{y2} ksi	A_{sv3} sq.in	A_{sh3} sq.in	f_{y3} ksi	A_{sv4} sq.in	A_{sh4} sq.in	f_{y4} ksi	A_{sv5} sq.in	A_{sh5} sq.in	f_{y5} ksi	A_{sv6} sq.in	f_{y6} ksi	V_v kips	V_h kips	V_u kips	EQUIVALENT P_u kips.
168-5	EQ	49	.775	.631	.057	.129	83.5		.05	44.1		.11	55.2	.2		48.1						11.15	12.0	23.15	46.3
168-6	EQ	45	.809	.588	.116	.261	72.9		.11	55.2		.2	48.1	.31		49.7						19.30	20.37	39.67	79.3
168-7	EQ	41.5	.824	.565	.376	.521	72.9		.11	55.2		.2	48.1	.88		43.5						54.15	30.33	84.48	169
168-8	LHS	31	.675	.736		.044	87.8	.086		85.3	.232	.261	72.9		.05	44.1		.11	55.2	.2	48.1	22.80	22.90	45.70	66.7
168-8	RHS	60.9	.856	.514		.044	87.8	.072		85.3		.05	44.1		.11	55.2	.200		48.1			13.45	6.23	19.68	62.2
168-9	LHS	31	.707	.707	.174	.261	72.9	.252	.503	76.4		.11	55.2	.6	.2	48.1						42.90	51.70	94.60	138.1
168-9	RHS	58.5	.867	.495	.145	.174	72.9		.11	55.2	.2	.2	48.1									17.50	14.05	31.55	99.7
168-10	LHS	31	.675	.736		.044	87.8	.086		85.3	.174	.261	72.9	.05	.05	44.1		.11	55.2	.2	48.1	21.47	22.90	44.37	64.8
168-10	RHS	60.9	.856	.514		.044	87.8	.072		85.3	.05	.05	44.1		.11	55.2	.200		48.1			15.34	6.23	21.50	68
168-11	LHS	31	.707	.707	.086	.129	83.5	.377	.566	76.4		.11	55.2	.6	.2	48.1						45.84	49.28	95.10	138.9
168-11	RHS	58.5	.867	.495	.100	.100	83.5	.11	.11	55.2	.2	.2	48.1									20.85	11.90	32.70	103.5

NOTE:

a_{eff}: AS DEFINED IN FIG. 2.4

$V_v : \text{Cos}\,\alpha\,(A_{sv1} f_{y1} + A_{sv2} f_{y2} + \cdots + A_{svn} f_{yn})$

$V_h : \text{Sin}\,\alpha\,(A_{sh1} f_{y1} + A_{sh2} f_{y2} + \cdots + A_{shn} f_{yn})$

$V_u : V_v + V_h$

$P_u : \frac{l'}{a} V_u$

TABLE 5.3- CALCULATIONS ACCORDING TO DIAGONAL SPLITTING CONCEPT CONSIDERING WEB REINFORCEMENT WITHIN a_1.

PANEL TYPE	PORTION	a_i in	Cos α	Sin α	A_{sv1} sq.in	A_{sh1} sq.in	f_{y1} ksi	A_{sv2} sq.in	A_{sh2} sq.in	f_{y2} ksi	A_{sv3} sq.in	A_{sh3} sq.in	f_{y3} ksi	A_{sv4} sq.in	A_{sh4} sq.in	f_{y4} ksi	A_{sh5} sq.in	f_{y5} ksi	V_v kips.	V_h kips	V_u kips	EQUIVALENT P_u kips
168-5	EQ	39	.775	.631	.043	.129	83.5		.05	44.1		.11	55.2						2.78	12.0	14.78	29.6
168-6	EQ	36	.809	.588	.116	.261	72.9		.11	55.2		.2	48.1						6.83	20.37	27.20	54.4
168-7	EQ	27	.824	.565	.232	.521	72.9		.11	55.2		.2	48.1						13.90	30.33	44.24	88.5
168-8	LHS	18	.675	.736		.044	87.8	.043		85.3	.116	.261	72.9		.05	44.1	.11	55.2	8.17	22.90	31.07	45.4
168-8	RHS	54	.856	.514		.044	87.8	.057		85.3		.05	44.1		.11	55.2			4.18	6.23	10.41	32.9
168-9	LHS	14	.707	.707	.087	.261	72.9	.063	.503	76.4		.11	55.2		.2	48.1			7.87	51.70	59.54	86.9
168-9	RHS	50	[illegible]	.495	.145	.174	72.9		.11	55.2		.2	48.1						9.16	14.05	23.21	73.4
168-10	LHS	18	.675	.736		.044	87.8	.043		85.3	.087	.261	72.9	.05	.05	44.1	.11	55.2	8.23	22.90	31.13	45.5
168-10	RHS	54	.856	.514		.044	87.8	.072		85.3	.05	.05	44.1		.11	55.2			7.10	6.23	13.34	42.2
168-11	LHS	14	.707	.707	.043	.129	83.5	.189	.566	76.4		.11	55.2	.2	.2	48.1			19.50	49.28	68.8	100.5
168-11	RHS	30	.867	.495	.086	.100	82.5	.11	.11	55.2		.2	48.1						11.48	11.90	23.4	73.9

NOTE:

a_i : AS DEFINED IN FIG. 2.4

V_v : $\cos\alpha\,(A_{sv1}f_{y1} + A_{sv2}f_{y2} + \cdots + A_{svn}f_{yn})$

V_h : $\sin\alpha\,(A_{sh1}f_{y1} + A_{sh2}f_{y2} + \cdots + A_{shn}f_{yn})$

V_u : $V_v + V_h$

P_u : $\frac{l'}{a} V_u$

In our case, we have to consider the section for maximum moment at mid-distance between the center line of the concentrated load to the center line of the support, i.e. a/2 (see Fig. 2.4).

Accordingly, $\frac{M_u}{V_u d} = \frac{V\frac{a}{2}}{Vd} = \frac{a}{2d}$.

In this case, ACI Equation (11.22) describing concrete strength capacity in shear can be written as follows:

$$v_c = (3.5 - 2.5\ \frac{a}{2d})(1.9\sqrt{f'_c} + 2500\,\rho_w\ \frac{2d}{a}) \qquad (5.1)$$

Now, we can define the maximum ultimate shear stress v_u allowable by ACI practice on the basis of Equation (11.24):

$$\frac{A_v}{s}\left(\frac{1+\frac{\ell_n}{d}}{12}\right) + \frac{A_{vh}}{s_2}\left(\frac{11-\frac{\ell_n}{d}}{12}\right) = \frac{(v_u - v_c)b_w}{f_y}$$

considering that for all samples

ℓ_n = 88 in

d = 47 in

b_w = 1.5 in

f_y = 60,000 psi max allowed by ACI

and accordingly

$$\frac{\ell_n}{d} = 1.872 < 2$$

therefore

$$v_u \leq 8\sqrt{f'_c}$$

$$\frac{b_w}{f_y} = 2.5 \times 10^{-5}$$

$$(1+\frac{\ell_n}{d})/12 = 0.24$$

$$(11-\frac{\ell_n}{d})/12 = 0.76$$

ACI Equation (11.24) can be written as follows:

$$v_u = v_c + 9560\ (\frac{A_v}{s}) + 30,400(\frac{A_{vh}}{s_2}) \leq 8\sqrt{f'_c} \qquad (5.2)$$

Equation (5.2) can also be written in terms of yield stress in steel as:

$$f_y = \frac{1.5(v_u - v_c)}{0.239(\frac{A_v}{s}) + 0.760(\frac{A_{vh}}{s_2})} \qquad (5.3)$$

This gives the yield stress in the web reinforcement after the limitation of $v_u \leq 8\sqrt{f'_c}$ has been applied.

Table 5.4 shows a summary of the calculations according to the above-developed equations.

Table 5.5 presents a comparison of the ultimate load-carrying capacities (P_u), computed according to ACI and

TABLE 5.4 - CALCULATIONS ACCORDING TO ACI-318-71, SECTION 11.9.

PANEL TYPE	PORTION	a in	a/2d	A_s sq.in	$\rho_2 = \frac{A_s}{b_w d}$	f'_c psi	$3.5 - 2.5\frac{a}{2d} \le 2.5$	$1.9\sqrt{f'_c}$	$2500\rho_w\frac{2d}{a}$	$v_c \le 6\sqrt{f'_c}$ psi	A_v/s	A_{vh}/S_2	$v_u \le 8\sqrt{f'_c}$ psi	$V_u = v_u b_w d$ kips	EQUIVALENT P_u kips	EQUIVALENT f_y IN WEB REINF. psi
168-5	EQ	49	0.52	0.62	.0088	5070	2.2	135.3	42.3	391 ⊕	.00413	.0055	569.6 *	40.2	80.3	50,450
168-6	EQ	49	0.52	0.88	.01248	4050	2.2	121.0	60	382.2 ⊕	.0088	.0109	509.6 *	35.9	71.9	18,410
168-7	EQ	49	0.52	2.0	.0284	5023	2.2	134.7	136.5	425.4 ⊕	.02188	.01629	567.2 *	40	80	12,080
168-8	LHS	31	0.33	0.88	.0125	5306	2.5	138.5	94.7	425.7 ⊕	.0154	.0092	583.2 *	41.1	60	22,140
168-8	RHS	67	0.713	0.88	.0125	5306	1.72	138.5	43.8	313.6 ⊕	.00388	.00377	466.3	32.8	102.7	60,000
168-9	LHS	31	0.33	1.1	.0156	5259	2.5	137.8	118.2	435 ⊕	.0266	.02135	580 *	40.9	59.7	9,630
168-9	RHS	67	0.713	1.1	.0156	5259	1.72	137.8	54.7	331	.00856	.0090	580 *	40.9	129.2	42,020
168-10	LHS	31	0.33	0.88	.0125	4698	2.5	130.2	113.6	411 ⊕	.01473	.0092	548 *	38.6	56.4	19,550
168-10	RHS	67	0.713	0.88	.0125	4698	1.72	130.2	43.8	299.2	.00422	.00377	454.2 *	32	101.2	60,000
168-11	LHS	31	0.33	1.1	.0156	5073	2.5	135.3	118.2	427.2 ⊕	.0330	.0199	569.6 *	40.2	58.6	9,290
168-11	RHS	67	0.713	1.1	.0156	5073	1.72	135.3	54.7	326.8	.0094	.00753	569.6 *	40.2	126.9	45,680

NOTE: STEEL CONSIDERED WITHIN DISTANCE a ONLY

* - $8\sqrt{f'_c}$

⊕ - $6\sqrt{f'_c}$

$d = 47$ in

$b_w = 1.5$ in

$l_n = 88$ in

$$\frac{M_u}{V_u d} = \frac{V_u(a/2)}{V_u d} = \frac{a}{2d}$$

$$\frac{l_n}{d} = 1.87 < 2$$

$$v_c = \left(3.5 - 2.5\frac{a}{2d}\right)\left(1.9\sqrt{f'_c} + 2500\rho_w\frac{2d}{a}\right) \le 6\sqrt{f'_c}$$

$$v_u = v_c + \frac{A_v}{s}(9560) + \frac{A_{vh}}{S_2}(30400) \le 8\sqrt{f'_c}$$

$$f_y = \frac{1.5(v_u - v_c)}{0.239\left(\frac{A_v}{s}\right) + 0.76\left(\frac{A_{vh}}{S_2}\right)} \le 60{,}000 \text{ psi}$$

a : DISTANCE BETWEEN ℄ OF SUPPORT AND CONCENTRATED LOAD

TABLE 5.5 - COMPARISON OF CALCULATIONS AND TEST RESULTS.

LOADING	PANEL TYPE	P_u test k. fail. side		$\frac{a}{h}$		$P_{u a_{eff}}$ k.		$P_{u a_i}$ k.		$P_{u ACI}$ k.		$f_{y ACI}$ ksi		P_u test avg.
		LHS	RHS	LHS	RHS	LHS	RHS	LHS	RHS	LHS	RHS	LHS	RHS	
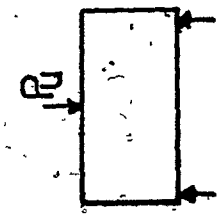	168-5-2	42		1.23	1.23	46.3	46.3	29.6	29.6	80.3	80.3	50.5	50.5	47.5
	168-5-3	53												
	168-6-2	60		1.3	1.3	79.3	79.3	54.4	54.4	71.9	71.9	18.4	18.4	57.5
	168-6-3		55											
	168-7-1		95	1.46	1.46	169	169	88.5	88.5	80	80	12.1	12.1	102.5
	168-7-2	110												
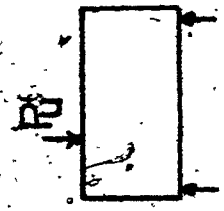	168-8-1	60		0.92	1.67	66.7	62.2	45.4	32.9	60	103.7	22.1	60	63.8
	168-8-2	67.5												
	168-9-1		63	1.0	1.75	138.1	99.7	86.9	73.4	59.7	129.2	9.6	42	75
	168-9-3		87											
	168-10-1		60	0.92	1.67	64.8	68	45.5	42.2	56.4	101.2	19.6	60	59
	168-10-2		58											
	168-11-1		90	1.0	1.75	138.9	103.5	100.5	73.9	58.6	126.9	9.3	45.7	87.5
	168-11-2	85												

to our proposed methods, with the values recorded from tests.

The comparison of P_u values shows that applying our formula (2.15) when considering the web reinforcement within a_{eff} would tend to overestimate the ultimate load-carrying capacity of the panels.

The ultimate capacity values P_u obtained from our formula (2.15) when considering the web reinforcement within a_i, were generally less than P_u test values, i.e., the ultimate load-carrying capacity was underestimated.

The comparison of P_u values estimated according to ACI-318-71 practice with the test values of P_u, showed no single trend, but overestimation, in some cases, and underestimation in others.

It should be noted also, that ACI equation (5.3) gives very low tensile stresses in the web reinforcement, as compared to actual yield observed during the tests. The proposed design formulas herein, assume a reach of yield in the web reinforcement.

Table 5.6 gives strength values averaged for each similar a_2/h ratio, i.e., the ratio of the length-to-height of the diagonal splitting support-segment. This table includes only the results from the support-segments in which failure had occurred.

TABLE 5.6 - COMPARISON OF P_u(test)/P_u(calculated) VALUES

$\frac{a_2}{h}$	P_u (test) kips.	P_u (a_{eff}) kips.	P_u (a_i) kips	P_u (ACI) kips.	$\frac{P_u(test)}{P_u(a_{eff})}$	$\frac{P_u(test)}{P_u(a_i)}$	$\frac{P_u(test)}{P_u(ACI)}$
0.92	63.8	66.8	45.4	60	0.96	1.40	1.06
1.00	85	138.9	100.5	58.6	0.61	0.85	1.45
1.23	47.5	46.3	29.6	80.3	1.03	1.60	0.59
1.30	57.5	79.4	54.4	71.9	0.72	1.06	0.80
1.46	102.5	169	88.5	80	0.61	1.16	1.28
1.67	59	68	42.2	101.2	0.87	1.40	0.58
1.75	80	101	73.5	128.4	0.79	1.08	0.62

Comparing the results, we can now derive the following important conclusions:

1) Until now, we do not have an adequate theory defining the ultimate strength of a deep beam under high shear, and also, describing the ultimate splitting strength in the vicinity of support. Available theories do not correspond to real behaviour and test results.

2) ACI-318-71 Equations for deep beams, with all the factors of safety incorporated therein, give results which do not always compare with tests and do not describe sufficiently the ultimate strength of deep beams in the vicinity of support. Those equations provide excessive safety and thus ask for an excessive amount of web reinforcement for a_2/h ratios of 0.90 to 1.15 and 1.40 to 1.55. For a_2/h ratios of 1.15 to 1.40 and of over 1.55, ACI practice leads to dangerous over-estimation of the carrying capacity of the web reinforcement. This situation should be corrected.

3) The diagonal splitting strength can be estimated with sufficient accuracy for design practice, on the basis of the formulas proposed herein, assuming as effective, the web reinforcement only, in the region between the faces of the support pads and the load-bearing pads, i.e., within a_1, Fig. 2.4 . The proposed formula for the

calculation of strength expressed in terms of a shear force is:

$$V_u = V_v + V_h = \cos\alpha \sum_{i=1}^{n} A_{svi} f_{yi} + \sin\alpha \sum_{i=1}^{n} A_{shi} f_{yi} \quad (2.15)$$

This formula describes the ultimate diagonal splitting state in the support-segment (see Fig. (2.4)). It takes into account different cases of a_2/h ratios and provides an adjusted factor of safety and web reinforcement. (A design example is presented in Appendix A).

The horizontal web reinforcement appears to be more effective in carrying the diagonal splitting force.

While columns V_h in Tables 5.2 and 5.3 remain unchanged, the values in columns V_v change according to the region within which the vertical web reinforcement was considered to be effective.

The above method of design does not apply to beams carrying a uniform load.

However, we feel that it is necessary to stress here, that a limited number of panels were tested. More experiments would be required to check further and solidify

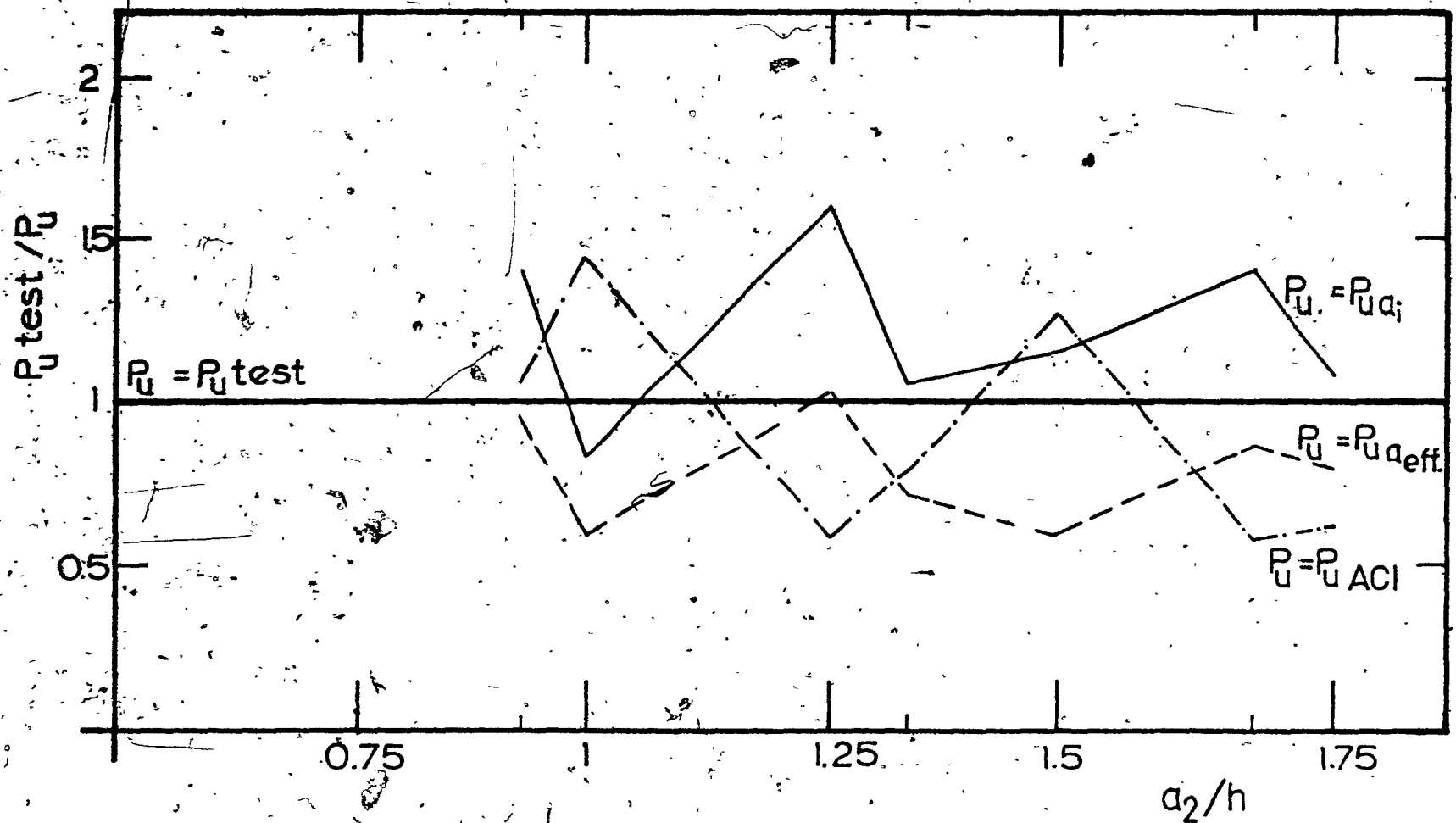

FIG. 5.1 - COMPARISON OF P_u(test)/P_u(calc.) RATIOS.

our findings before making final recommendations for revision of the present ACI practice, which in some cases, appears to be dangerous (Fig. 5.1).

Panels loaded at two points and with different wire meshes having new a_2/h ratios, should be tested. Also, an analysis could be further developed, using the finite elements method. A photoelastic analysis of comparable models would also be required, in order to better define the stress pattern in the inclined splitting support-segment.

REFERENCES

REFERENCES

[1] ACI Committee 318, "Building Code Requirements for Reinforced Concrete (ACI-318-71)", American Concrete Institute, Detroit, 1972.

[2] Bresler, B., and Scordelis, A.C., "Shear Strength of Reinforced Concrete Beams", University of California, Berkeley, 1961.

[3] Ferguson, P.M., "Reinforced Concrete Fundamentals", John Wiley and Sons, Inc., 2nd Edition, 1965.

[4] Proceedings of the International Symposium on Low Cost Housing Problems Related to Urban Renewal and Development. University of Missouri, Rolla, 1964.

[5] Zielinski, Z.A., "Research on Ultimate Strength in Shear of Bonded and Unbonded Reinforced Concrete Beams", International Symposium on Shear, Torsion and Bond in Reinforced and Prestressed Concrete, P.S.G. College of Technology, Coimbatore, India, January, 1969.

[6] Zielinski, Z.A., "Behaviour and Ultimate Strength of Rectangular Reinforced Concrete Beams in Bending and High Shear", North Carolina State University, Bulletin No. 81, 1967.

[7] Zielinski, Z.A., "A New Approach to Ultimate Strength of Reinforced Concrete Beams in Inclined Cracking and Reduction of Web Reinforcement in Bridge Girders", Second International Symposium Concrete Bridge Design, ACI Publication SP.26, pp.411-456, 1971.

[8] Short, D.R., Kong, F.K., Robins, P.J., and Kirby, D.P., "Deep Beams With Inclined Web Reinforcement", J. American Concrete Institute, Vol. 69-16, March, 1972, pp.172-176.

[9] Winter, G., Urquhart, L.C., O'Rourke, C.E., and Nilson, A.H., "Design of Concrete Structures", McGraw-Hill Book Co., 7th Edition, 1964.

[10] ACI-ASCE Committee 326, Report, "Shear and Diagonal Tension", J. American Concrete Institute, Nos. 1,2,3. January, February and March, 1962.

APPENDIX A

DESIGN EXAMPLE

APPENDIX A

DESIGN EXAMPLE

A design example, using the data for Panel 168-9 is presented herein.

The three approaches discussed in this thesis are used. They are:

1) Applying our formula (2.15) and considering the web reinforcement within a_{eff} as effective.

2) Applying our formula (2.15) and considering the web reinforcement within a_i as effective.

3) Applying Section (11.9) of ACI-318-71.

Panel 168-9 (Figure in Appendix B), bearing plates 10" long, were used at the support, and 24" long under the load.

A1.1 SOLUTION NO. 1

Considering the RHS support-segment (failure side) and the web reinforcement within a_{eff} (see Table 5.2):

a_{eff} = 58.5 in (fig.2.4)

cosα = 0.867

sinα = 0.495

as obtained from the geometry of Fig. 2.4 by substituting the dimensions of the support-load segment.

From Table 3.3:

f_y for 6/6 wire mesh = 72.9 ksi

f_y for #3 rebar = 55.2 ksi

f_y for #4 rebar = 48.1 ksi

$$V_v = \cos\alpha \sum_{i=1}^{n} A_{svi} f_{yi} \qquad \text{(formula 2.13)}$$

where

A_{sv} = 5 wire gage No. 6 + 1 #4 rebars

V_v = 0.867 [0.145 x 72.9 + 0.2 x 48.1] = 17.5 kips

$$V_h = \sin\alpha \sum_{i=1}^{n} A_{shi} f_{yi} \qquad \text{(formula 2.14)}$$

where

A_{sh} = 6 wire gage No. 6 + 1 #3 + 1 #4 rebars and neglecting the tensile flexural reinforcement.

V_h = 0.495[0.174 x 72.9 + 0.11 x 55.2 + 0.2 x 48.1] = 14.1 kips

$V_u = V_v + V_h$ = 17.5 + 14.1 = 31.6 kips (formula 2.15)

which can be produced by a concentrated load P_u, applied at $\frac{1}{3}$ span, of $\frac{31+67}{31} \times 31.6 = 99.7$ kips.

A1.2 SOLUTION NO. 2

Considering the RHS support-segment (failure side) and the web reinforcement within a_i (Table 5.3):

$a_i = 50$ in (figure 2.4)

$\cos\alpha = 0.867$

$\sin\alpha = 0.495$

From Table 3.3:

f_y for 6/6 wire mesh = 72.9 ksi

f_y for #3 rebar = 55.2 ksi

f_y for #4 rebar = 48.1 ksi

$$V_v = \cos\alpha \sum_{i=1}^{n} A_{svi} f_{yi} \quad \text{(formula 2.13)}$$

where

A_{sv} = 5 wire gage No. 6

$V_v = 0.867[0.145 \times 72.9] = 9.2$ kips

$$V_h = \sin\alpha \sum_{i=1}^{n} A_{shi} f_{yi} \quad \text{(formula 2.14)}$$

where

A_{sh} = 6 wire gage No. 6 + 1 #3 + 1 #4 rebars and neglecting the tensile flexural reinforcement.

$V_h = 0.495[0.174 \times 72.9 + 0.11 \times 55.2 + 0.2 \times 48.1] =$

$= 14.1$ kips

$V_u = V_v + V_h = 9.2 + 14.1 = 23.3$ kips (formula 2.15)

P_u @ $\frac{1}{3}$ span $= \frac{31+67}{31} \times 23.3 = 73.4$ kips

Solution No. 2, is the design approach which we are recommending.

A1.3 SOLUTION NO. 3

Considering the same support-segment and applying Section (11.9) of ACI-318-71 (Table 5.4):

$a = 67$ in (Fig. 2.4)

$b_w = 1.5$ in

$d = 47$ in

$f'_c = 5260$ psi

$\sqrt{f'_c} = 72.5$ psi

$A_s = 1$ #8 + 1 #5 rebars

To apply formula (5.1) i.e. ACI Equation (11.22):

$$\rho_w = \frac{A_s}{b_w d} = \frac{.79+.31}{1.5 \times 47} = 0.0156$$

$$\frac{a}{2d} = \frac{67}{2 \times 47} = 0.713$$

The term = $3.5 - (2.5\frac{a}{2d}) = 1.72 < 2.5$

$$v_c = 1.72[1.9\sqrt{f'_c} + 2500\,\rho_w\,\frac{2d}{a}] \quad \text{(formula 5.1)}$$

$$v_c = 1.72[137.8 + \frac{2500 \times 0.0156}{0.713}] = 331 \text{ psi}$$

$$6\sqrt{f'_c} = 435 \text{ psi} > 331 \text{ psi}$$

Therefore

$$v_c = 331 \text{ psi}$$

Considering the web reinforcement within a, (Fig.2.4):

$$\frac{A_v}{s} = 0.00856$$

$$\frac{A_{vh}}{s_2} = 0.009$$

Applying Formula 5.2, i.e., ACI Equation (11.24):

$$v_u = 331 + 9560(0.00856) + 30400(0.009) = 686.4 \text{ psi}$$

$$8\sqrt{f'_c} = 580 \text{ psi} < 686.4 \text{ psi}$$

Therefore

$$v_u = 580 \text{ psi}$$

$$V_u = v_u\, b_w d = 580 \times 1.5 \times 47 = 40.9 \text{ kips}$$

$$P_u \text{ @ } \tfrac{1}{3} \text{ span} = \frac{31+67}{31} \times 40.9 = 129.2 \text{ kips}$$

To find the stress in the web reinforcement as induced by the above computed force V_u = 40.9 kips.

Applying formula (5.3):

$$f_y = \frac{1.5(580-331)}{0.239(0.00856)+0.76(0.009)} = 42{,}020 \text{ psi}$$

which is less than 60,000 psi.

APPENDIX B

DETAILED DRAWINGS OF TEST PANELS

APPENDIX B

DETAILED DRAWINGS OF TEST PANELS

The detailed drawings of the tested panels are presented herein.

For the loading condition of each panel type, see Table 3.1.

The hardboard bearing pads used at the supports were 4 in x 10 in for all panel types.

The hardboard bearing pads used under the load were 4 inches wide and their length varied for each panel type, according to its load capacity. These lengths are shown in the respective figures in Appendix C.

Panels 168-10 and 168-11 had two identical intermediate ribs 6 inches deep, located at 1/6 and 5/6 of the span.

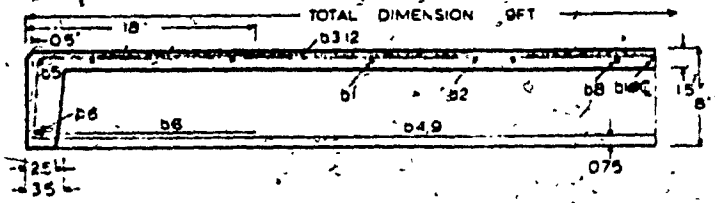

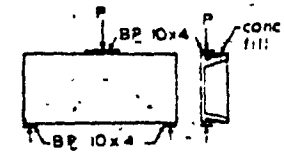

LOADING ARRANGEMENT

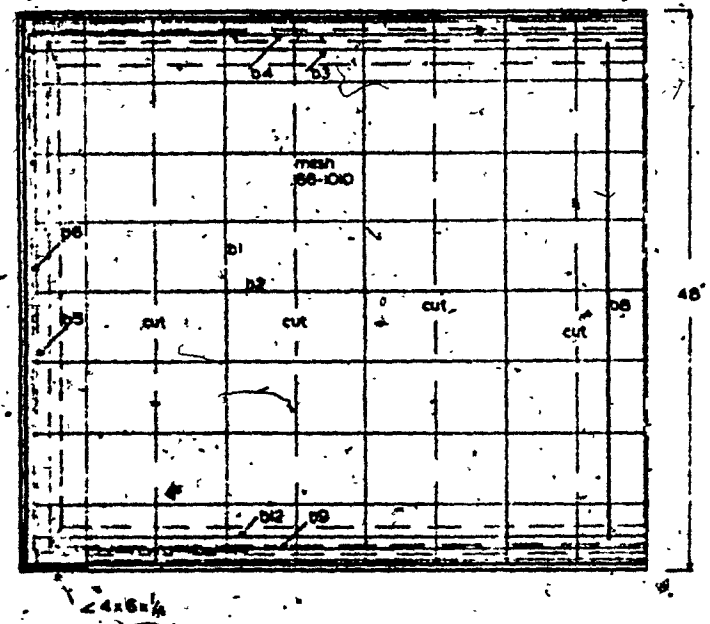

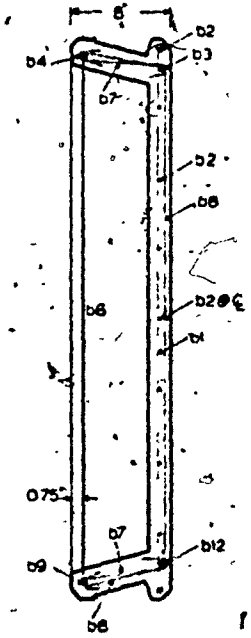

REINFORCEMENT TYPE 188-5

BAR No.	TYPE & SIZE OF BARS	No. OF BARS	LENGTH OF BAR in	F_y ksi
b1	mesh 66-1010	17	18.25	
b2		2	12.25	
b3	#2	1	12.25	40
b4	#3	1	11.25	40
b5	#2	2	46.25	40
b6	#2	2	82.25	40
b7	#2	38	10.75	40
b8	#4	2	65.25	40
b9	#5	1	108	40
b12	#5	1	108	40

USE CONCRETE f'_c = 4000# PSI

WEIGHT OF PANEL = 500 LBS

UCOPAN PANELS		
REINFORCEMENT DETAILING		
DR Z A ZIELINSKI		
ALFRED ABDULEZER		
SCALE 1" = 1'	9th DEC '71	188-5

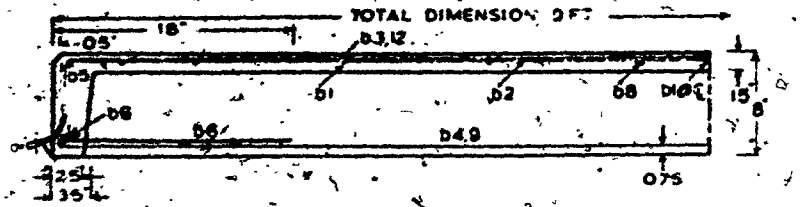

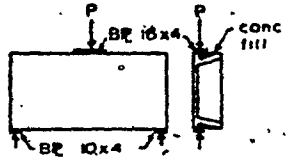

LOADING ARRANGEMENT

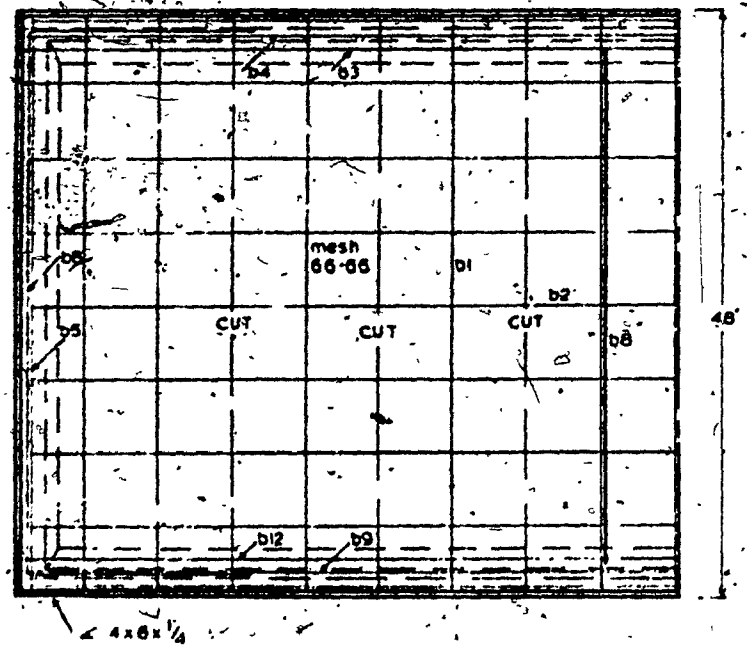

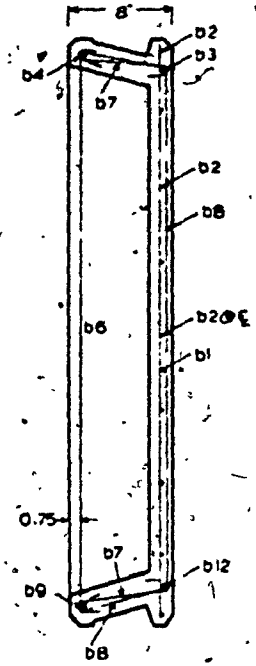

REINFORCEMENT - TYPE 188 - 6				
BAR №	TYPE & SIZE OF BARS	№ OF BARS	LENGTH OF BAR, in	F_y KSI
b1	mesh 66-66	17 cross	48.25	-
b2		9	122.5	-
b3	◆3	1	122.5	40
b4	◆4	1	119.5	40
b5	◆2	2	48.25	40
b6	◆2	2	82.25	40
b7	◆2	38	30.75	40
b8	◆5	2	65.25	40
b9	◆6	1	108	60
b12	◆6	1	108	60

USE CONCRETE f'c 4000 PSI

WEIGHT OF PANEL = 1500 LBS

UCOPAN PANELS		
REINFORCEMENT DETAILING		
DR Z A ZIELINSKI		
ALFRED ABDULEZER		
SCALE 1:6	12th DEC 1971	188 - 6

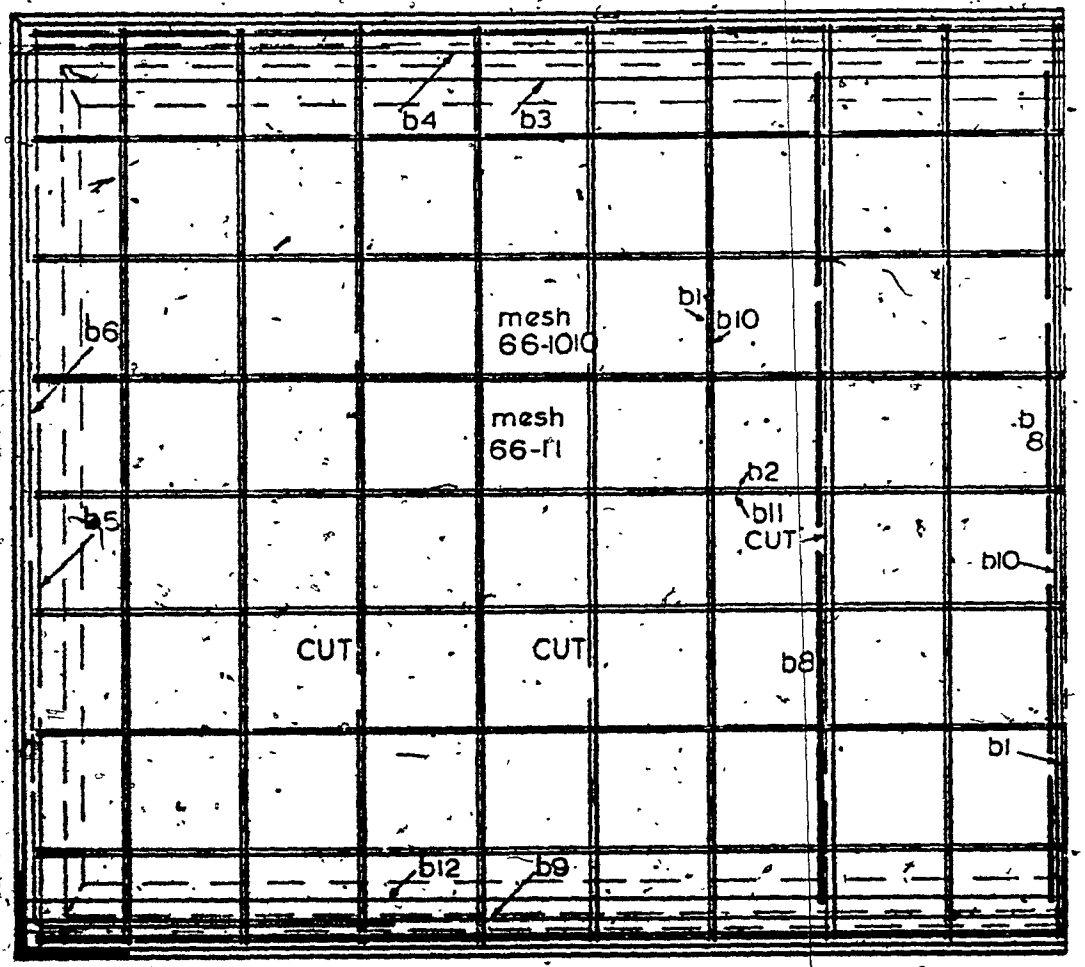

BAR Nº	TYPE & SIZE OF BARS	Nº OF BARS	LENGTH OF BAR, in	F_y ksi.
b1	mesh 66-66	17 CUT	46.25	
b2		9	122.5	
b3	#3	1	122.5	40
b4	#4	1	119.5	40
b5	#2	2	46.25	40
b6	#2	2	82.25	40
b7	#2	38	10.75	40
b8	#8	3	65.25	60
b9	#9	1	108	60
b10	mesh 66-66	17	46.25	
b11		9	122.5	
b12	#9	1	108	60

CUT - WHOLE WIRE TO BE CUT OFF

168 - 7

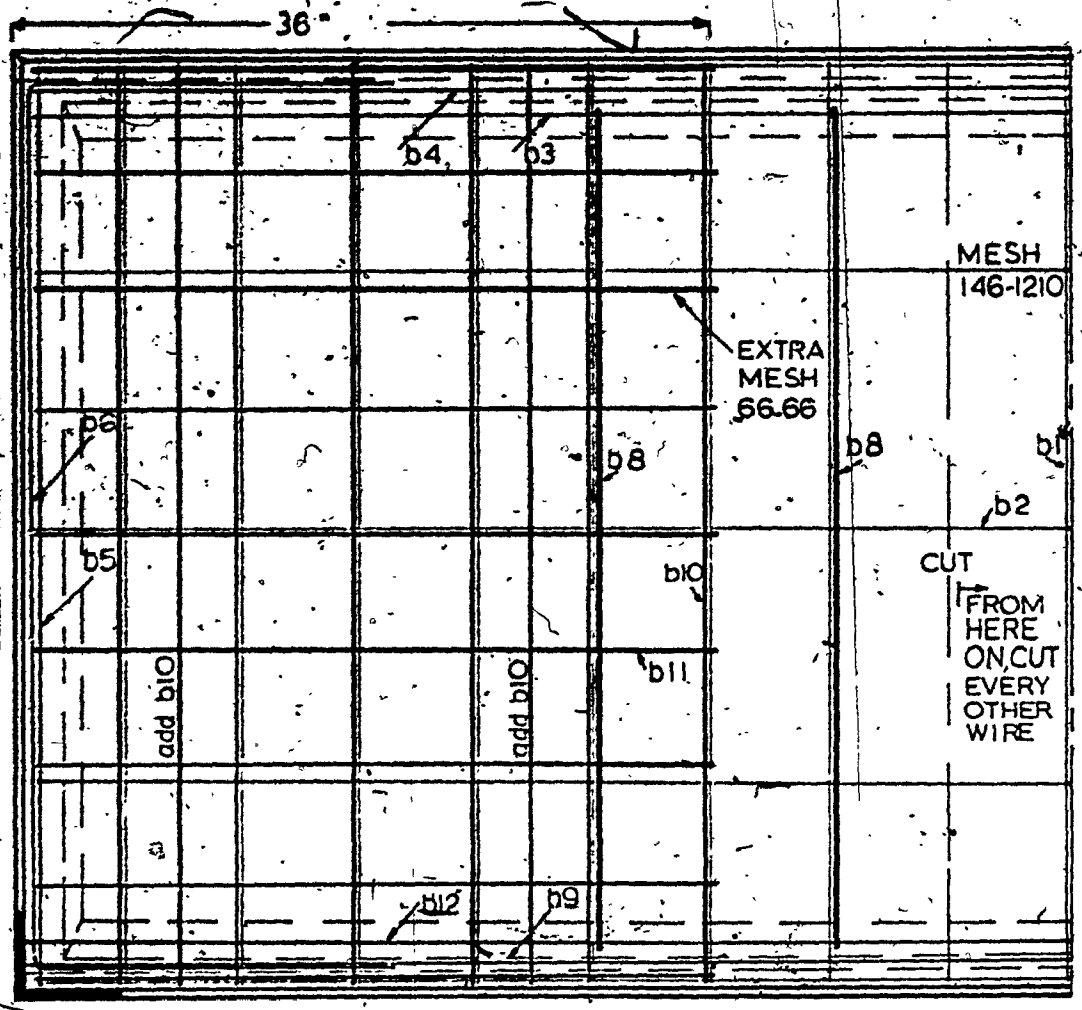

CUT- WHOLE WIRE TO BE CUT OFF

BAR Nº	TYPE & SIZE OF BARS	Nº OF BARS	LENGTH OF BAR, in.	F_y ksi.
b1	mesh 146-1210	17 cut 5	46.25	
b2		5	122.5	
b3	#2	1	122.5	40
b4	#3	1	119.5	40
b5	#2	2	46.25	40
b6	#2	2	82.25	40
b7	#2		10.75	40
b8	#4	2	65.25	40
b9	#5	1	108	60
b10	mesh 66-66	6 add 2	134	
b11		9	35.5	
b12	#5	1	108	60

168 - 8

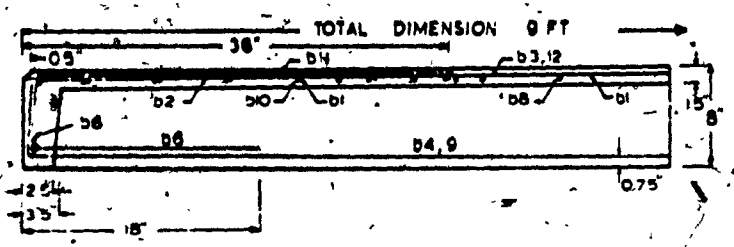

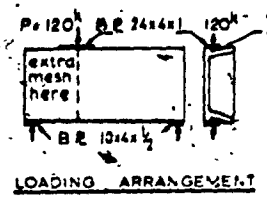

LOADING ARRANGEMENT

EXTRA MESH LEFT HAND SIDE ONLY

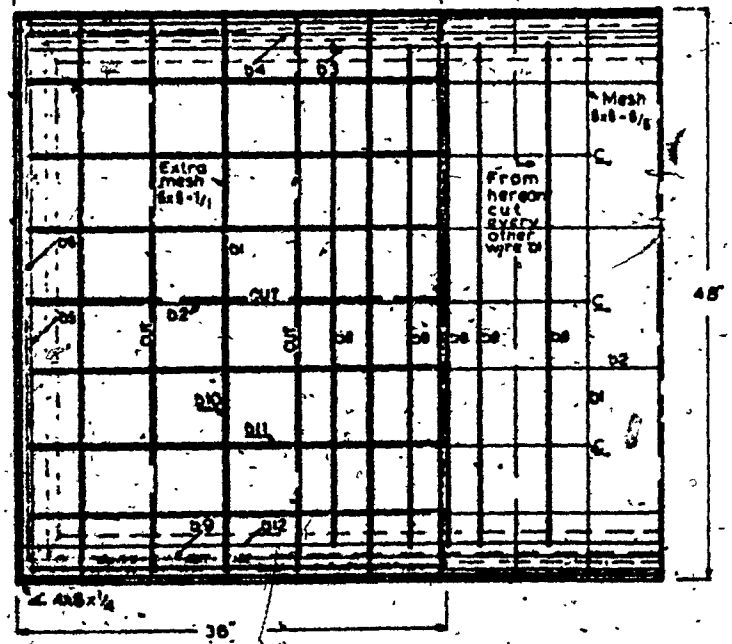

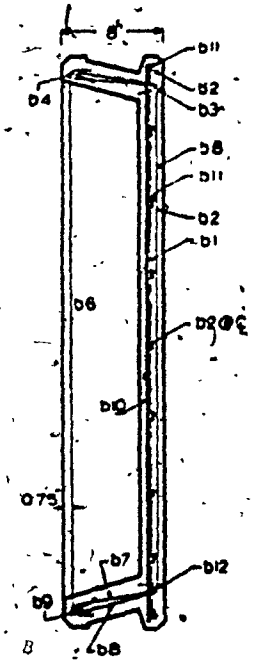

REINFORCEMENT TYPE 168-9				
BAR No	TYPE & SIZE OF BARS	NO OF BARS	LENGTH OF BAR, in	F_y ksi
b1	MESH 6x6-5/5	17 cut 5	48.25	
b2		9 cut 3	122.5	
b3	#3	1	122.5	40
b4	#4	1	119.5	40
b5	#2	2	48.25	40
b6	#2	2	82.25	40
b7	#2	38	10.75	40
b8	#4	5	65.25	40
b9	#6	4	108	60
b10	EXTRA MESH 6x6-1/1	8 cut 2	134	
b11		9 cut 1	35.5	
b12	#6	4	108	40

USE CONCRETE f'_c = 3000 PSI

WEIGHT OF PANEL = 1500 LBS

CUT - where wire to be cut off

C - Cut off remaining wire

UCOPAN PANELS		
REINFORCEMENT DETAILING		
DR Z. A ZIELINSKI		
ALFRED ABDULEZER		
SCALE 1 6	17th DEC. 1971	168-9

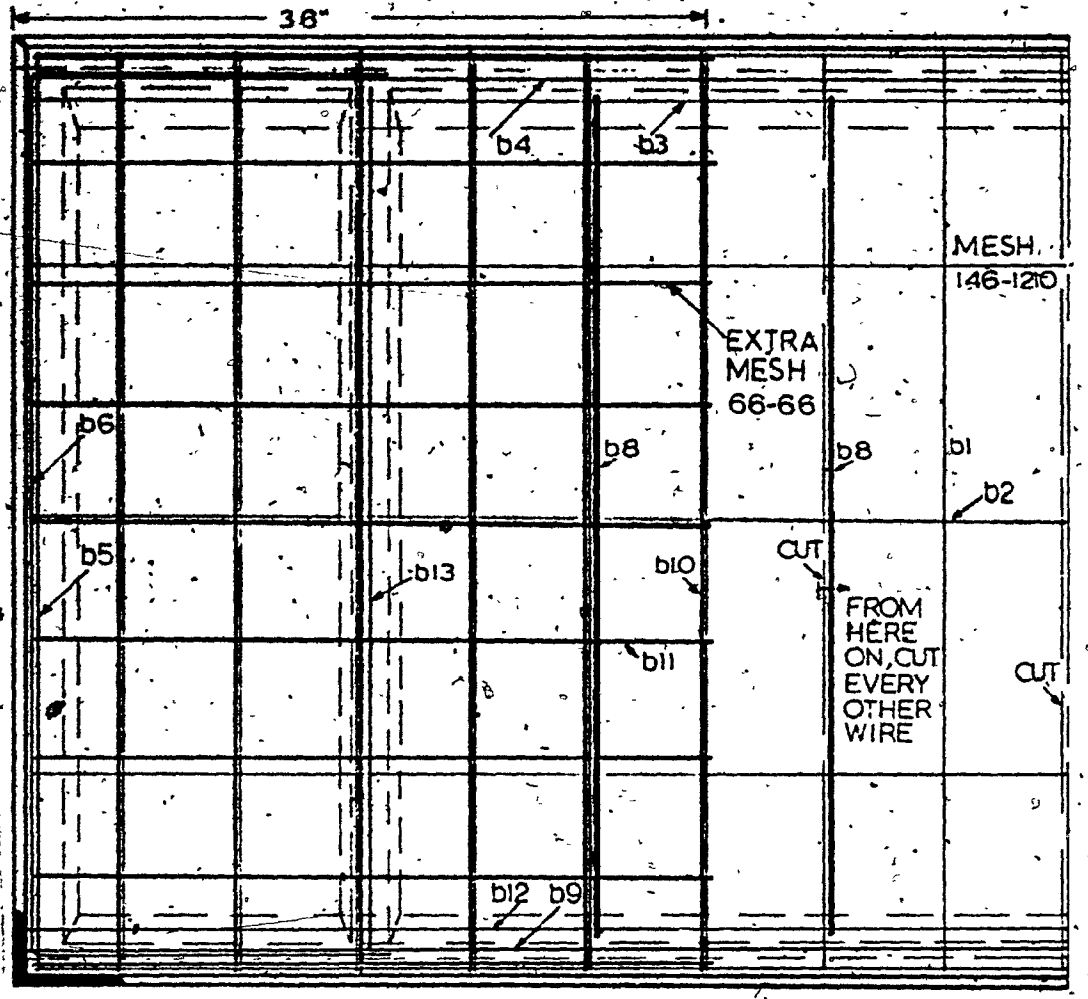

BAR Nº	TYPE & SIZE OF BARS	Nº OF BARS	LENGTH OF BAR, in.	F_y ksi.
b1	mesh 146 - 1210	17 cut 6	46.25	
b2		5	122.5	
b3	#2	1	122.5	40
b4	#3	1	119.5	40
b5	#2	2	46.25	40
b6	#2	2	82.25	40
b7	#2		10.75	40
b8	#4	2	65.25	40
b9	#5	1	108	60
b10	mesh 66-66	6	134	
b11		9	35.5	
b12	#5	1	108	60
b13	#2	2	56.75	40

CUT - WHOLE WIRE TO BE CUT OFF

168 - 10

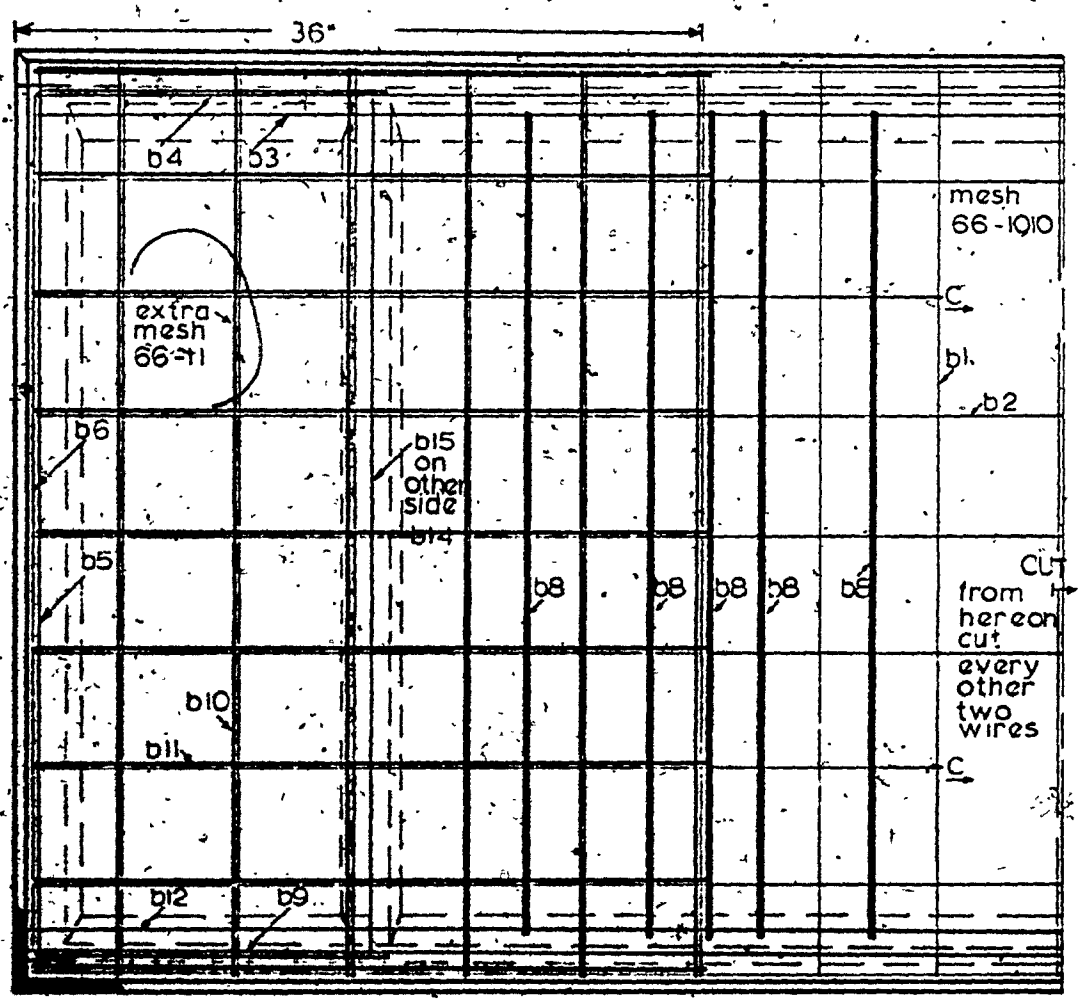

BAR Nº	TYPE & SIZE OF BARS	Nº OF BARS	LENGTH OF BAR, in.	F_y ksi.
b1	mesh 66-1010	17	46.25	
b2		9	122.5	
b3	#3	1	122.5	40
b4	#4	1	119.5	40
b5	#2	2	46.25	40
b6	#2	2	82.25	40
b7	#2		10.75	40
b8	#4	5	6525	40
b9	#8	1	108	60
b10	mesh 66-11	6	13.4	
b11		9	35.5	
b12	#5	1	108	60
b_{15}^{14}	#3 rhs rib #4 lhs rib	1	56.75	40

CUT - WHOLE WIRE TO BE CUT OFF.
C - CUT OFF REMAINING WIRE

168-11

APPENDIX C

CRACK PATTERNS

APPENDIX C

CRACK PATTERNS

The crack patterns of the tested panels are presented herein.

The numbers shown on the crack patterns represent the loads in kips, at which the cracks propagated to the points defined.

The letters F, B and S mean, flexural, inclined and diagonal splitting cracks, respectively. (Compare with Figure 2.1).

The bearing pads shown under the load and the supports are 4 inches wide.

Photographs of the cracked panels are also presented in Appendix E.

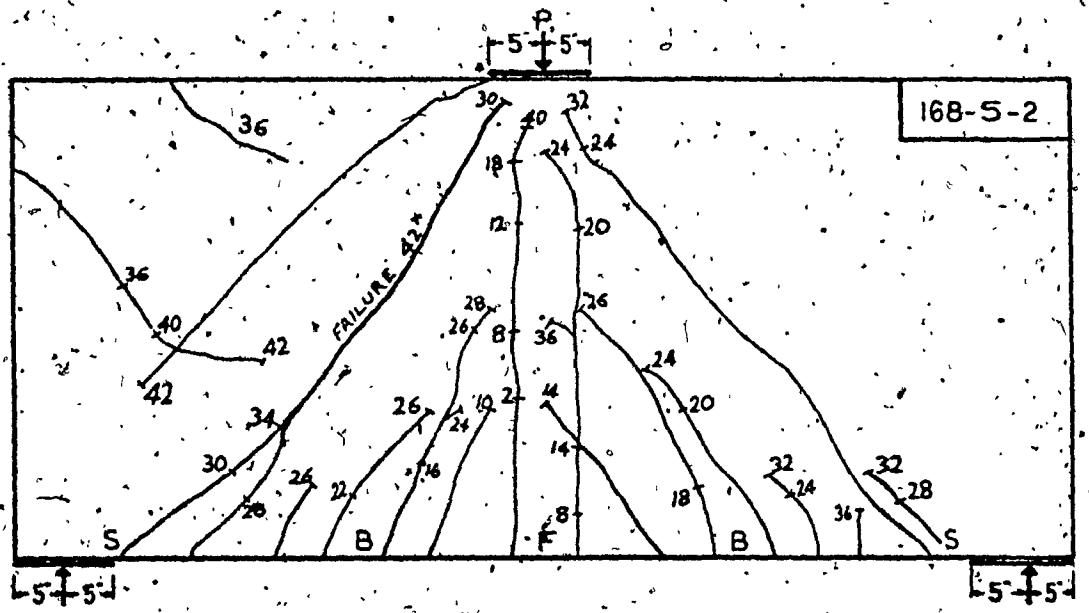
P
5'
5'
168-S-2
36
30
40
32
18
24
24
12
20
FAILURE 42+
36
40
42
42
28
26
8
36
26
24
34
26
10
2
24
44
20
30
24
22
16
14
32
24
32
28
18
36
8
S
B
F
B
S
5'
5'
5'
5'

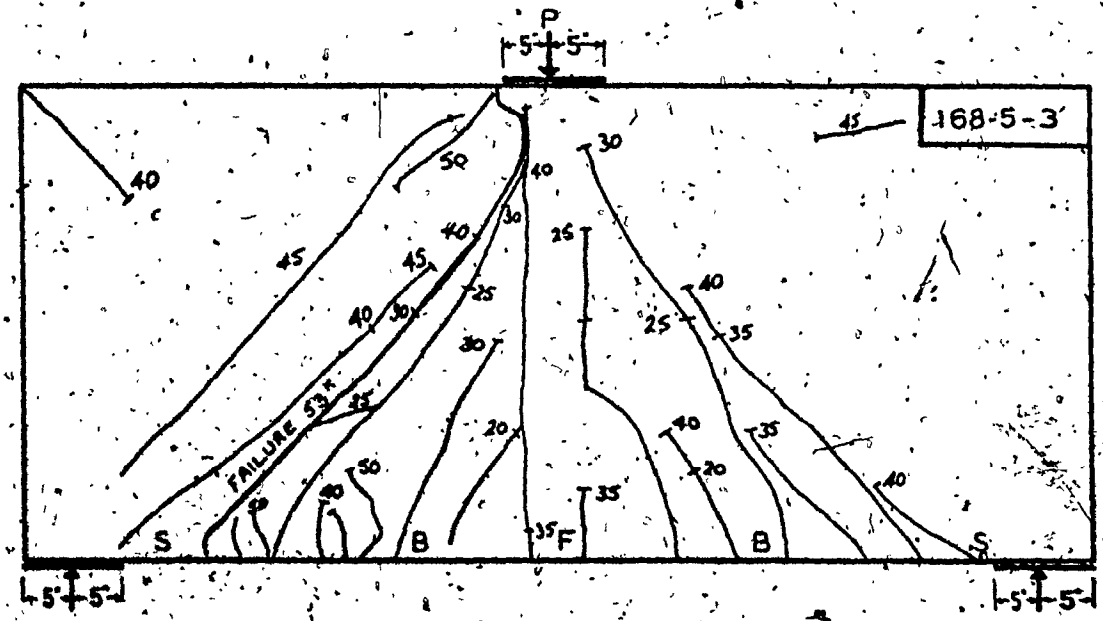
P
5'
5'
168-5-3'
45
40
50
40
30
30
25
45
40
45
25
40
35
40
30
30
FAILURE 53+
20
40
35
20
50
35
40
35
S
B
F
B
S
5'
5'
5'
5'

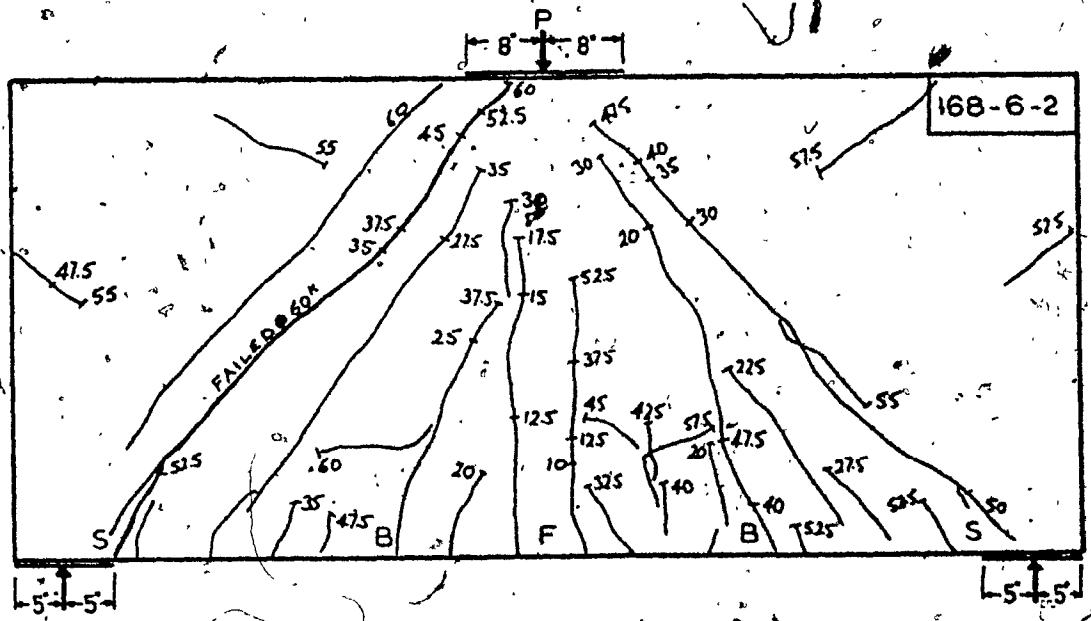
P
8'
8'
168-6-2
FAILED @ 60K
S
B
F
B
S
5'
5'
5'
5'

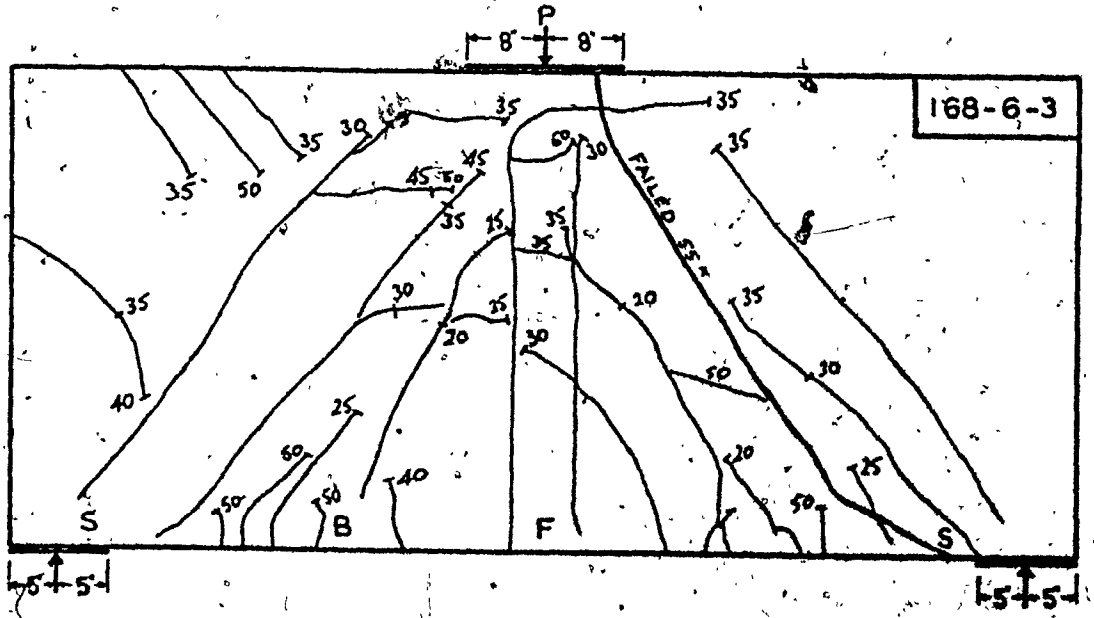
P
8'
8'
168-6-3
FAILED @ 55K
S
B
F
S
5'
5'
5'
5'

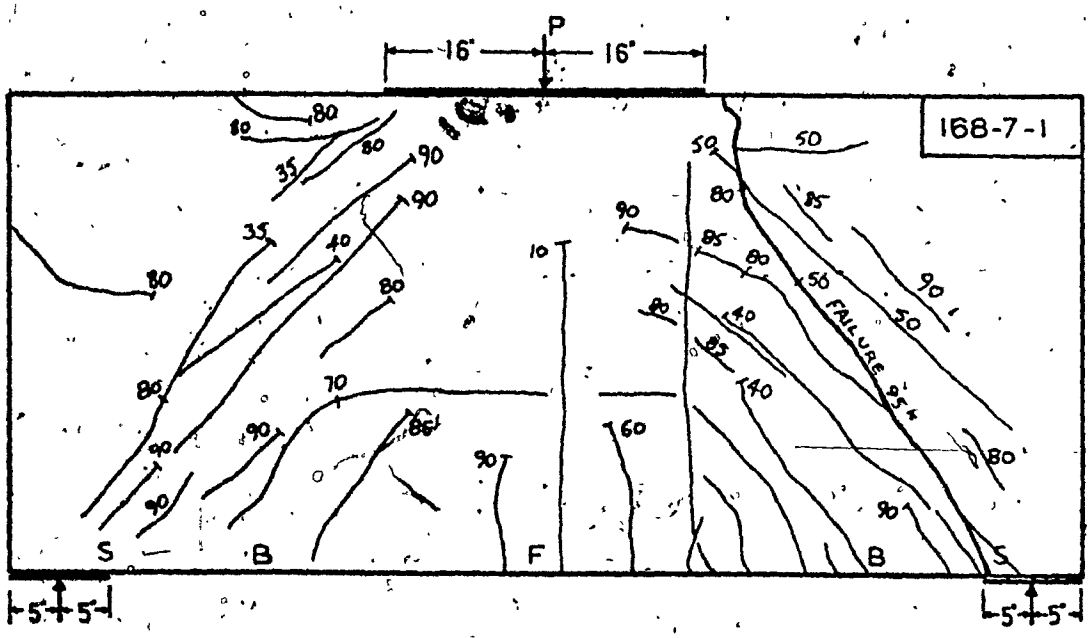
P
16"
16"
168-7-1
S
B
F
B
S
5"
5"
5"
5"
FAILURE 95%

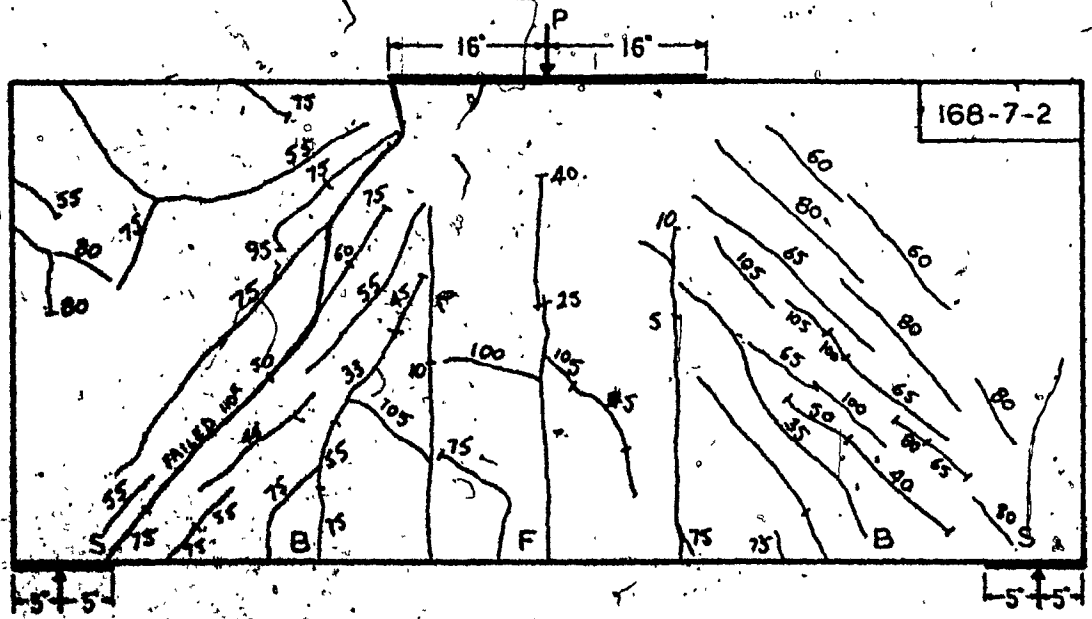
P
16"
16"
168-7-2
FAILED 10%
S
B
F
B
S
5"
5"
5"
5"

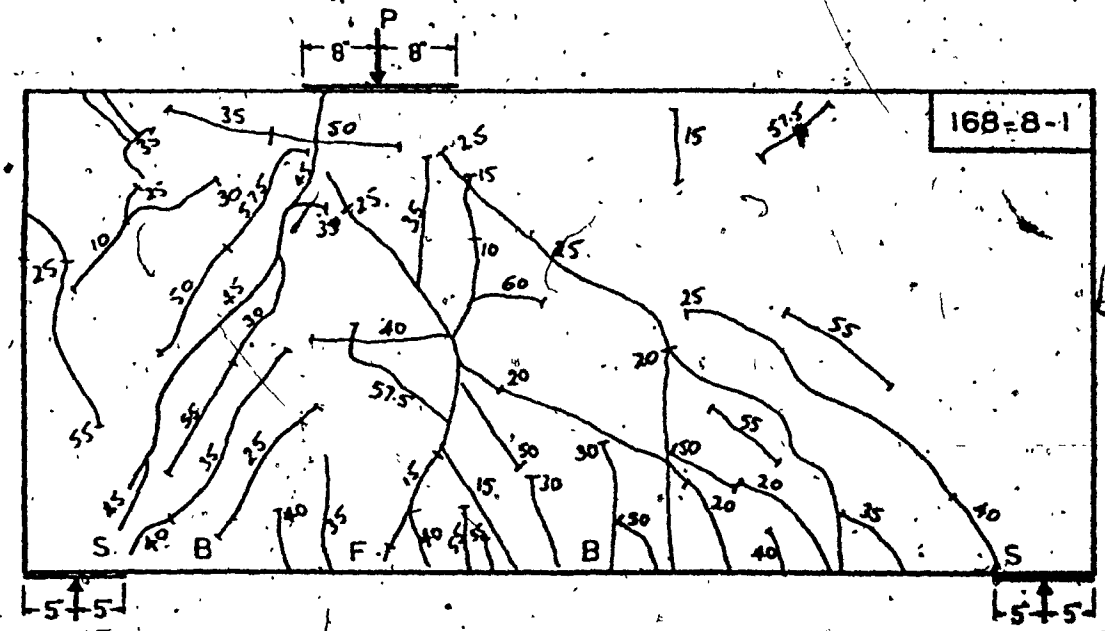
P
8'
8'
168-8-1
S
B
F
B
S
5'
5'
5'
5'

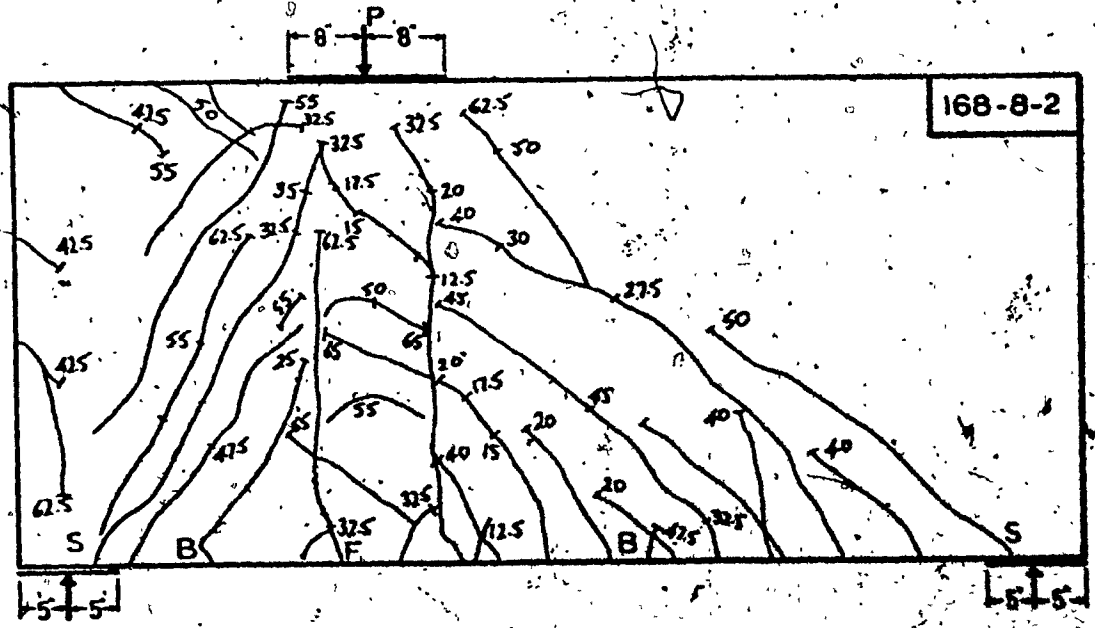
P
8'
8'
168-8-2
S
B
F
B
S
5'
5'
5'
5'

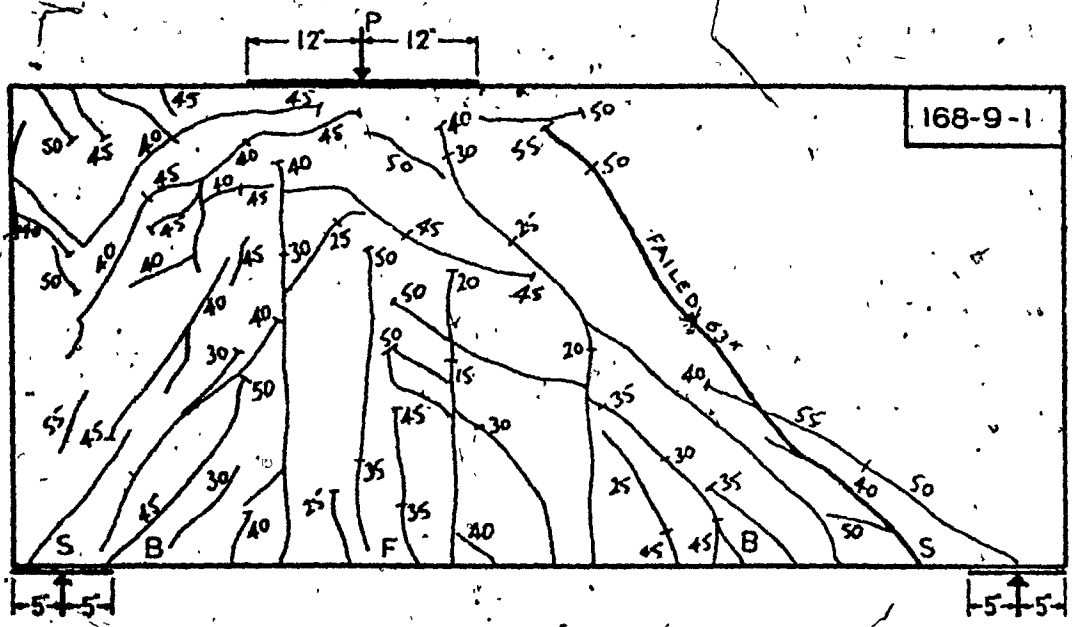
12"
P
12"
168-9-1
FAILED 63%
S
B
F
B
S
5"
5"
5"
5"

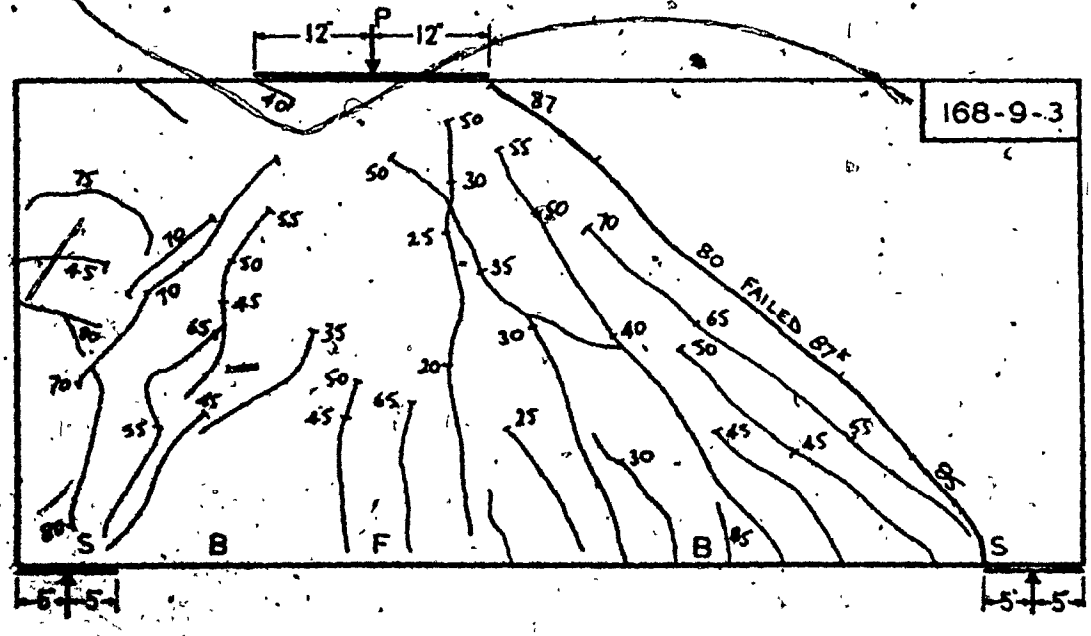
12"
P
12"
168-9-3
80 FAILED 87%
S
B
F
B
S
5"
5"
5"
5"

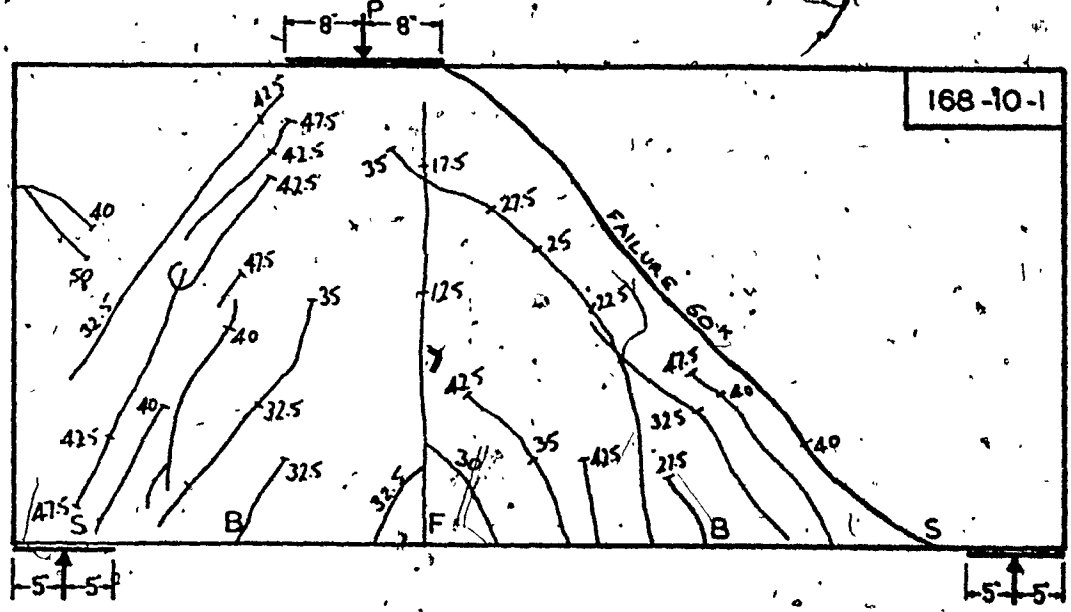
8"
P
8"
168-10-1
42.5
47.5
42.5
42.5
40
SP
32.5
47.5
40
35
42.5
40
32.5
42.5
32.5
47.5
S
B
32.5
F
35
17.5
27.5
25
12.5
22.5
FAILURE BOX
42.5
30
35
42.5
47.5
40
32.5
21.5
40
B
S
5
5
5
5

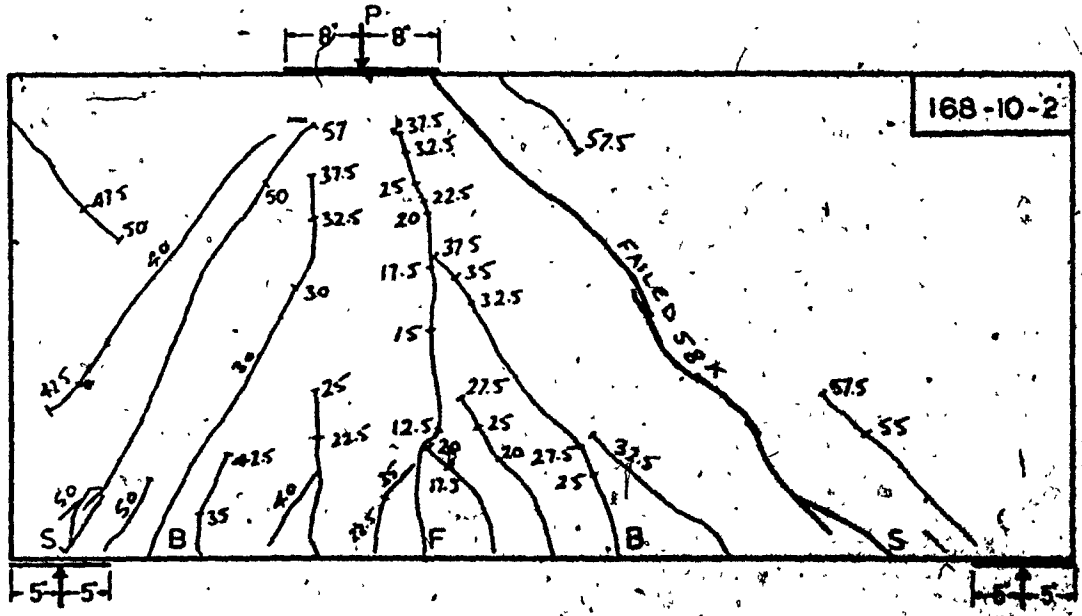
8"
P
8"
168-10-2
57
37.5
32.5
57.5
47.5
50
37.5
50
32.5
40
25
22.5
20
37.5
17.5
35
32.5
30
15
FAILED SBX
42.5
40
25
22.5
12.5
27.5
25
32.5
57.5
55
40
50
42.5
35
40
35
17.5
F
B
S
5
5
5
5

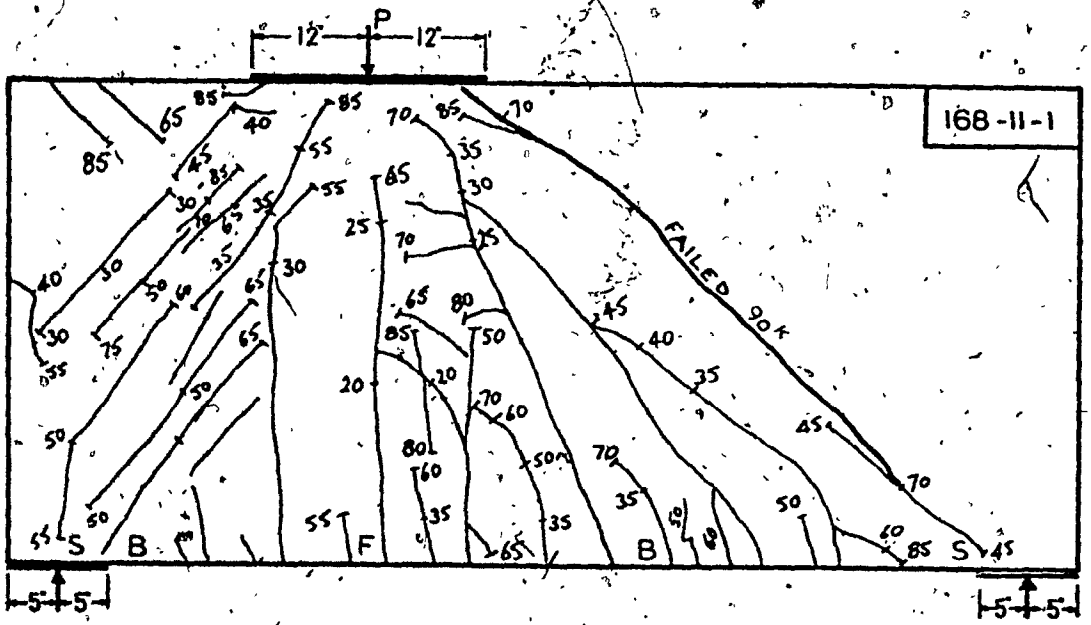
12'
P
12'
168-11-1
FAILED 90K
S
B
F
B
S
5'
5'
5'
5'

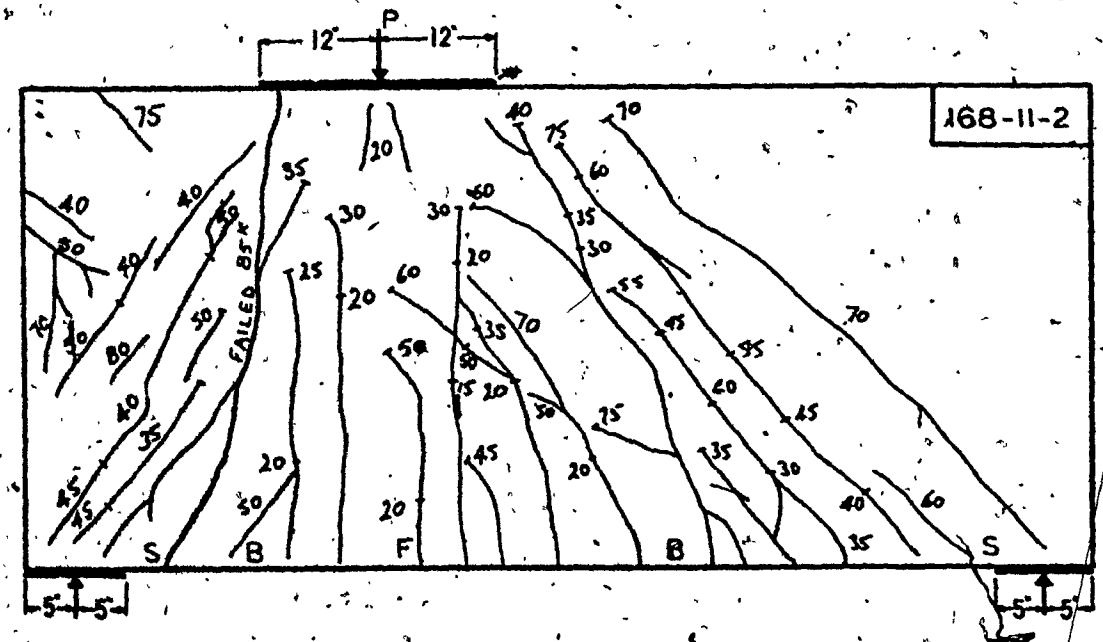
12'
P
12'
168-11-2
FAILED 85K
S
B
F
B
S
5'
5'
5'
5'

APPENDIX D

STRAIN AND DISPLACEMENT DIAGRAMS FOR PANEL 168-9-3

APPENDIX D

STRAIN AND DISPLACEMENT DIAGRAMS FOR PANEL 168-9-3

Considering Panel 168-9-3 as an example, comparison diagrams of tension strains, compression strains and displacements in the horizontal axis are given herein.

The stress-strain diagram of the test-cylinders is given in Figure D.1.

In Figures D.2 and D.3, it is interesting to note the sharp increase of strain, at failure, which occurs at the middle of the tension diagonal (see Figure 3.5(c)).

In Figures D.4 and D.5, note that a parallel sharp increase in strain at the compression diagonals occurs (see Figure 3.4(b)).

Figures D.6 to D.11 show the displacement of the panel in the horizontal axis. Note that the maximum displacements were occurring at the load-line and at the free (unbraced) corner of the panel (see Figure 3.6(b)).

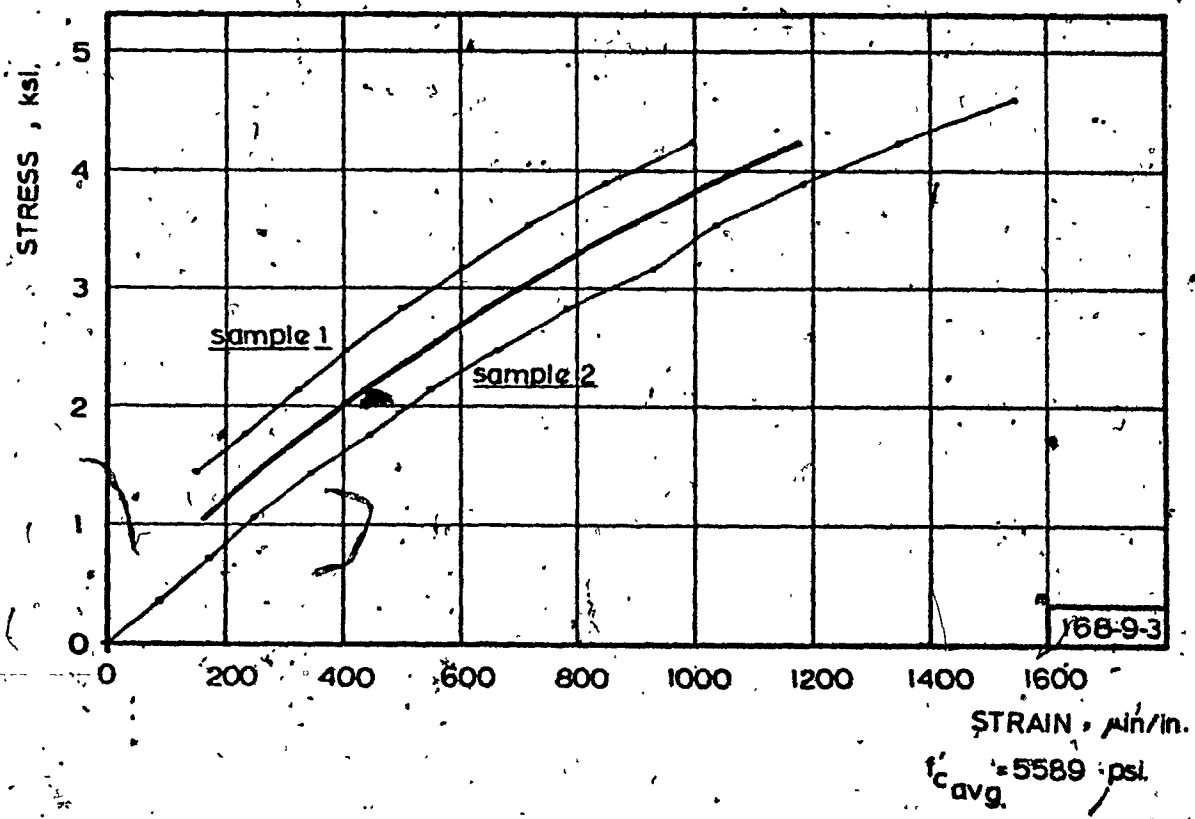

FIG. D.1- CONCRETE STRESS - STRAIN CURVES

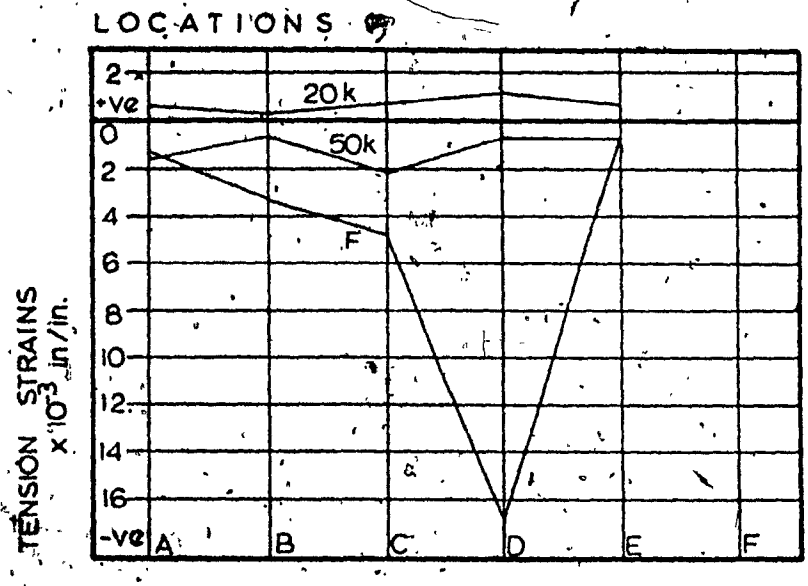

FIG. D2 - COMPARISON OF STRAINS ALONG TENSION DIAGONAL A-F, PANEL 168-9-3.

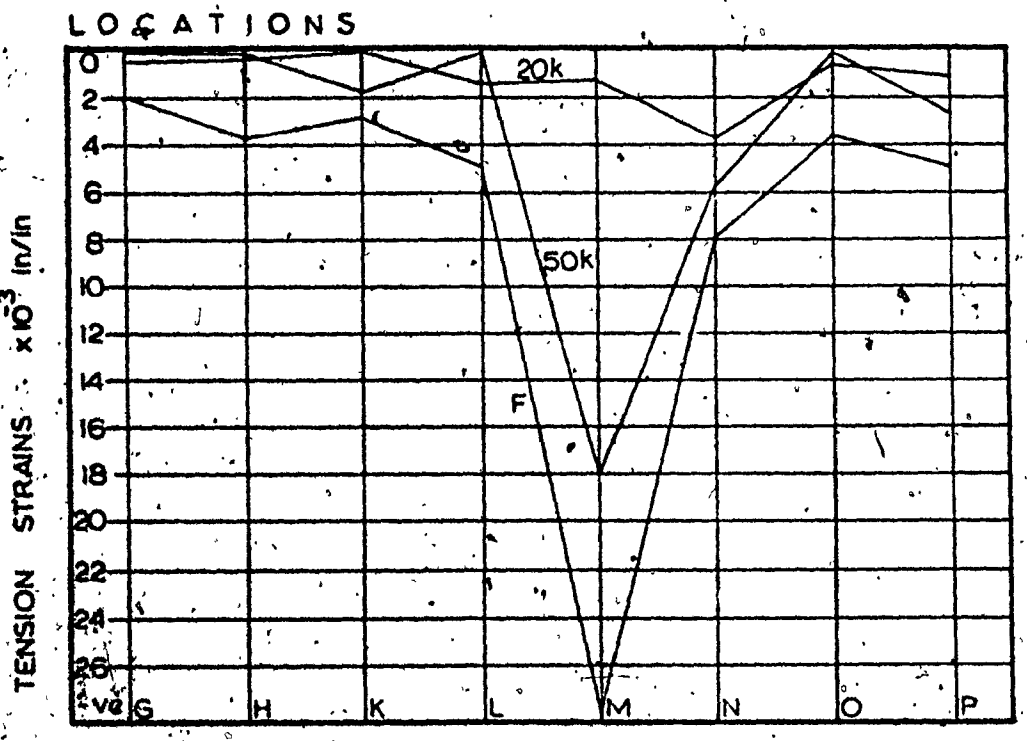

FIG. D3- COMPARISON OF STRAINS ALONG TENSION DIAGONAL G-P PANEL 168-9-3

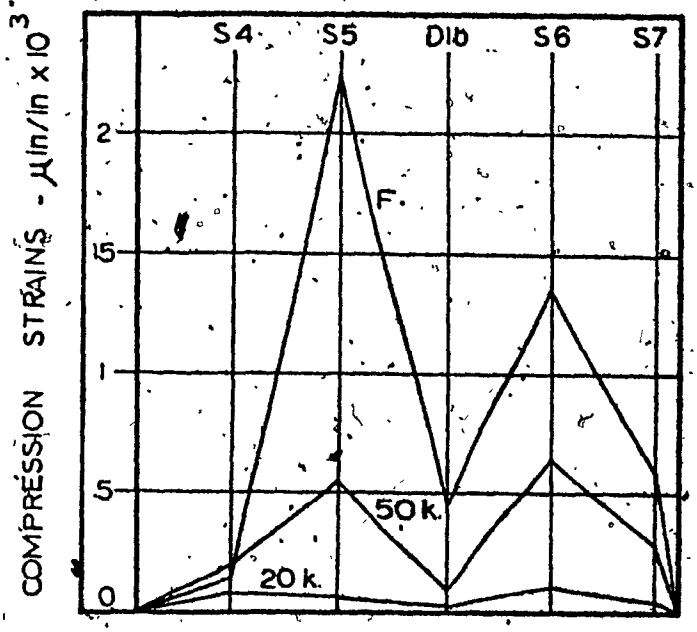

FIG. D.4 - COMPARISON OF STRAINS ALONG DIAGONAL S4 - S7 PANEL 168-9-3

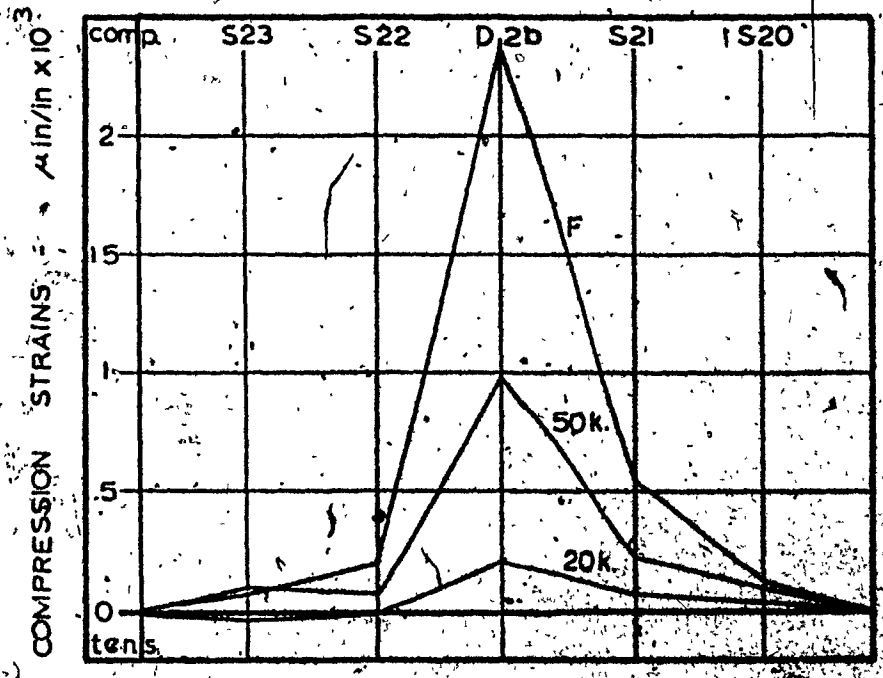

FIG. D5 - COMPARISON OF STRAINS ALONG COMPRESSION DIAGONAL S23 - S20 PANEL - 168 - 9 - 3

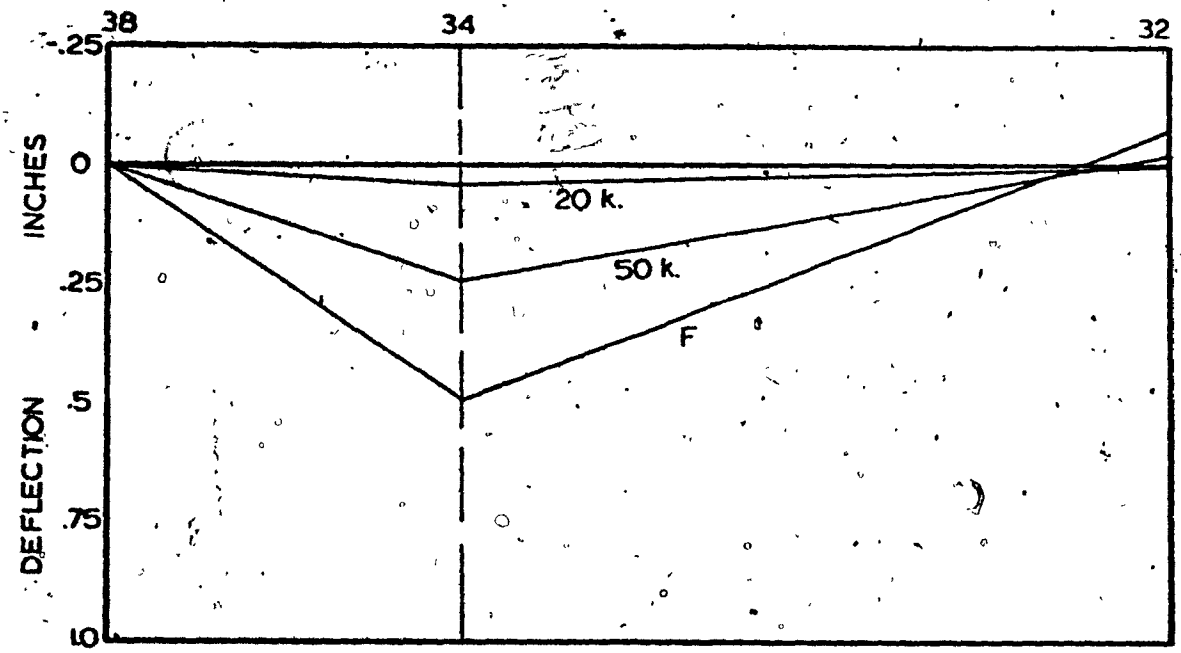

FIG. D.6- LOWER EDGE TWISTING IN X-Z PLANE
EDGE 32 - 38 . PANEL 168-9-3

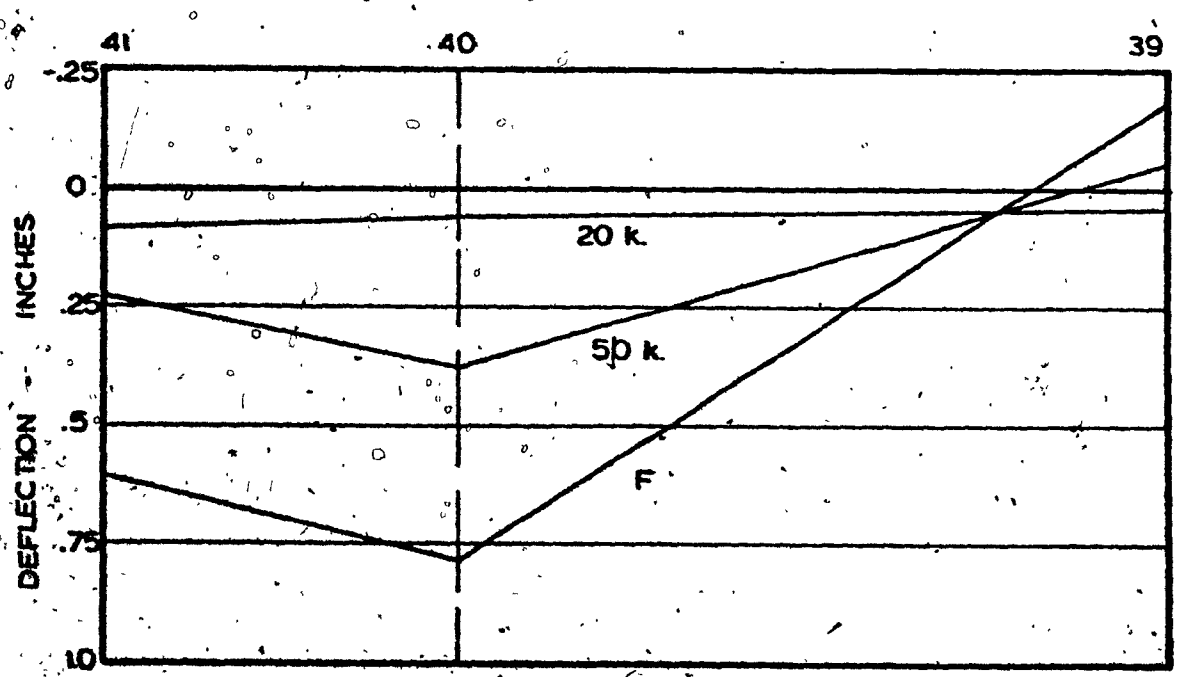

FIG. D.7- MIDDLE TWISTING IN X - Z PLANE
LINE 39 - 41 PANEL 168-9-3

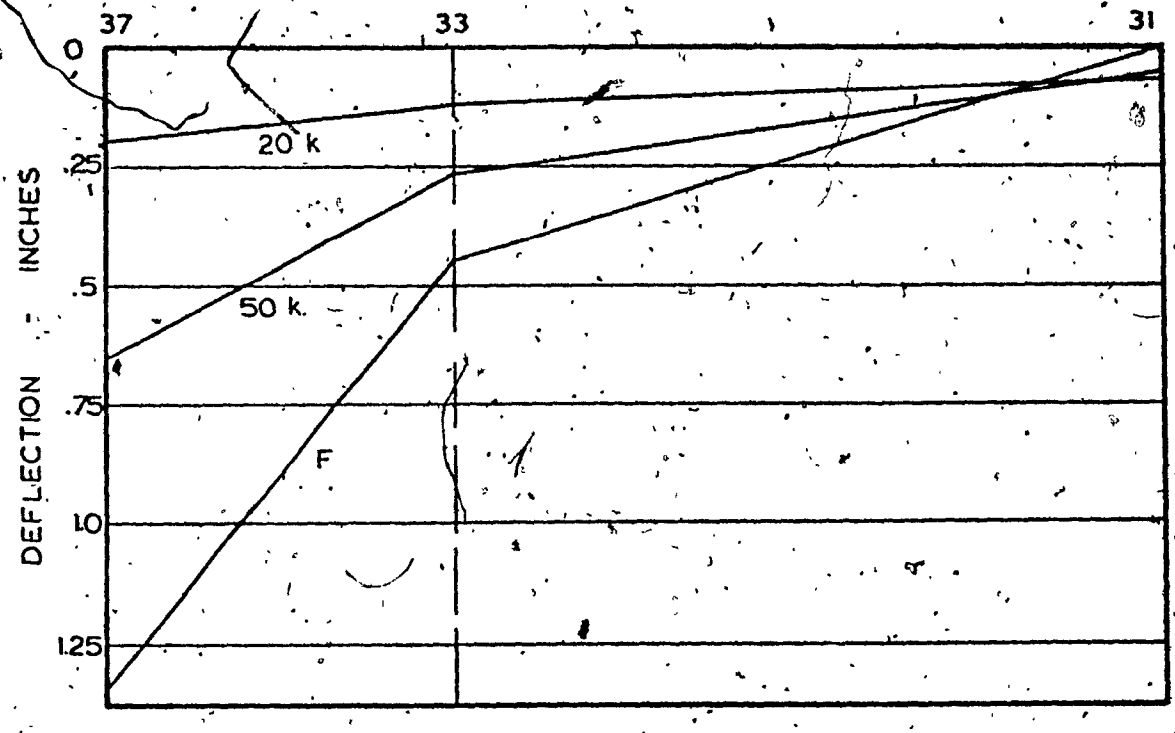

FIG D.8- UPPER EDGE DEFLECTION IN X-Z' PLANE
EDGE 31 - 37 , PANEL 168-9-3

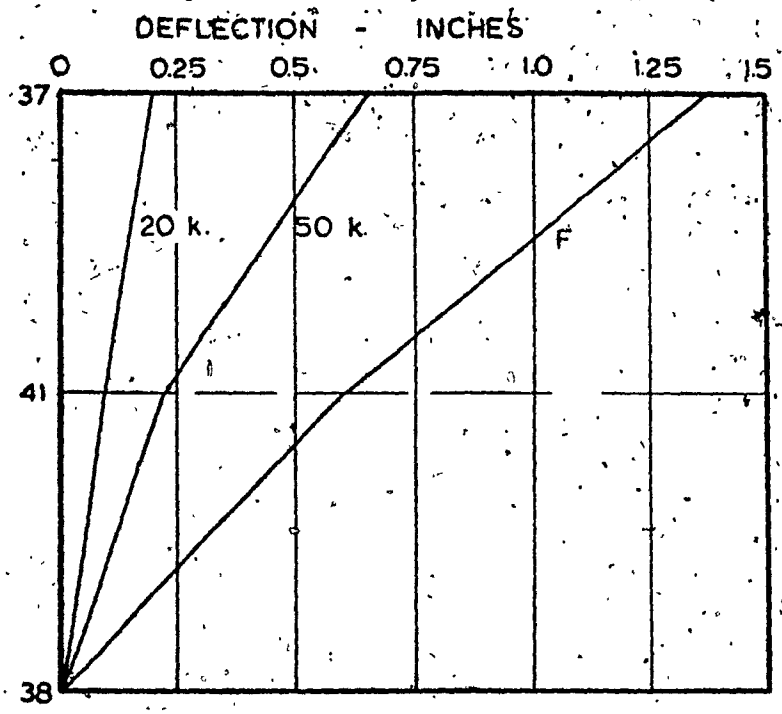

FIG. D.9- LEFT END TWISTING IN Y-Z PLANE
END 37 - 38 PANEL 168-9-3

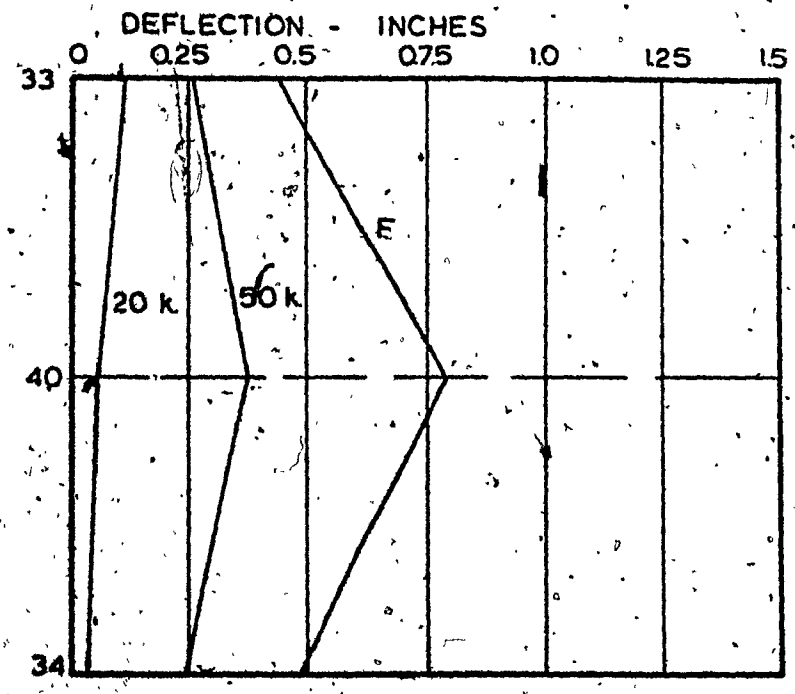

FIG. D.10- MIDDLE LINE 33-34 TWISTING IN
Y-Z PLANE PANEL 168-9-3

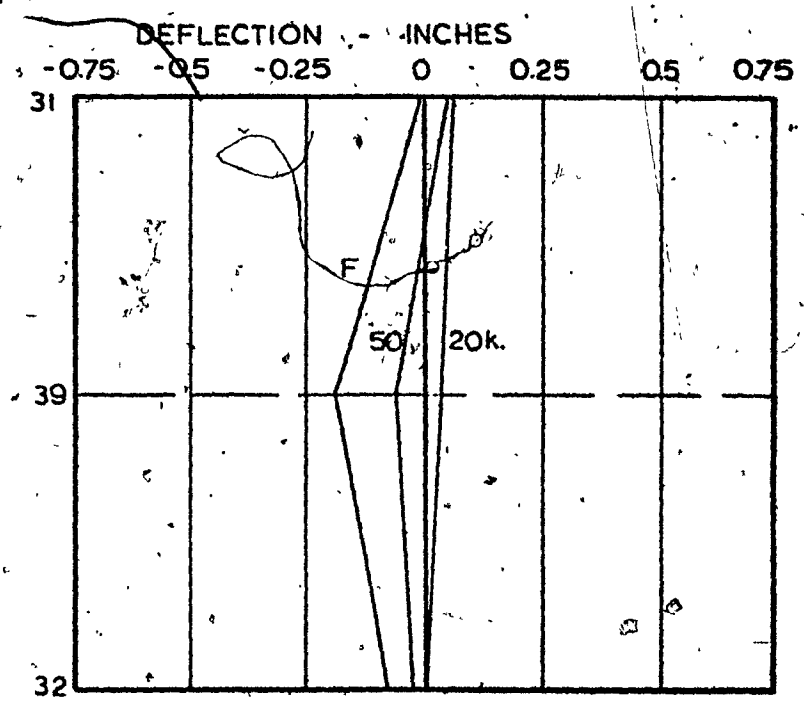

FIG. D.11 - RIGHT END TWISTING IN Y - Z PLANE
END 31 - 32 PANEL 168 - 9 - 3

APPENDIX E

TEST PHOTOGRAPHS

APPENDIX E

TEST PHOTOGRAPHS

Photographs of the test frame and of the failed panels are presented herein.

Photographs E.1 and E.2 show a typical panel in the test frame. Note the load cell which is placed between the hydraulic cylinder and a stiffened wide flange beam. Also note the displacement measuring devices mounted on the standing clamped angles. The bolts holding the columns of the test frame were post-tensioned. The left-hand side pin support is visible in photograph E.2.

Photographs E.3 to E.16 are for the failed panels 168-5 to 168-11, respectively.

In photograph E.3, note the diagonal splitting cracks D1 and D2.

In photograph E.11, note the snapped wires of the web reinforcement at the diagonal splitting crack. (Compare with the figures in Appendix C).

PHOTOGRAPH E.1

PHOTOGRAPH E.2

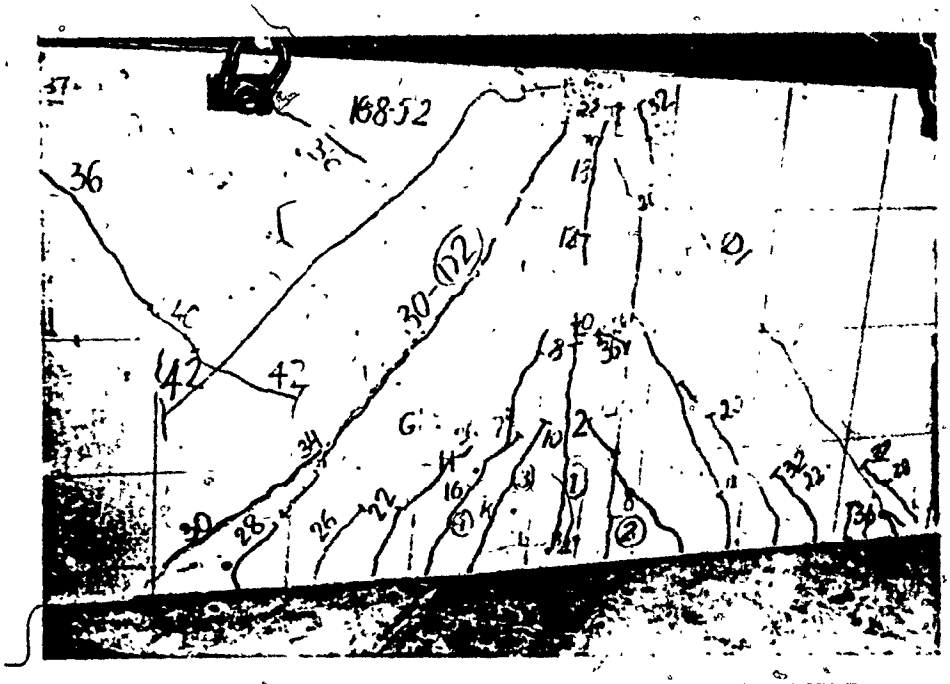

PHOTOGRAPH E.3

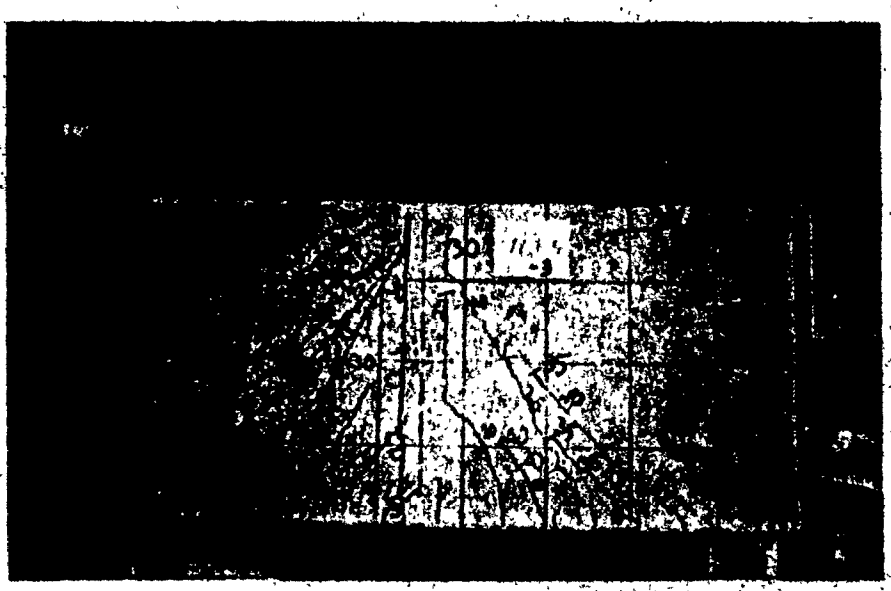

PHOTOGRAPH E.4

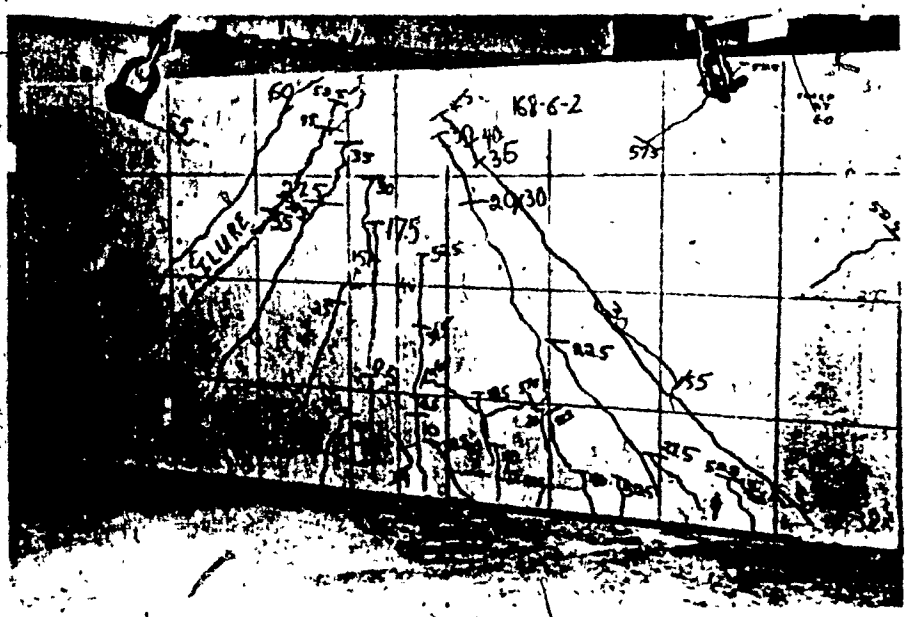

PHOTOGRAPH E.5

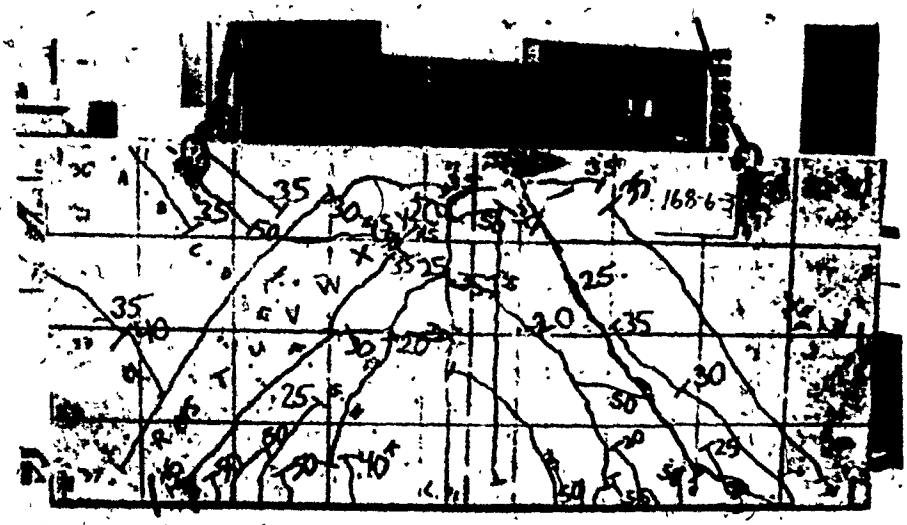

PHOTOGRAPH E.6

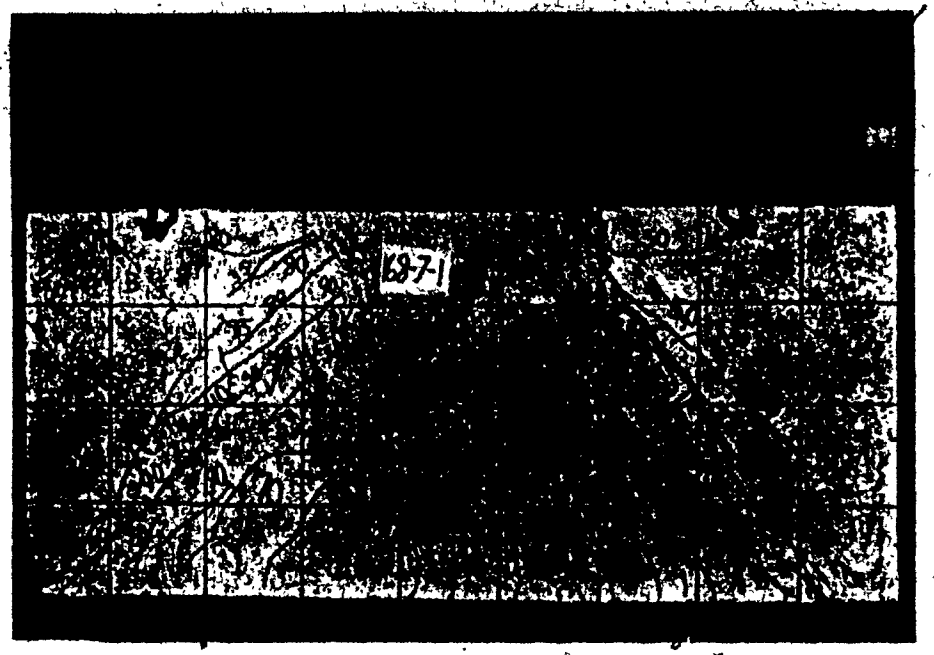

PHOTOGRAPH E.7

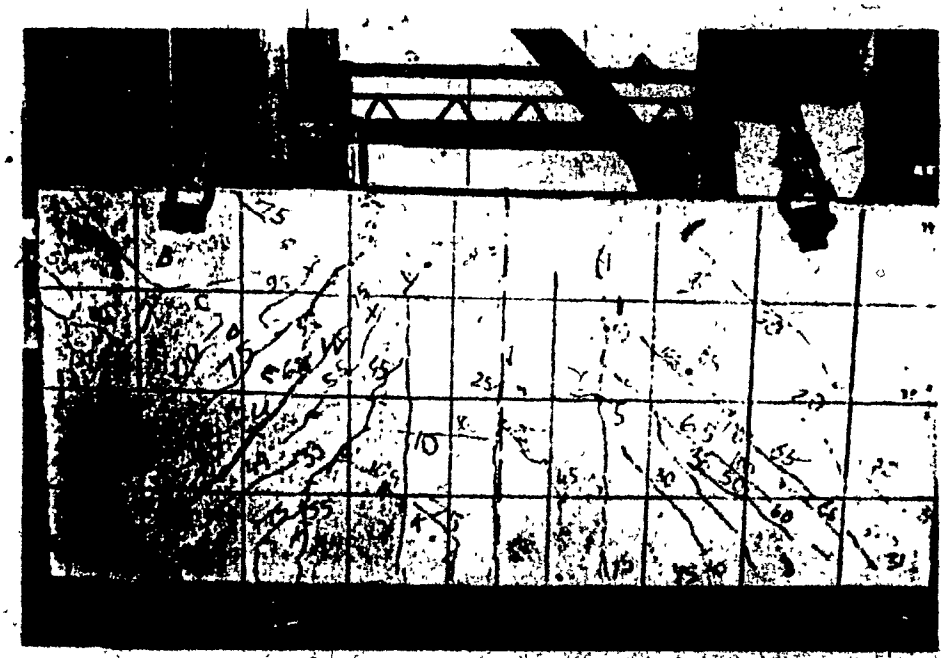

PHOTOGRAPH E.8

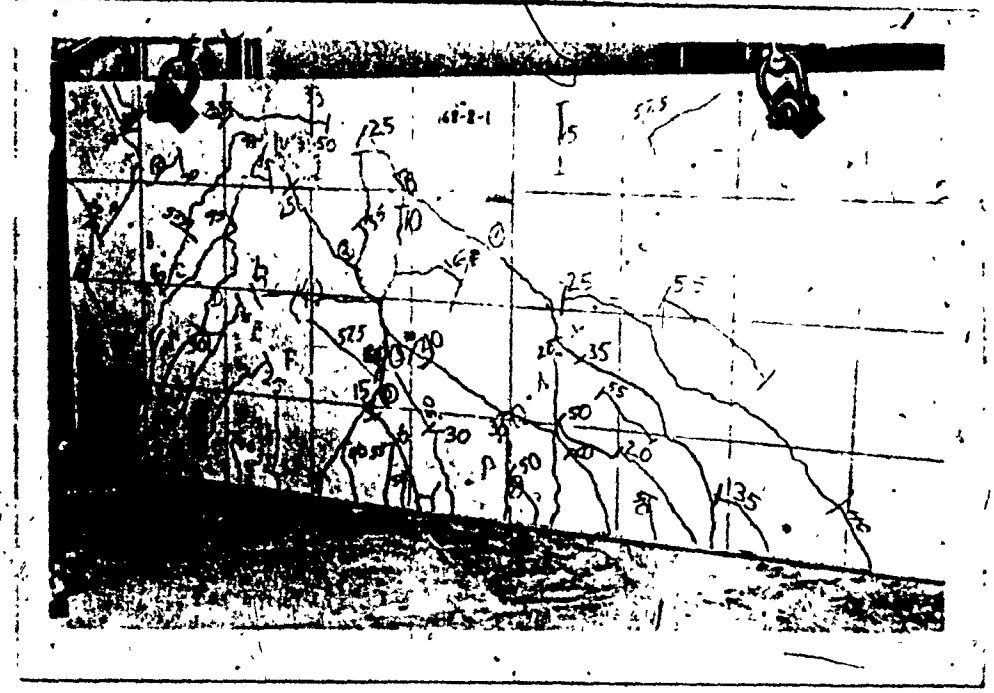

PHOTOGRAPH E.9

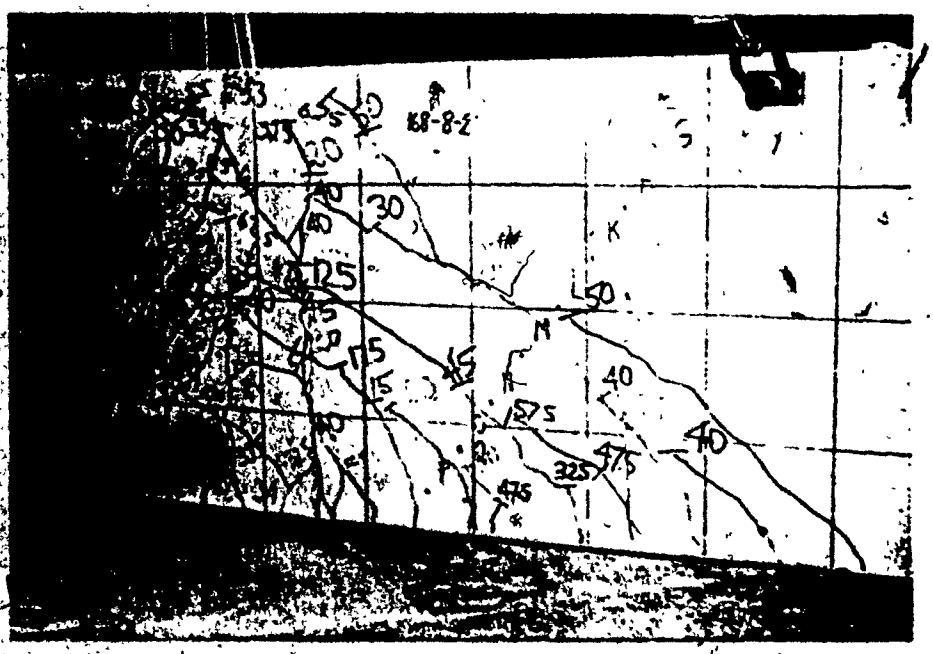

PHOTOGRAPH E.10

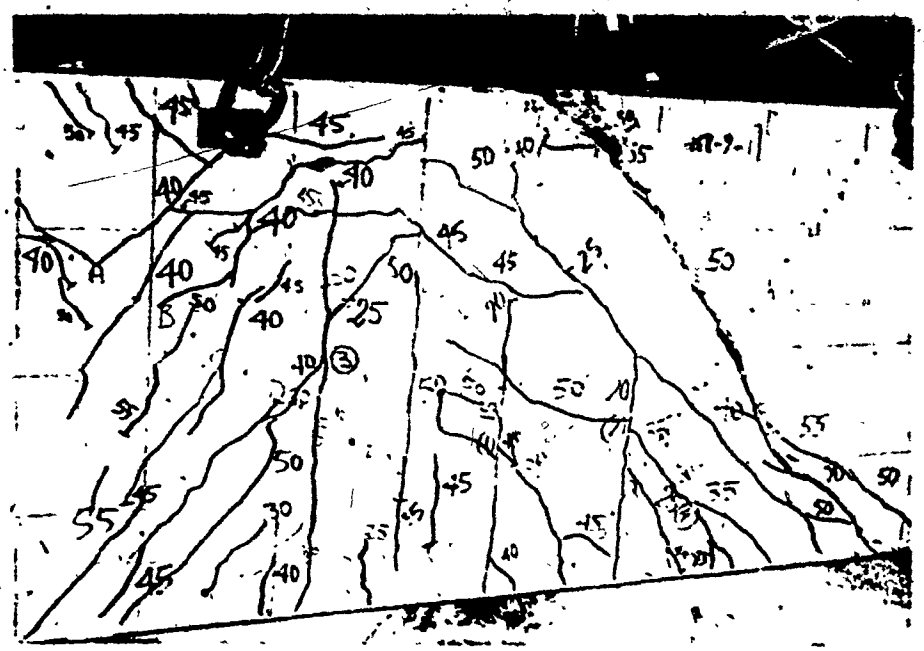

PHOTOGRAPH E.11

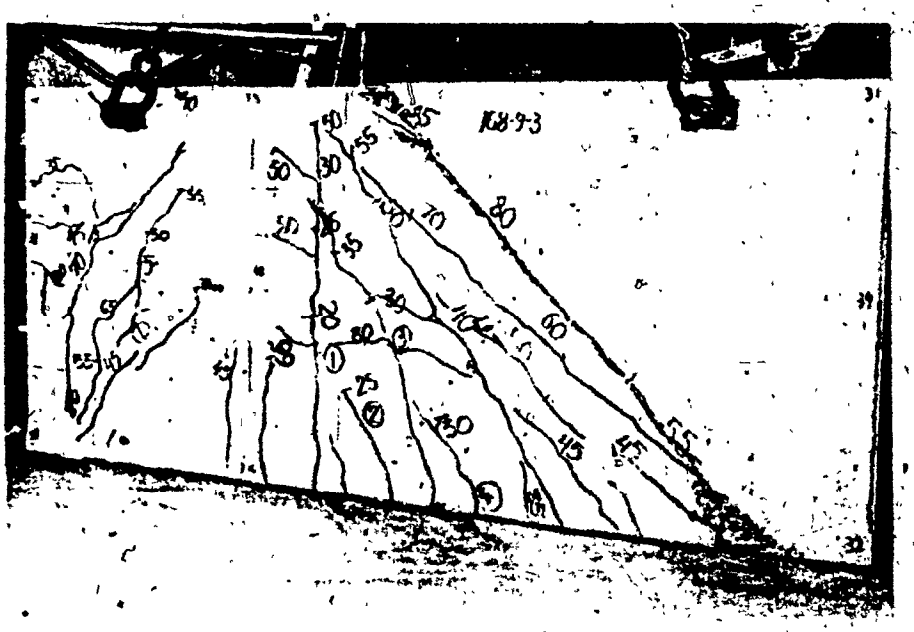

PHOTOGRAPH E.12

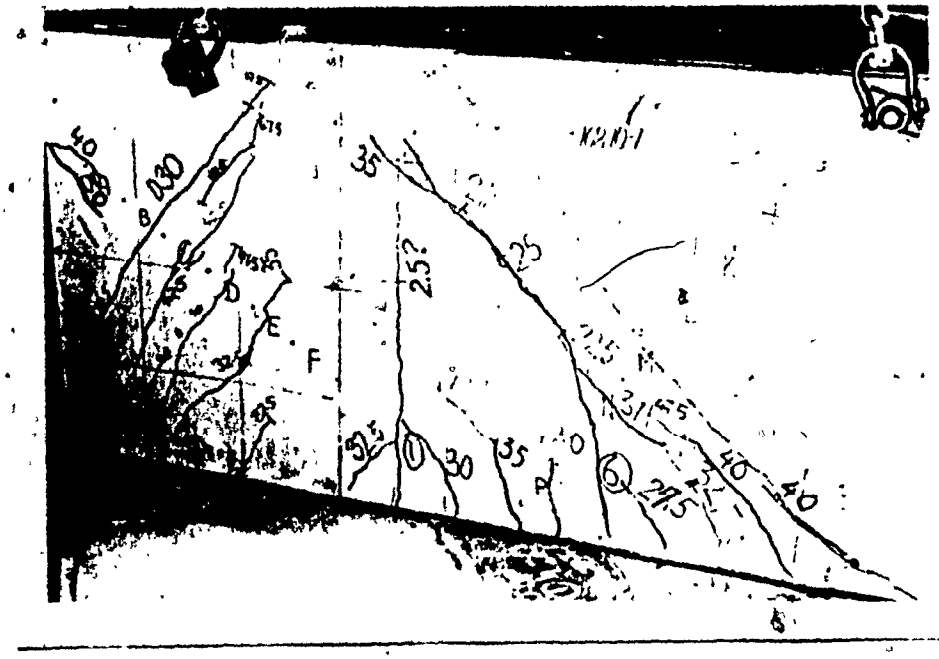

PHOTOGRAPH E.13

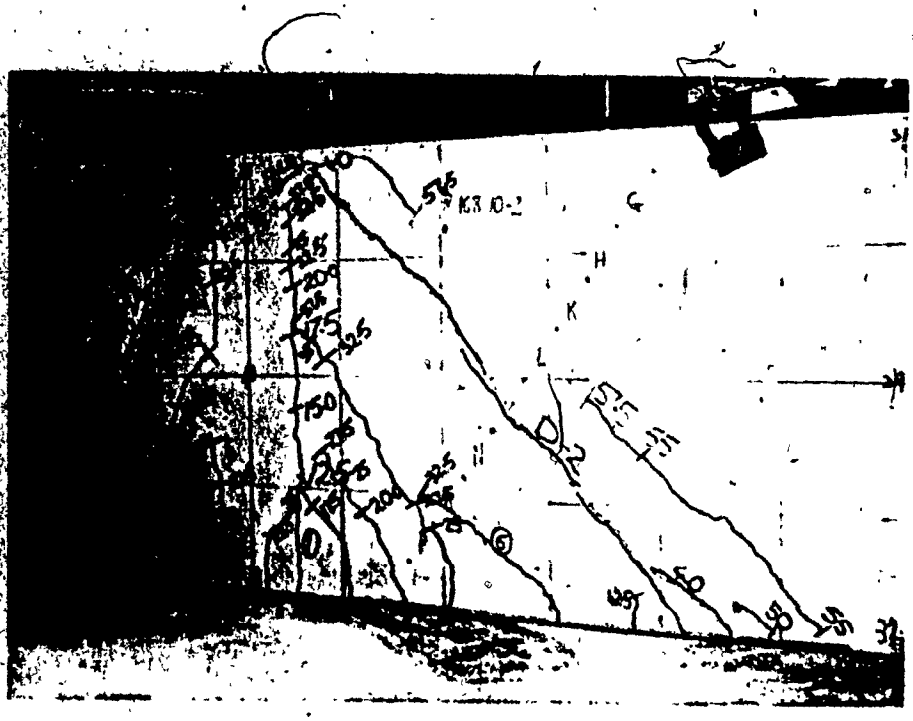

PHOTOGRAPH E.14

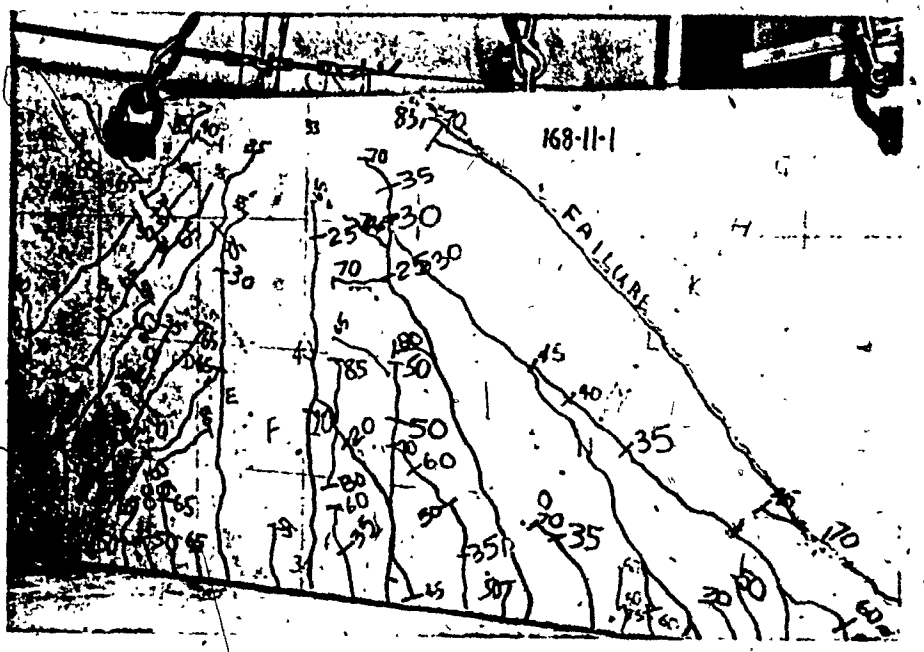

PHOTOGRAPH E.15

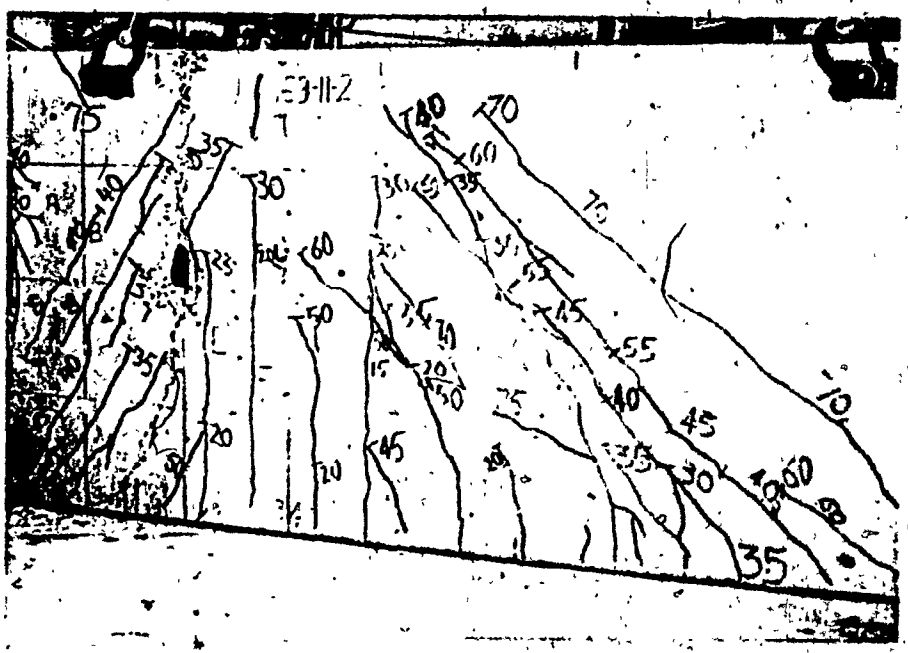

PHOTOGRAPH E.16